RAMAN STUDIES OF THIN POLYPYRROLE FILMS

by

William Stephen Conder

Dissertation submitted to the Faculty of the
Virginia Polytechnic Institute and State University
in partial fulfillment of the requirements for the degree of
Doctor of Philosophy in Chemistry

APPROVED:

Raymond E. Dessy, Chairman

John G. Mason

James P. Wightman

Michael A. Ogliaruso

Paul J. Harris

August, 1985

Blacksburg, Virginia

RAMAN STUDIES OF THIN POLYPYRROLE FILMS

by

William Stephen Conder

Raymond E. Dessy, Chairman

Chemistry

(ABSTRACT)

Polypyrrole is an electrochemically synthesized conductive polymer that has physical properties which impede efforts to develop structure-properties relationships. The extent of conjugation, as limited by the presence of structural disorders in the polymer, is important in determining its inherent conductivity. The extent of conjugation in thin electrochemically generated films of polypyrrole and poly-N-methylpyrrole has been examined with resonance Raman spectrosopy. The Raman experiment was performed within the electrochemical cell and does not suffer from exposure to the contaminants encountered when transfer techniques are employed.

Electrochemically reduced films of polypyrrole exhibited intense resonance Raman spectra of the carbon-carbon stretching frequencies. The position of these bands is a function of the number of double bonds in conjugation. The conjugation length within the polymer chain was found to be

between 3 and 4 rings for PP and slightly less in PNMP (2-3 rings). This is the first reported determination of the conjugation length in PP and PNMP. This data confirms the idea that PNMP is less conductive than PP due to reduced planarity within the chain, thus less conjugation.

Reduced films of PP and PNMP yielded intense luminescence that disappeared upon oxidation. The luminescence is a broad featureless band that consumes the weakly enhanced Raman of PNMP. The intensity of the luminescence increased as the reduction potential increased and the highest intensities occurred at potentials far cathodic of the E_0 for the film. The explanation for this is still obscure but may involve either further reduction of highly luminescent segments or a decrease in the amount of quenching by solvent or counter-ion interactions with the luminescer.

ACKNOWLEDGEMENTS

I would like to thank for the craftmanship and numerous rescue operations performed on the glassware used in this research. provided functional parts from my flawed designs necessary to perform electrochemistry inside the sample compartment of the spectrometer. The potentiostat design and many helpful discussions on electrochemistry were generously contributed by Dr. Harry Finklea. gave indispensable assistance with the sample imaging and the Raman cell design. provided advice and helped with the implementation of the FORTH research software. introduced me to polypyrrole and contributed much to my understanding of its chemistry and properties. 's experience in spectroscopy and the general aspects of research helped focus my efforts. gave the advice and encouragement necessary to complete this project. I am greatly indebted to my parents for their financial and moral support, given without question, throughout all the years of my education. Finally, the love and understanding of pulled me through the rough times and I dedicate this work to her.

TABLE OF CONTENTS

LIST OF ILLUSTRATIONS

LIST OF TABLES

1.0 INTRODUCTION

The search for a polymer with the conductivity of a metal and the processibility of a plastic has lead to the development and analysis of many conductive polymer systems. Some examples are polyacetylene, polysulfurnitride, polyparaphenylene, and the heteroaromatic polypyrroles and polythiophenes. Potential applications lie in the battery, electronics, and solar energy fields. The need to develop characterization methods for these polymers is essential for success in this area. Standard polymer characterization methods often fail to provide a clear view of the structures involved. The lack of structural information impedes synthetic efforts to create polymers with improved conductivity and physical properties.

Polypyrrole and its nitrogen substituted derivatives are unique because of the ability to synthesize thin films via controlled electrochemical methods. The films, adhered to the electrode surface, can be electrochemically switched between the conducting (oxidized) and insulating (reduced) states. Several research groups have directed efforts towards the electrochemical characterization of these materials[1-2]. Polypyrrole films have been used as electrode materials[3], ion gate membranes[4], catalysts in the reduction

of oxygen[5], and as a photocorrosion inhibitor in a solar cell[6].

Polypyrrole is an amorphous, insoluble material sensitive to air oxidation when reduced. It has been therefore difficult to obtain good structural information supporting the electrochemists' assertions as to the conducting nature of the material. Spectroscopic data has been obtained by developing dry box techniques to transfer the film into the cell of the desired instrument. Electronic absorption[7], UPS[8], XPS[9], Infrared[12], ^{13}C nmr[11], and other tools have yielded useful information by this procedure. However, the transfer technique inevitably provokes some chemical or physical change in the film, and destroys the film-solution interface. An <u>in situ</u> method of characterization is desirable.

Raman spectroscopy has found many successful applications to polymer analysis[12]. It places few restrictions on the size, shape, and transparency of the sample. Non-polar groupings yield strong Raman signals important for the study of the carbon backbone present in many polymers. Strong absorption of highly conjugated systems further augments the method's sensitivity and yields resonance enhanced spectra with excellent signal-to-noise characteristics.

Resonance Raman techniques have been combined with electrochemistry to obtain structural data of the electrode-solution interface[13]. The electrochemical data (current, potential, charge) can be supplemented with spectroscopic data. Much valuable information can be obtained in one cell and in one experiment.

Combining laser Raman spectroscopy with electrochemistry creates a powerful technique for the characterization of pyrrole-type conductive polymers. The electrochemical arrangement controls the polymerization and subsequent switching of the film. The laser Raman acts as a structural probe of the film in the as-grown, oxidized, reduced, and intermediate states. It provides a unique opportunity to view the transformation that occurs during electrochemical cycling of the polymer.

This thesis presents the results of a Raman spectroelectrochemical investigation of polypyrrole and some its N-substituted derivatives. It reports the Raman spectra of the as-grown, oxidized, and reduced forms of polypyrrole (PP), poly-N-methylpyrrole (PNMP), and poly-N-phenylpyrrole (PNPP). Polypyrrole exhibits strong resonant enhanced spectra in the reduced form. The first known report of photoluminescent spectra from the reduced forms of each of the polymers is described. Comparison of the spectra for the

reduced and oxidized forms suggest homogeneous charge extraction from the aromatic system.

The Raman data for polypyrrole is similar to that of polyacetylene and this observation is used in this work to determine the extent of conjugation and the distribution of conjugation lengths within a polymer chain. Comparison of the spectra between polypyrrole and the N-substituted derivatives supports a relationship between conductivity and planarity only speculated on previously. This data is useful in explaining the difference in the electrochemical behavior and conductivity between the unsubstituted and substituted forms.

2.0 HISTORICAL

2.1 PYRROLE BLACK

The material that came to be known as "pyrrole black" was first discovered by Italian workers in 1916[14]. It was formed from the oxidation of pyrrole by H_2O_2 in acetic acid. Oxidative degradation with $KMnO_4$ gave several dicarboxylic acids of which pyrrole-2,5-dicarboxylic acid was the most prevalent. This suggested that the material consisted of α,α' linked pyrrole units. Further characterization was impeded by insolubility in all organic solvents and a limited solubility in aqueous alkali.

2.2 ELECTROCHEMICAL SYNTHESIS OF POLYPYRROLE

The first electrochemical synthesis was achieved by electrooxidation of pyrrole in aqueous sulfuric acid by Dall'Olio[15]. The resulting film had a conductivity of 8 ohm^{-1} cm^{-1} and was described as an "insoluble, brittle, powdery film" on a Pt electrode[15]. These films gave a strong epr signal indicative of many unpaired electrons and elemental analysis suggested one positive charge per 3-4 pyrrole rings.

Extensive characterization of polypyrrole began with the development of an electrochemical method for creating mechanically stable films. This was accomplished by Diaz, et al[16] in 1979 by galvanostatic synthesis of polypyrrole (PP) in a two electrode cell. These films of PP adhered strongly to the electrode surface and performed well as an electrode for voltammetry of ferrocene in acetonitrile. Thick films (5-50 μm) could be separated from the electrode surface for further physical and structural characterization.

Diaz and Castillo[17] were the first to synthesize thin (0.1 μm) PP films which could be cycled or "switched" between the conductive (oxidized) and insulative (reduced) states. They noted the redox potential for PP at -0.22 V vs. sodium saturated calomelelectrode. The films' color changed from a light yellow when reduced to a brown-black when oxidized. The redox process seemed to involve the extended π-electron system of the polymer backbone making PP an inherently electroactive polymer, not just a polymer with attached electroactive pendant groups. Although the oxidized form supported ferrocene elctrochemistry, the reduced form inhibited the reduction of nitrobenzene and the resulting reduction wave came from the slow diffusion of nitrobenzene to the Pt surface.

2.3 MECHANISM OF POLYMERIZATION

A simplified mechanism for the formation of polypyrrole (PP) is shown in Figure 1. Film growth proceeds by a radical cation coupling process forming the more readily oxidizeable oligomers and eliminating two protons. Once formed, the oligomeric cations continue to react with monomeric cations, which are in high concentration adjacent to the electrode surface. The oligomers eventually become insoluble and attach themselves to the electrode surface. Film growth proceeds until the chain becomes unreactive, probably for steric reasons.

The overall n (the number of electrons) for the reaction was determined to be 2.25. Further evidence to support this mechanism has been reported by Street, *et al*[18] who also noted the decrease in the cell pH due to proton elimination during polymerization. Monitoring of the film growth by uv-vis absorption at a transparent indium oxide electrode verified the cessation of film growth at potentials insufficient to oxidize the monomer[19]. Use of 2-substituted monomers prevented film formation, supporting the α,α' linked pyrrole linear chain structure[20].

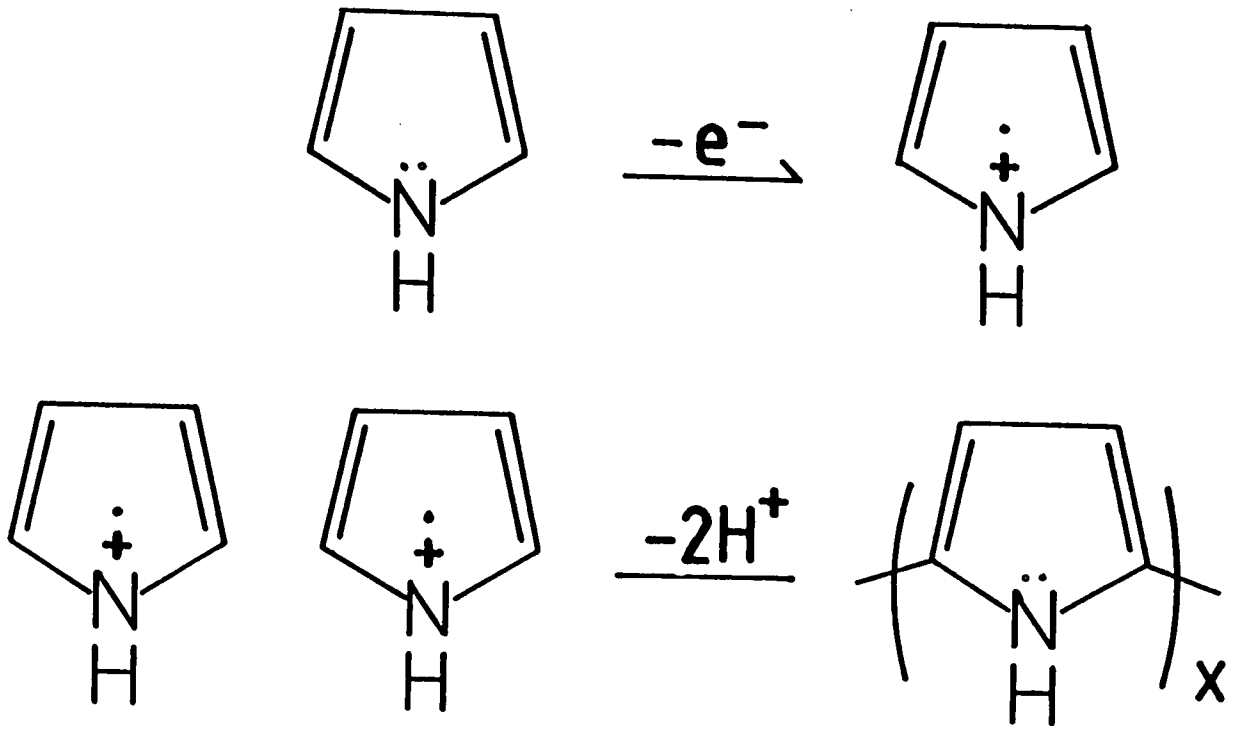

Figure 1. Mechanism of Polypyrrole Formation.

2.4 CHARACTERIZATION OF POLYPYRROLE

The development of the generalized methods for both thin and thick film polymerizations opened the way for extensive characterization of polypyrrole. Research efforts centered around two areas: thin film electrochemical investigations into anion effects and structure-property relationships, and thick film physical and structural characterization.

2.5 PHYSICAL CHARACTERIZATION

Kanazawa, *et al*[21] found PP to be a nonfibrous continuous film that is thermally stable up to 250°C. Its room temperature conductivity is in the metallic range ($\approx$100 $ohm^{-1}cm^{-1}$), as determined by the four-probe method[22], and the positive thermopower measurement suggests that it is a p-type conductor[23]. Elemental analysis of oxidized PP found 70% pyrrole and 30% anion. The lack of peaks in the x-ray analysis[23] are indicative of a noncrystalline material. The results of all physical characterization experiments are consistent with the conduction in PP being due to oxidation of the π-electron system.

2.6 ELECTROCHEMISTRY OF POLYPYRROLE

Thin films which are in contact with the electrode surface have been studied extensively by electrochemical methods. An exhaustive review of the electrochemical aspects of PP research has been written by Diaz and Kanazawa[24]. The impetus behind these efforts are an understanding of the properties of PP as related to structure.

Oxidation of the film removes π-electron density from the pyrrole backbone. The positive charge must be balanced and requires the movement of polymer chains as well as ion migration into the film[25]. SEM (Scanning Electron Microscopy) analysis of neutral and oxidized films show no gross distortions of the surface topology due to these processes[26].

Several studies on the cyclic voltammetric behavior of PP and its N-substituted derivatives have been done. Diaz, *et al*[27] assert that the non-Nernstian behavior of the surface localized film (i.e. inequality of the peak anodic and cathodic voltages) is a result of the slow ion mobility into and out of the film. Salmon, *et al*[28] performed electrochemical studies of chemically modified PP and found that the nature of the anion influences the redox kinetics and the conductivity of PP. The conductivity of the polymer

can be varied over a range of 10^4 simply by changing the anion from fluoroborate to fluorosulfonate. This is quite puzzling considering that the extent of oxidation and the pyrrole ring/anion ratio remain constant.

The conductivity of poly-N-methylpyrrole (PNMP) is $10^{-1}ohm^{-1}cm^{-1}$, which is in the semiconductor range and 10^5 less than PP[29]. The peak anodic voltage in PNMP is shifted anodically by 650 mV, and the reduced form is less sensitive to air oxidation. One explanation for this change is the destabilization of the cation species of PNMP due to sterically induced torsion about the α,α linkage. Put simply, the positive charge in the cationic species of PNMP is not as delocalized as in PP due to a reduction in ring coplanarity. Increasing the size of the substituent on the nitrogen reduces the conductivity and N-cyclohexylpyrrole film formation is prevented altogether.

The large difference between the redox potential of the monomer ($\simeq$+1.2 V) and the polymer (-0.2 V) of pyrrole created interest in developing a relationship between the observed redox potential and the number of rings in a PP chain. Diaz, et al[30] established a linear relationship between the redox potential, low-energy electronic absorption, and N (the number of monomer units) for pyrrole, dipyrrole, tripyrrole,

and polypyrrole. Plots of the peak anodic potential versus 1/N are linear and suggests that N for PP is greater than 10.

2.7 STRUCTURAL CHARACTERIZATION OF PP

The amorphous unordered films of PP have been given the idealized chemical structure as depicted in Figure 2. All research findings to date are consistent with this structure, however things are not quite that simple. Elemental analysis, for example, consistently yields a C-to-N ratio of 4-to-1, but with 10% excess hydrogen. This value is in excess of that attributeable to chain ends[31]. Obviously, there is a need to characterize the material structurally.

The most compelling evidence to date that PP consists of alternating pyrrole rings was obtained by Street *et al*[32]. They performed x-ray and ir analsis of pyrrole dimer and trimer and compared the results to PP. Infra-red spectra of PP are quite similar to those of the dimer and trimer with a number of peaks in the area of the pyrrole ring vibrations (800-1600cm^{-1}). The X-ray analysis showed peak data supportive of the alternating ring structure and a planar crystal packing of the chains similar to that found in graphite.

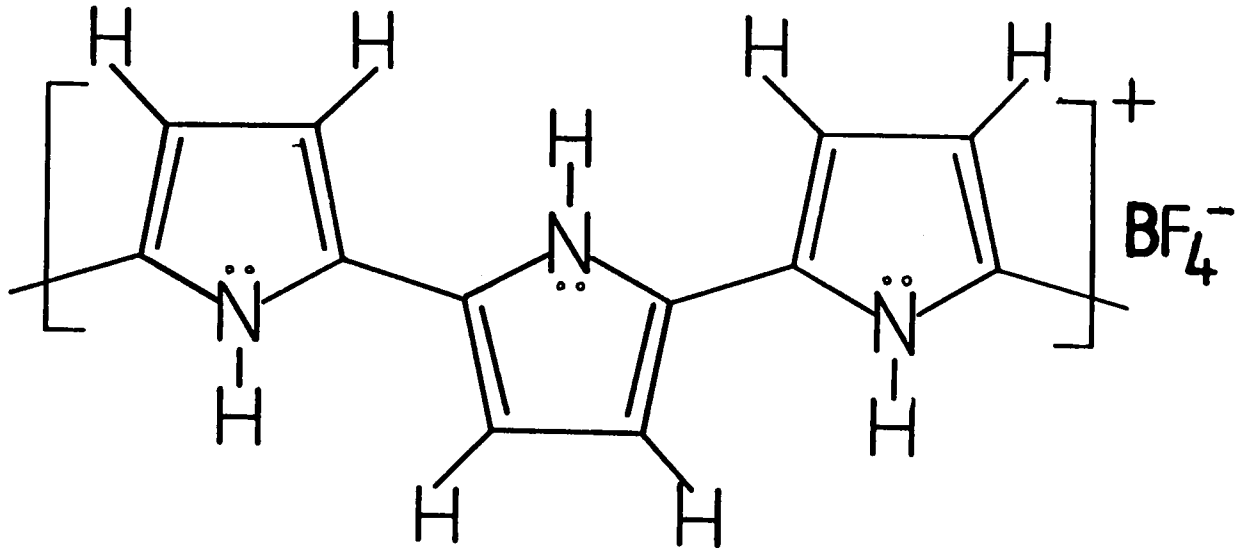

Figure 2. Simplified structure of PP.

Additional evidence supporting the presence of the pyrrole moiety in PP was provided by ^{13}C-nmr[11] using magic angle spinning techniques. Their results showed that the chemical shifts of the α-carbon resonances in the polymer are consistent with an α-substituted pyrrole. Also, XPS[33] (X-ray Photoelectron Spectroscopy) studies of pyrrole and PP reveal similar C(1s) and N(1s) peak data.

However, in addition to supporting a generalized structure these tools also provide strong evidence that suggests the presence of two types of disorders in PP films. Pfluger's[33] XPS spectra of the C(1s) region in PP have peaks attributed to the presence of α,β linked or sp^3 hybridized ring carbons. The presence of sp^3 C-H moieties in partially saturated pyrrole rings within the polymer chain was verified by ^{13}C-nmr[11]. This result is consistent with the presence of excess hydrogen in the elemental analysis of PP. Furthermore, the presence of α,β linkages can lead to cross-linking in the polymer, explaining the intractable properties of the film.

The two types of structural disorders are shown in Figure 3. The sp^3 carbons destroys the conjugation along the chain. Non-linearities in the chain structure are caused by non-α,α' linked rings which eventually leads to a lack of planarity within the chain.

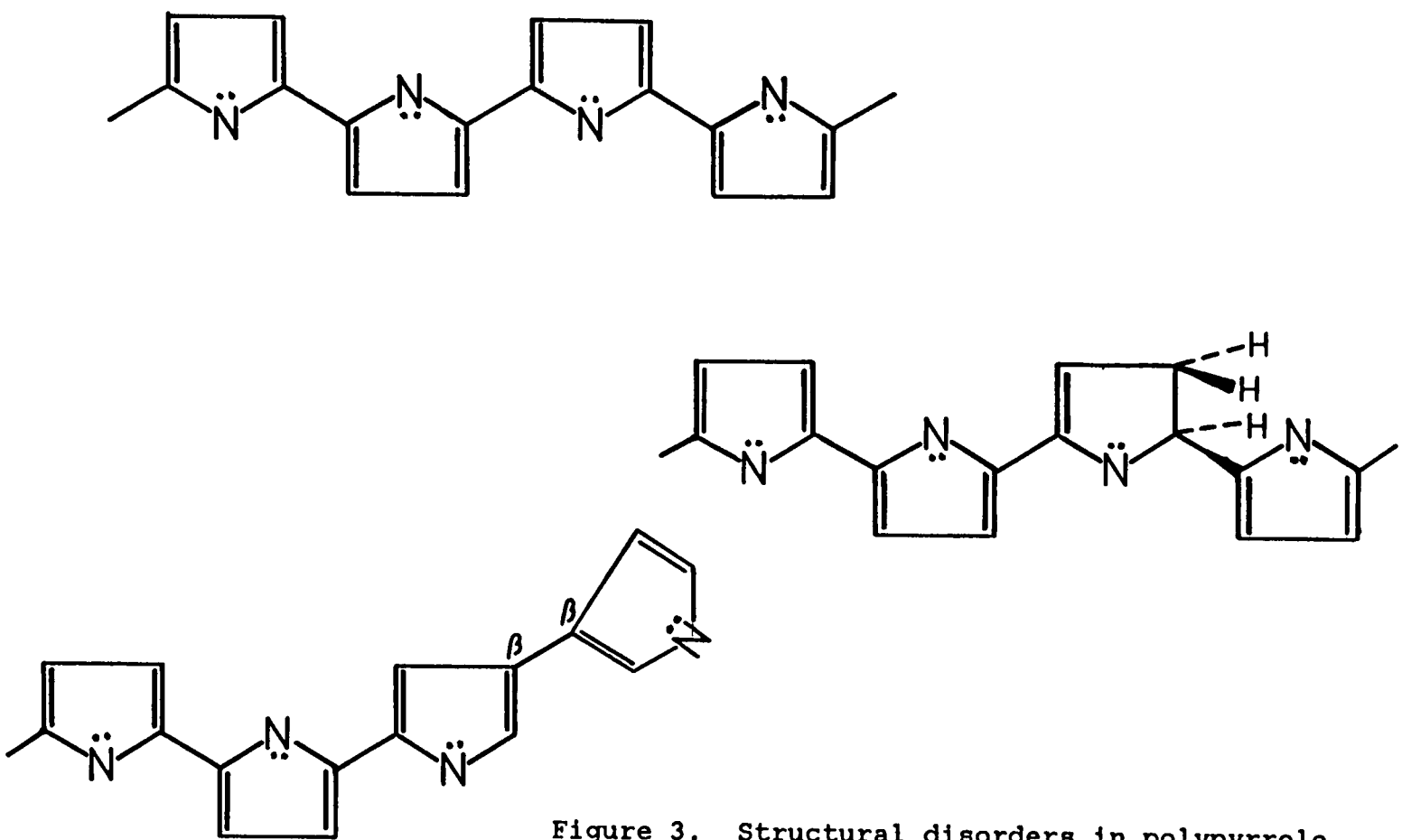

Figure 3. Structural disorders in polypyrrole.

2.8 CONJUGATION LENGTH AND CHAIN LENGTH

The presence of structural disorders in PP lead to the distinction between chain length and conjugation length or the number of coplanar pyrrole rings. Results of UPS[35] (Ultra-violet Photoelectron Spectroscopy) studies have determined that the PP chain length to be in excess of 4 rings. However, PP has the mechanical properties and solubility of a much higher molecular weight material. Radiochemical methods with electrochemically synthesized poly-(β,β')-dimethylpyrrole (the β positions on the pyrrole ring are blocked to prevent α,β links) have determined the chain length to be between 100 and 1000 rings[36].

Yakushi's optical absorption study[37] of oxidized and reduced films suggest the presence of short chain oligomers and a wide distribution of conjugation lengths. However, the exact length is unknown and the current knowledge depicts a conjugation length of at least 4 rings but does not restrict the maximum length. The presence of a single peak in the cyclic voltammogram is indicative of a single conjugation length predominating the distribution. Elemental analysis has determined the minimum conjugation length to be 3 rings. If longer cojugation lengths are present then they may significantly effect the transport properties (e.g. conductivity) of the film. The principal charge carrier in

PP is either a polaron (cation) or bipolaron (dication). Bredas *et al*[38] have determined the length of a bipolaron to be 4 rings. A suitable method for determing the conjugation length in PP would help develop a relationship between conductivity and conjugation. Comparison of this data to polyacetylene (PA) may help to explain its higher conductivity and poorer stability.

3.0 RAMAN THEORY

3.1 BASIC RAMAN PROCESS

The Raman effect is a molecular scattering phenomena first predicted by Smekal in 1923[39] and experimentally verified by Sir C. V. Raman[40] in 1928. The process is depicted in Figure 4 as the promotion of the molecule to an unstable excited state after a collision with a uv-vis photon. The scattered radiation is created when the molecule returns to the ground state. If the initial and final states, which are vibrational energy levels of the molecule, are the same, then the collison is considered elastic. Elastic collisions do not involve energy transfer between the photon and the molecule. The resultant scattered radiation is known as Rayleigh scattering and occurs at the same frequency as the incident radiation.

Raman scatter occurs when the final and initial states are energetically inequivalent. The collision is inelastic and involves energy transfer between the molecule and the photon. This type of scatter is very weak, when compared to Rayleigh scattering, as only one photon in 10^{10} is effected.

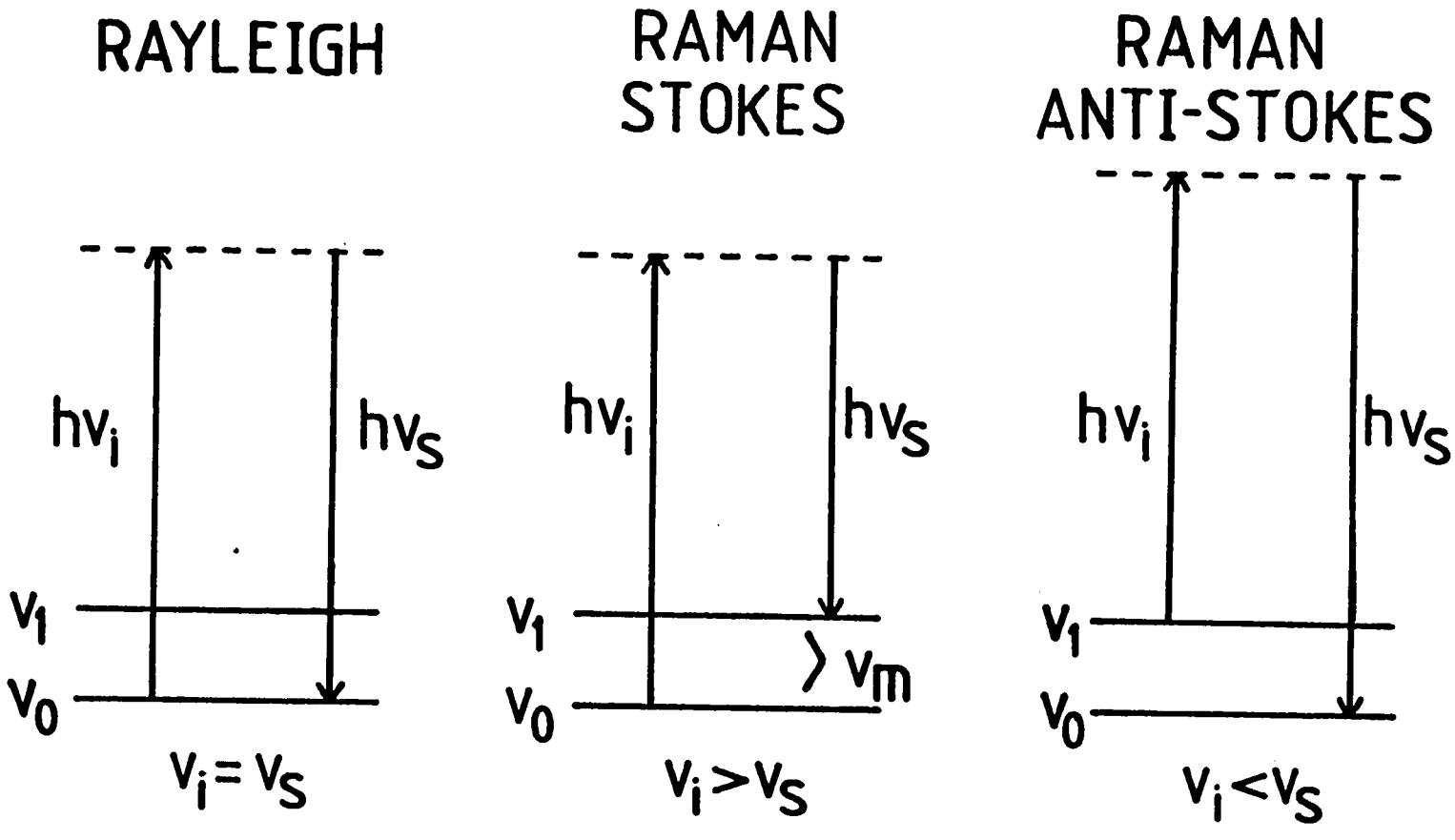

Figure 4. Energy level description of Raman.

The energy is transferred in discreet quanta resulting in a series of lines shifted in frequency from the incident light by an amount equal to a vibrational frequency of the molecule. The same vibrational energy is sometimes measured directly by infra-red absorption.

The entire Raman spectrum of a molecule contains two sets of lines: Anti-Stokes and Stokes. In Figure 4, the Stokes lines appear when the molecules vibrational energy is increased by transfer of energy from the photon to the molecule. The result is a red-shift in the scattered radiation. Anti-Stokes lines are blue-shifted, to higher energy, by transfer of energy from the molecule to the photon. Stokes lines are the most intense due to the higher population of the ground vibrational level at room temperature, thus they are the most often measured experimentally.

Raman and infra-red yield complementary information about the vibrational structure of the molecule. They differ in the mechanism of energy transfer between the molecule and the incident radiation. Several excellent works have been published detailing this difference, and only the most salient features will be discussed here[41].

Raman active vibrations change the polarizability of the molecule (in contrast to a change in the dipole moment of the molecule for an infra-red active vibration). Certain vibrations, such as symmetric vibrations of homonuclear diatomics, are Raman active, and ir inactive because they involve changes in the polarizability without changes in the dipole moment. Raman and infra-red activity are not mutually exclusive because many vibrations involve both types of changes. Thus they yield complementary information.

3.2 RESONANCE RAMAN

In normal Raman spectroscopy (NRS) the frequency of the exciting light is below that required to promote an electron into the first electronic excited state. However, the linear polyenes and PNA's have significant absorption in the the uv-vis region and consequently their Raman spectra have bands with greatly increased intensities when acquired with excitation wavelengths that fall within an allowed electronic transition. This process is depicted in Figure 5. These spectra are resonance enhanced spectra and some band intensities increase by a factor of 10^6 over their normal Raman equivalents.

An abbreviated review of the theory of resonance Raman spectroscopy (RRS) has been done by Strommen and Nakamoto[42].

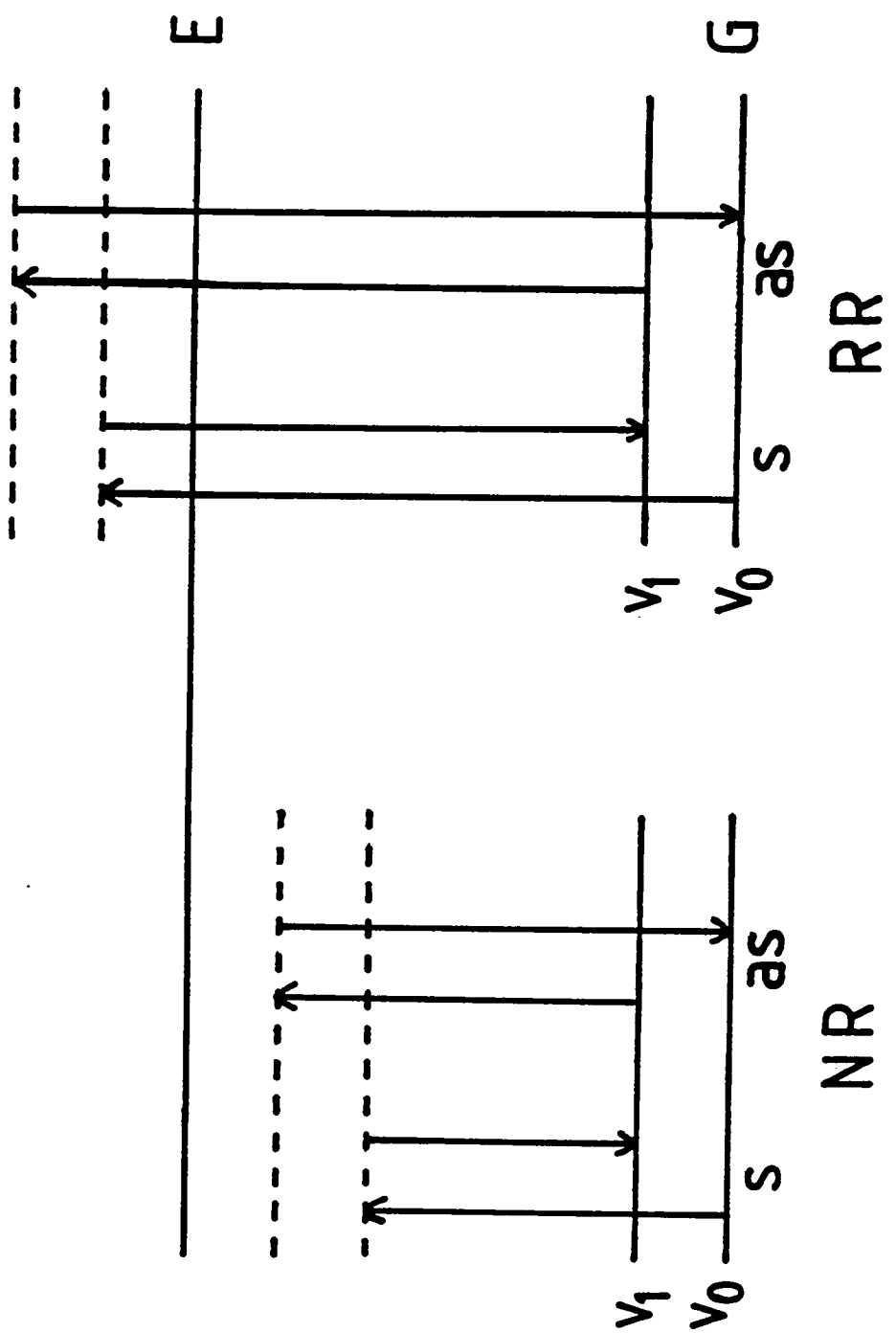

Figure 5. Comparison of NRS to RRS.

The important distinction is that not all bands in the NRS are enhanced in the RRS. The explanation for the selectivity is that only vibrational modes which are affected by the electronic transition are enhanced. In aromatics and highly conjugated polyenes the uv-vis absorption bands are $\pi \rightarrow \pi^*$ transitions of the delocalized π-electron system. The intensity of the carbon-carbon stretching frequencies (both double and single bond) are enhanced when excitation wavelengths are employed that promote $\pi \rightarrow \pi^*$ transitions.

Albrect's[43] theoretical approach to explaining RRS involves the changes in the scattering intensitiy that occur when the excitation wavelength is brought into resonance with the lowest lying electronic excited state. This theory states that only totally symmetric vibrations are intensified at the wavelength of the electronic transition. The result is that symmetric stretches of the carbon-carbon bonds in linear polyenes and aromatic systems are specifically enhanced by the resonance Raman method.

3.3 ADVANTAGES OF RAMAN SPECTROSOPY TO POLYMER ANALYSIS

Raman spectroscopy has several important advantages, both as a general method, and in its application to polymer analysis. Gerrard[44] has published a recent review of the application of Raman to analysis of various polymer systems. Raman is

capable of analyzing all types of samples; liquid, gaseous, or solid (opaque or transparent). This is particularly important for polymers because of their various shapes and sizes.

Raman spectroscopy has been aided by photon counting techniques employing advances in digital electronics and thermoelectrically cooled photomultiplier tubes. But the laser has been the obvious technical advance to promote the viability of Raman spectroscopy as an analytical tool. The small (50 micron) spot size of the laser has allowed spatial analysis of solid samples. Spectral aquisition times have been improved by using optical multichannel analyzers, such as the microchannel plate detectors used in night vision equipment.

The greatest advantage of Raman spectroscopy in the study of polymer systems is the inherent sensitivity to the non-polar carbon-carbon bonds so often found in the backbone of the polymer. This sensitivity is increased further by applying resonance Raman methods. It has proven to be useful for the study of degraded polyvinylchloride and polyacetylene.

3.4 APPLICATIONS OF RRS TO LINEAR POLYENES

Applications of RRS to the study of linear polyenes takes advantage of their uv-vis absorption and the invention of visible wavelength lasers. Strong absorption throughout the visible region is possible. Sondheimer *et al*[45] reported the absorption data for $H(CH=CH)_n-H$ for n=3, 5, 6, 8, and 10. They noted the shift to longer wavelengths of the absorption maxima as n increases.

The Raman spectra of linear polyenes is distinguished by two series of lines at $\approx 1600 cm^{-1}$ ($\bar{\nu}_2$) and $1140 cm^{-1}$. The analysis of the planar vibrations of conjugated chain polyenes assigns these lines to C=C and C-C stretching frequencies respectively[46]. These same bands are enhanced when using the appropriate laser excitation.

Subsequent research of the C=C stretching frequency ($\approx 1600 cm^{-1}$) revealed that its value is dependent on n as well. The C=C stretching frequency for a series of diethyl esters of 2-butenedioic acid are presented in Table 1[47]. The general trend is opposite to that observed for absorption; $\bar{\nu}_2$ decreases as n increases. Thus it is possible to determine the extent of conjugation by measurement of the C=C stretching frequency.

Table 1. $\tilde{\nu}_2$ values for $EtO_2C-(CH=CH)_n-CO_2Et$.

n	$\tilde{\nu}_2$ (cm^{-1})
1	1664
2	1644
3	1621
4	1596
5	1570
6	1562
7	1550
8	1542

Polyacetylene (PA) is a linear polyene which is conductive in the oxidized form. Its conjugation has been studied extensively by Raman spectroscopy and several equations relating $\bar{\nu}_2$ and the conjugation sequence length have been developed. Three of these equations are listed in Table 2.

The first equation was developed by Lichtmann et al[48], and was obtained by plotting published values of $\bar{\nu}_2$ for low molecular weight polyenes against log n. It was found to yield less than satisfactory results for large values of n encountered in some polymers. Equations 2[49] and 3[50] were developed from asymptotic regression analysis and yield better fits for large values for n. The fact that two similar equations exist is due to some controversy over the the exact experimental value of $\bar{\nu}_2$ as $n\rightarrow\infty$ ($1474cm^{-1}$ in equation 2 and $1461cm^{-1}$ in equation 3). Baruya et al[50] state that their value ($1461cm^{-1}$) is the best because it was acquired from a sample with a known n of 30 and excited by the 752.5 nm laser line from a Kr^+ laser. This excitation line is necessary to obtain RRS from such a long conjugated segment.

A plot of $\bar{\nu}_2$ against n for n=1 to 10 using all three equations is shown in Figure 6. It shows that for values of n<10 there is very little difference in the C=C stretching frequency calculated by using equations 2 and 3. Thus linear polyenes

Table 2. Equations relating $\bar{\nu}_2$ to n.

1.	Lichtmann, Temkin, & Fitchen	$\bar{\nu}_2 = 915/n + 1450$
2.	Gerrard & Maddams	$\bar{\nu}_2 = 1471 + 141.7e^{-0.0925n}$
3.	Baruya, Gerrard, & Maddams	$\bar{\nu}_2 = 1461 + 151.2e^{-0.078ln}$
	n = # of conjugated double bonds	
	$\bar{\nu}_2$ = C=C stretching frequency (cm^{-1})	

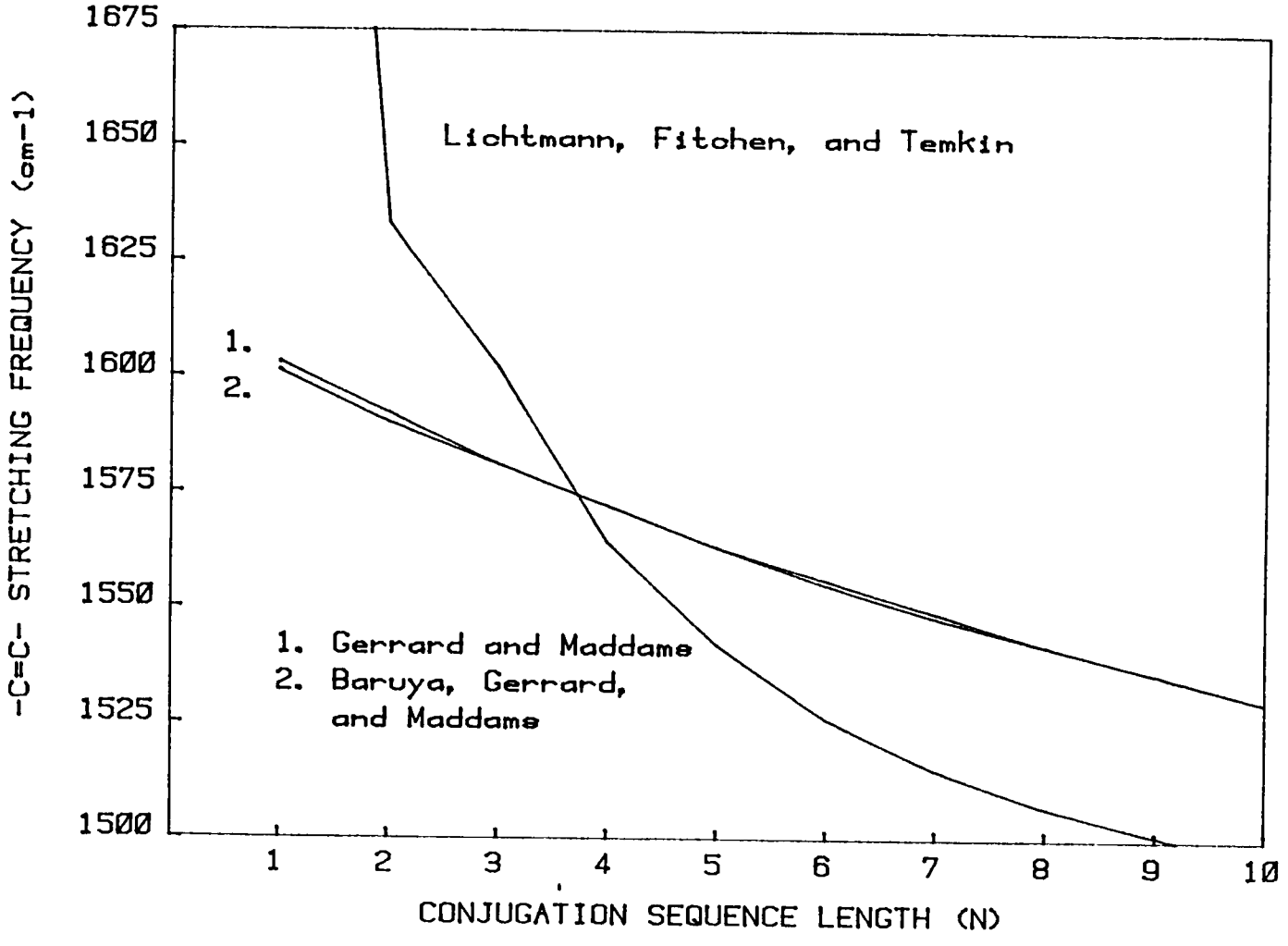

Figure 6. Plot of $\bar{\nu}_2$ vs. N

with less than 10 conjugated double bond are described by either equation.

PP is structurally very similar to PA in its carbon-carbon backbone. Figure 7 shows the C-C backbone structure for PA and PP. If one ignores the bridging nitrogens in PP, the C-C backbone is trans-cisoid (cis about the C-C single bond) in chains where the rings do not alternate (lower left of fig 7). In chains with alternating rings (lower right) a mixture of trans-cisoid and trans-transoid exist. Included within Figure 7 are the Raman band positions for the C=C and C-C stretching vibrations in PP and PA. The values for PP were obtained from the work presented in this dissertation. Clearly, their Raman spectra are similar. A published resonance Raman spectrum[51] for neutral PA is reproduced in Figure 8 for comparison with those obtained from reduced PP presented in Chapter 6.

The similarities in the structure and Raman spectra between PP and PA create the opportunity for an analysis of the conjugation length in reduced PP from the measured C=C stretching frequency. This research applies the equations developed for linear polyenes to an analysis of the conjugation in PP. It requires the experimental determination of the C=C stretching frequency for reduced PP. This presents an experimental challenge. The Raman

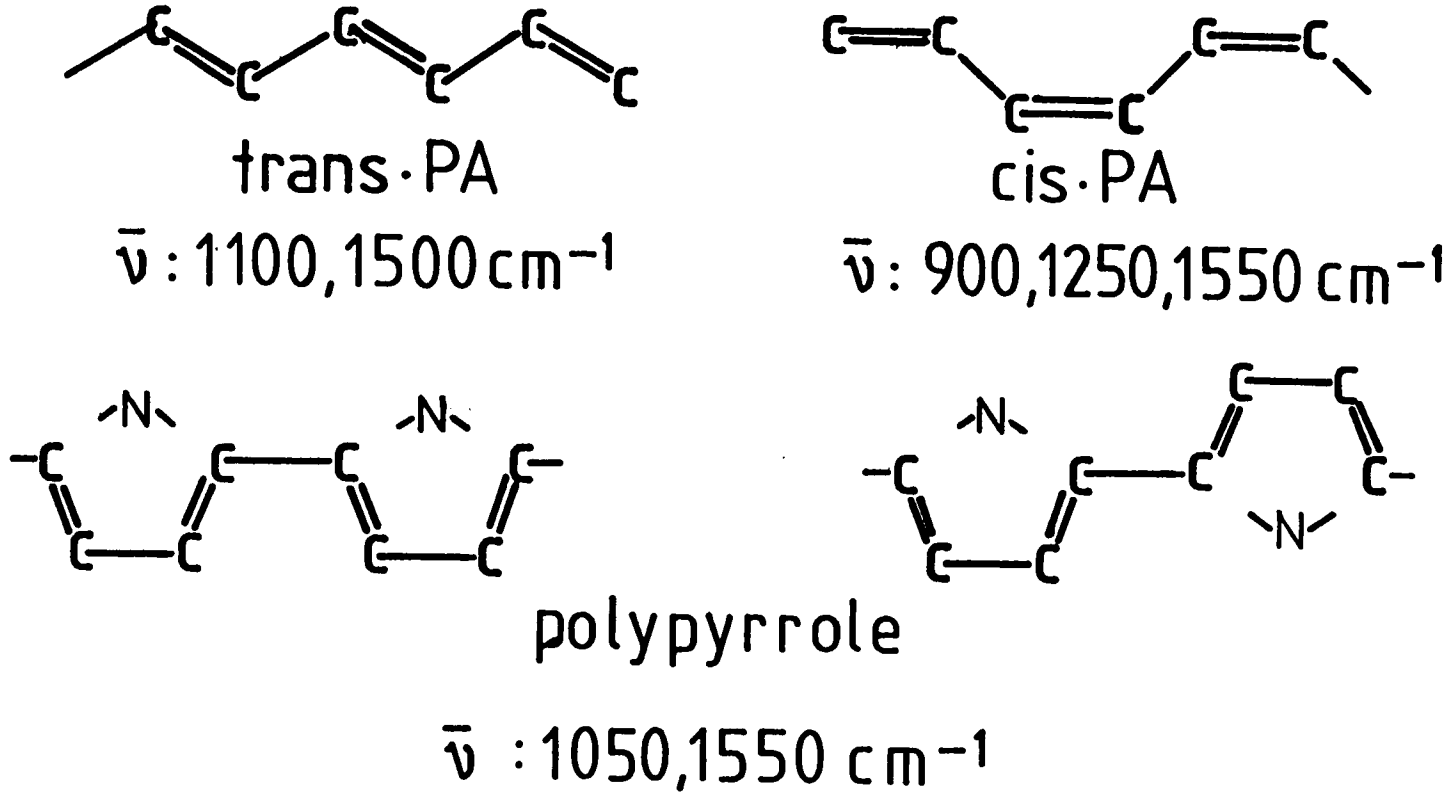

Figure 7. Carbon-carbon skeletal structure of PA & PP.

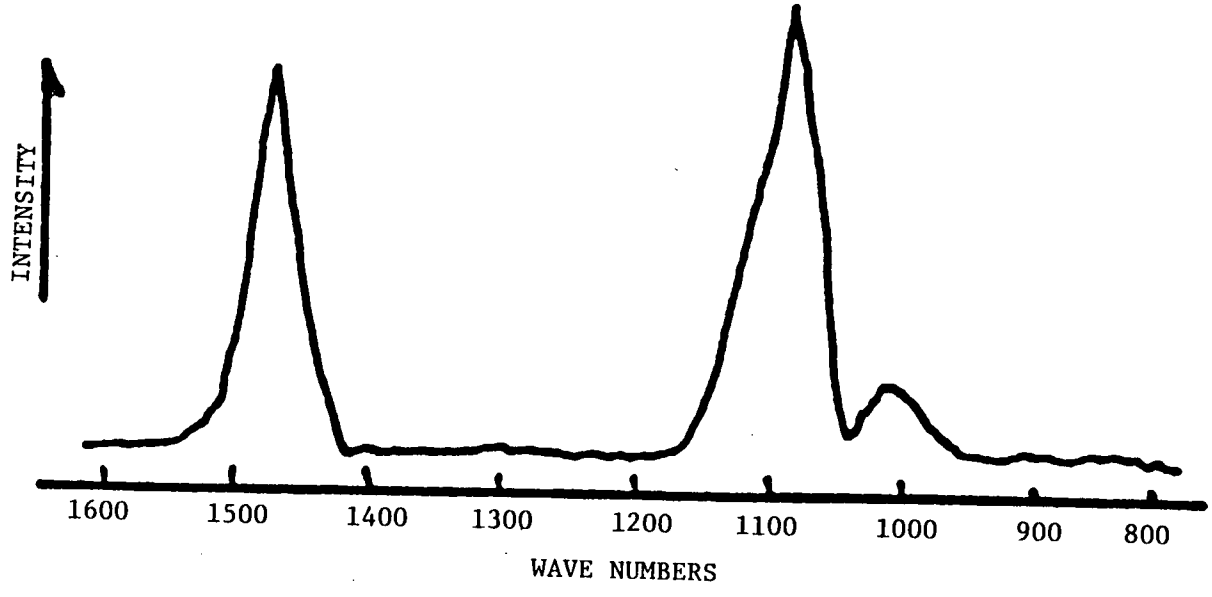

Figure 8. Raman spectrum of PA: 632.8 nm excitation.

experiment must be performed within the electrochemical cell to avoid decomposition and changes in in film structure because of the film transfer from the cell to the spectrometer. This unique approach allows the effect of the reduction potential upon the extent of conjugation to be studied.

4.0 INSTRUMENTATION

The instrumentation required for Raman spectroelectrochemistry is shown in Figure 9. It consists of two separate and independent instruments that are interfaced through the Raman/Electrochemistry cell. The electrochemical apparatus performs the necessary electrode pretreatment, film deposition, film oxidation or reduction, and cyclic voltammetry. The Raman instrument provides spectra of the film at various stages during these processes. The cell is the interface between the two systems and has attributes suitable to electrochemistry and spectroscopy. Each piece is described in detail in the following sections.

4.1 ELECTROCHEMICAL APPARATUS

The potentiostat required for the electrochemistry was built in our laboratory and is controlled by a Digital Equipment Corporation LSI-11 microcomputer. A schematic of the potentiostat is shown in Figure 10. A three electrode, single cell arrangement is used for all electrochemical experiments. The platinum working, gold counter, and reference electrodes are described in the materials section.

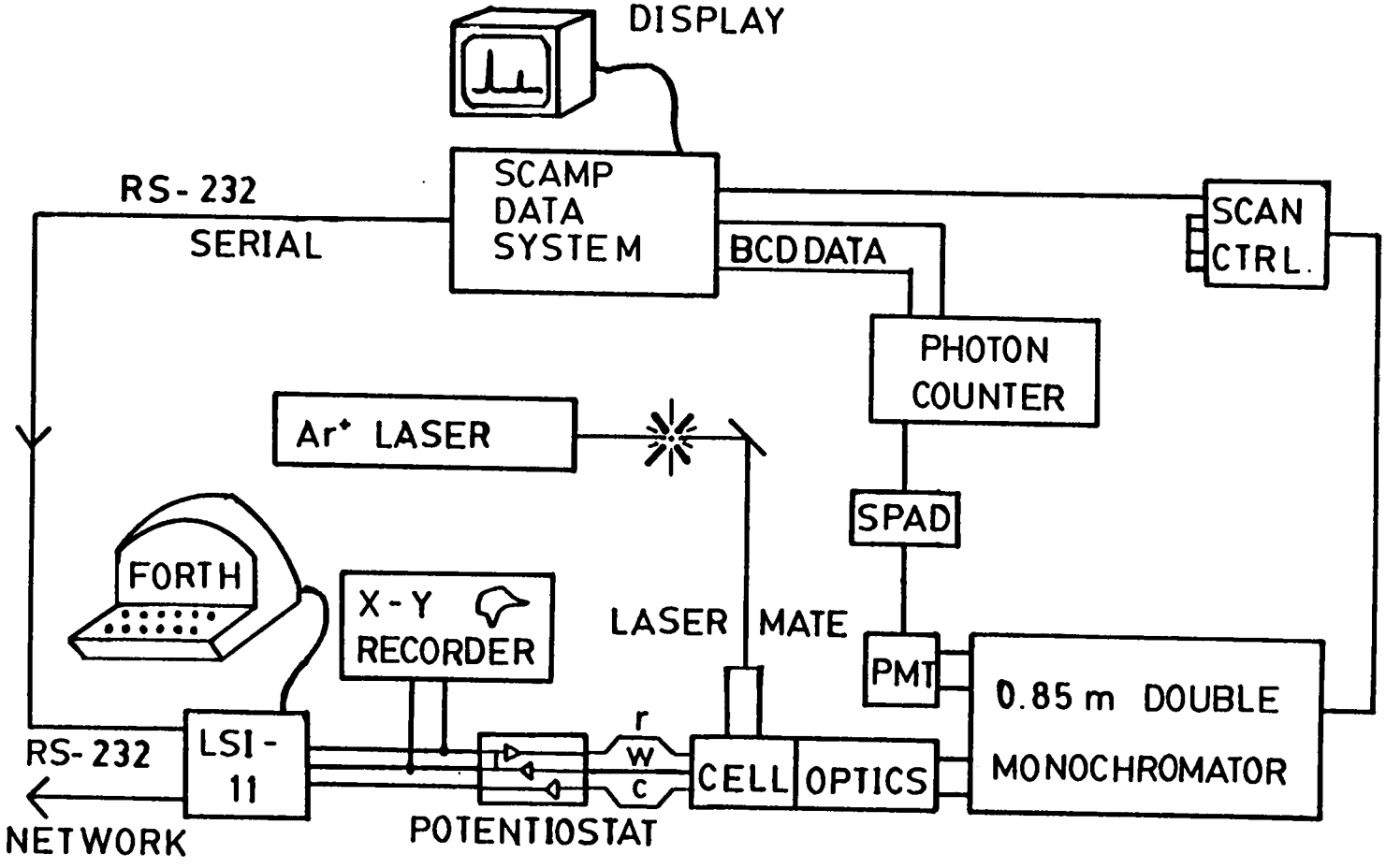

Figure 9. Raman/Electrochemistry instrumentation.

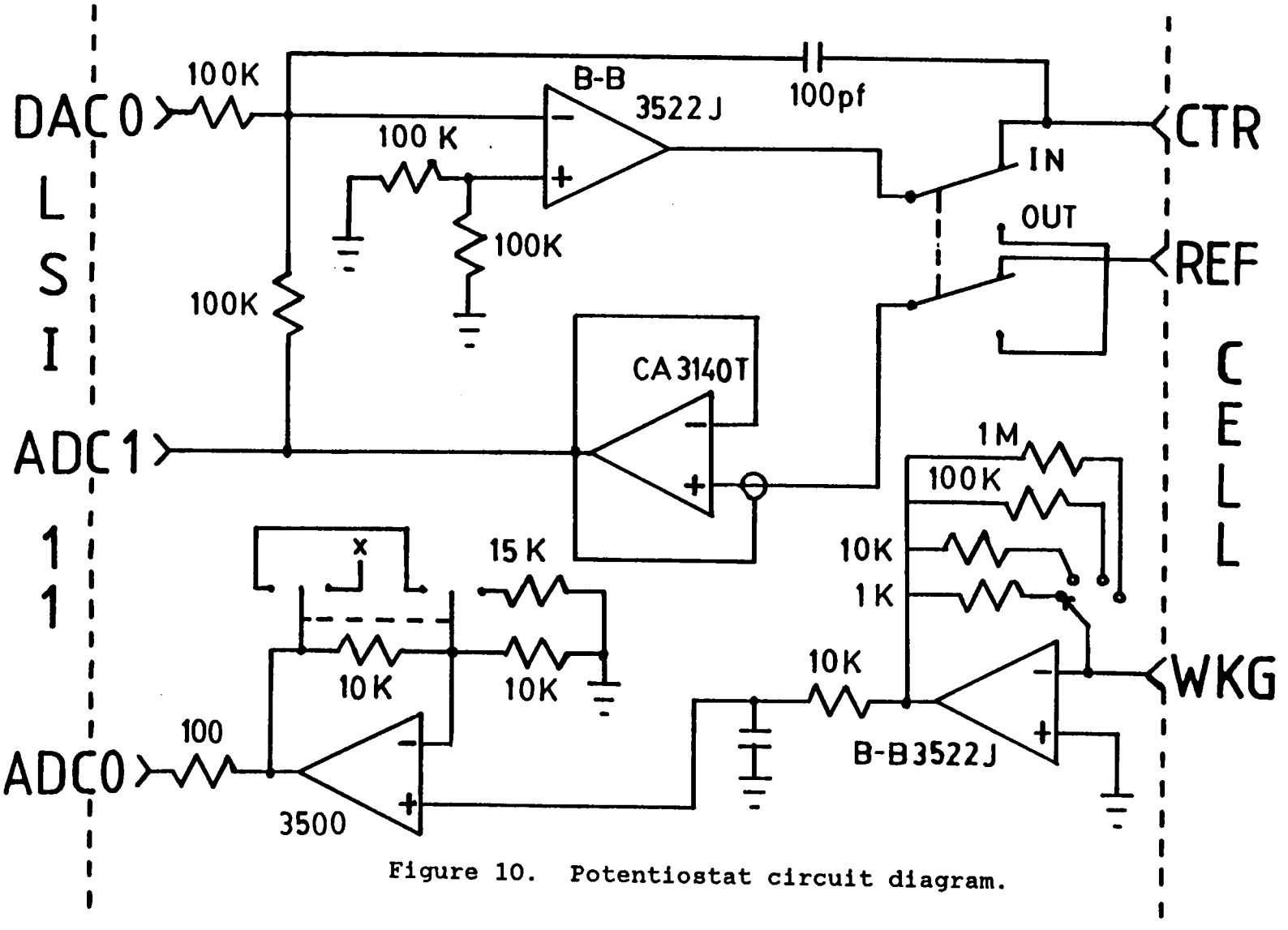

Figure 10. Potentiostat circuit diagram.

The computer system utilizes an analog I/O subsystem (ADAC Corp.,Model 1050) to apply all potentials to the working electrode through a 12-bit digital-to-analog converter (DAC0). It monitors the current and voltage on two channels of a 12-bit analog-to-digital converter (ADC0 and ADC1). The microcomputer system is based around a Digital Equipment Corporation LSI-11 16-bit central processor and 16K memory programmed in FORTH. The FORTH programs are detailed in Appendix A. All polymerization and triangle waveforms required for film deposition and cyclic voltammetry are computer generated. The electrochemical data is displayed locally on an X-Y recorder (Houston Instruments Model 2000) and acquired digitally for processing and transfer to the laboratory host computer for archiving and plotting.

The potentiostat is used in both the constant current and standard voltammetric configurations. The constant current configuration used for film formation is shown in Figure 11. It differs from the voltammetric configuration by a precision resistor placed in series with the working electrode and connection of this point to the reference input of the potentiostat. This forces a constant current through the cell. The amount of current is determined by Ohm's Law (dividing the applied potential by the resistance value). This has been verified by an ammeter. Simply removing the

resistor and reconnecting the reference electrode allows cyclic voltammetry to be performed.

4.2 RAMAN INSTRUMENTATION.

A list of the components that constitute a laser Raman spectrometer system is provided in Appendix B. Briefly, the Spectra-Physics Ar-ion laser provides laser output at nine wavelengths between 454.8 nm and 514.5 nm. The laser radiation is coupled into the cell compartment by the Laser Mate and Front-end Illuminator combination. This reduces spectral interferences from the Argon plasma and focuses a small (≈50 micron) laser spot into the sample area. The front-end has mirrored collection optics to focus the Raman scatter into the 0.85m double monochromator.

The Raman signal is detected with a thermoelectrically cooled photomultiplier tube. The Hamamatsu R955 PMT, amplifier-discriminater (SPAD), and digital electronics supplied by the DPC2 make up the photon counting system necessary for detection of weak Raman signals. The resolution of the monochromator, down to 0.015 nm at 500 nm, and photon counting detection provide an excellent system for Raman spectroscopy.

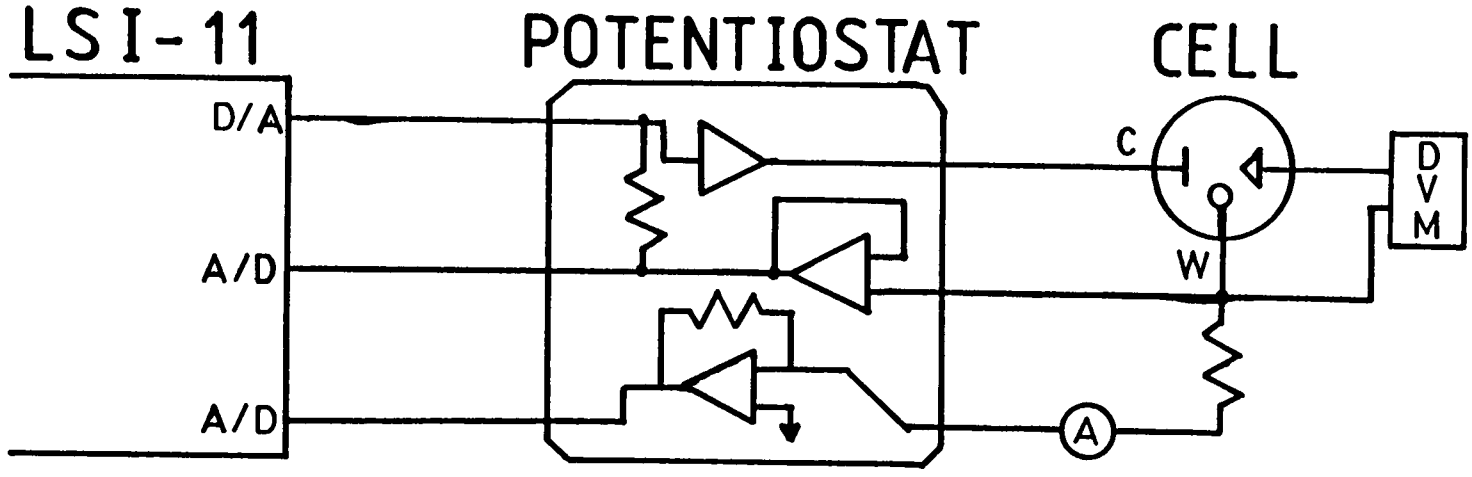

Figure 11. Polymerization configuration.

The photon counts are collected from the DPC-2 by the SCAMP data system for display, processing, and eventual transfer to the laboratory network host computer for storage and plot generation. All plots are created with a Hewlett-Packard 7225A digital plotter.

4.3 RAMAN/ELECTROCHEMISTRY CELL

The Raman spectroelectrochemistry cell is shown in figure 12. It must perform two functions. First, it serves as a cell for polymerization of the monomer onto the Pt electrode surface and subsequent electrochemical cycling. Second, it serves as a Raman cell for illumination of the film and collection of the scattered radiation. The cell is constructed from a 2.5 inch length of 1.5 inch diameter glass tube which has been cut in a "D" shape at one end to accept a flat quartz viewing window. A ground and polished quartz flat is used as the entrance window. The windows were sealed to the cell with Dow Corning silicone sealant in the standard 90 degree geometry used in Raman spectroscopy.

The other features of the cell include: a threaded glass joint (ACE Glass Co.) which accepts a solid glass rod for mounting the cell into the front-end illuminator, a drain tube with stopcock for draining the cell, and a standard taper glass joint which accepts the platinum electrode for

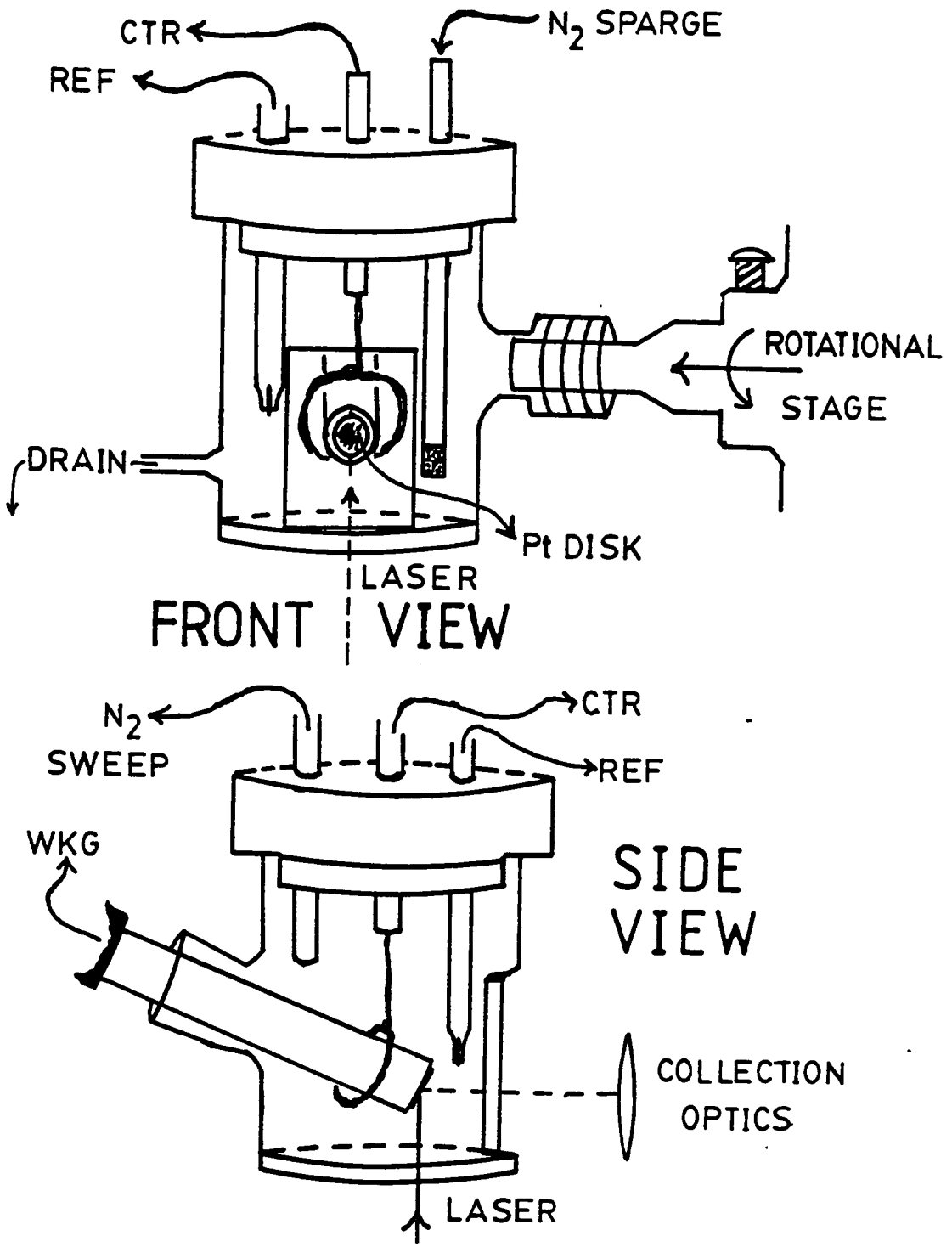

Figure 12. Raman spectroelectrochemistry cell.

positioning into the laser beam as shown in figure 12. The teflon lid holds the sparge and sweep tubes, Luggin capillary, and counter electrode connection completing the cell.

The three electrodes are positioned inside the cell without obscuring the Pt surface and in an acceptable manner for voltammetry. The gold counter electrode is coiled about the working electrode body to provide symmetrical current lines between the working and counter electrodes. The Luggin capillary is placed adjacent to the platinum surface and is easily visible through the front of the cell.

The position of the working electrode surface with respect to the excitation beam is a modification of the one chosen by Campion[52]. It provides for an incident angle of 70° from the normal to the electrode surface in the plane formed by the incident and reflected beams. This is similar to other designs for front-surface reflectance Raman spectroscopy, particularly surface enhanced Raman. The spot of laser radiation appears as an ellipse on the surface of the film when properly focused into the entrance slit of the monochromator.

5.0 FILM PREPARATION METHODOLOGY

5.1 ELECTRODES AND REAGENTS

The three electrodes used are a Corning Pt metallic electrode (VWR Scientific), a gold counter electrode fashioned from a 50 cm length of 0.5 mm diameter gold wire (Aesar Group, Johnson-Matthey Inc.), and a miniature saturated calomel reference electrode (Fisher Scientific). The calomel electrode was flushed with deionized water and refilled with saturated sodium chloride solution.

Spectral grade acetonitrile was purchased from Burdick & Jackson (American Scientific Products) and used from freshly opened bottles or distilled over phosphorous pentoxide under a nitrogen atmosphere. Diaz found no noticeable differences between the distilled and undistilled acetonitrile in his electrochemical characterization of polypyrrole[30]. Tetraethylammonium and tetra-n-butylammonium tetrafluoroborate were obtained in electrometric grade (Southwest Analytical) and used after drying in a vacuum oven at 90°C for 10-12 hours. Pyrrole and N-methylpyrrole were obtained from Aldrich Chemical and distilled over calcium hydride and stored in a dessicator under nitrogen at 0°C. N-phenylpyrrole (Aldrich) was purified by sublimation.

5.2 ELECTRODE PREPARATION

The platinum working electrode is a disk of 5mm diameter sealed into the end of a 12.5mm diameter glass tube. It was polished with 1.0 micron, 0.03 micron, and 0.05 micron alumina on a billiard cloth high-speed polishing wheel. Excessive polishing of the surface should be avoided to prevent degradation of the platinum to glass seal and scratching of the platinum surface.

Prior to each film deposition the Pt and Au electrodes were vigorously cleaned in a three step process. First, the electrodes were immersed in hot concentrated sulfuric acid for 10-15 minutes followed by a rinse with deionized water. This step is especially good for removing old films without physically disturbing the polished electrode surfaces. Second, they were cleaned electrochemically in a cell filled with 1.0M sulfuric acid, by potentiostating the electrode for 1-2 minutes at each of three potentials: anodically at +1.9V, cathodically at -0.3 V, and at a neutral +0.2V. Vigorous evolution of hydrogen gas was seen at the cathodic potential. Third, the electrodes were cycled anodically from -.225V to +1.425V at 75 to 100 mV sec^{-1}. until reproducible hydrogen waves were seen in the cathodic region[53]. The electrodes can be placed in the cell after one final rinse with deionized water and acetonitrile.

5.3 ELECTROCHEMICAL POLYMERIZATION

Thin films of PP and its derivatives were prepared by electrooxidation of the monomer in acetonitrile using a method similar to the one described by Diaz and Kanazawa[25]. The polymerization solution was 0.05M in monomer, 0.10M in electrolyte, and 1% H_2O in acetonitrile. Oxygen had to be rigorously excluded from the cell during the polymerization and subsequent electrochemical cycling to prevent irreversible oxidation of the film. The constant current configuration (Figure 11 in Chapter 4) was used with a 5K ohm 1% resistor in series with the working electrode. The applied potential (DACO) was 600 mV, yielding a current of 120 microamperes. Polymerization times of 100 tO 200 seconds, gave smooth, continuous films of a reproducible thickness as evidenced by their cyclic voltammograms.

Comparison of the peak anodic currents from the cyclic voltammograms of films prepared in this manner to those published by Diaz confirmed that the films were approximately 50-100 nm thick[30]. Diaz *et al*[25] determined that current densities of 8 mC cm^{-2} during the polymerization created a film ≈20 nm thick. This work employed a density of ≈16 mC cm^{-2}, with an approximate electrode area of 0.75 cm^{-2}. Absolute film thickness is unimportant as long as it is reproducible and less than the maximum thickness that can be

switched. The films prepared in this manner were used for the characterization of the oxidized and reduced forms by Raman spectroscopy.

6.0 RAMAN SPECTROSCOPY OF SWITCHABLE FILMS

6.1 EXPERIMENTAL

Films were prepared according to the method stated in the previous section. Prior to Raman characterization, the cell and film were rinsed to remove unreacted monomer and refilled with fresh solvent and electrolyte, taking care to avoid air contamination. The cell was then rinsed with dry deoxygenated acetonitrile, followed by filling with deoxygenated acetonitrile/0.1M $TEABF_4$. The reference electrode, and Luggin capillary are then placed in the cell and the appropriate potential applied to the film by way of the computer interface. The film remains potentiostated at the selected potential for 5 to 10 minutes prior to the Raman scan. All potentials stated were versus the sodium saturated calomel electrode (SSCE). Slight adjustments were made to the image of the laser spot on the film after disturbing the cell.

Raman scans were performed over the range $800cm^{-1}$ to $1800cm^{-1}$ at a 120 cm^{-1}/min. scan rate and a 1 second integration time (photon counting mode). The slit settings were chosen to yield 2 cm^{-1} resolution for the particular laser line (e.g. 146 microns at 488.0 nm). The broad bands associated with

amorphous polymers obviated the need for higher resolution scans. Care was taken to prevent photo-induced damage to the film from exposure to high laser powers, especially in the reduced films, where absorption isthe strongest. Typical laser power levels were 30 to 50 mW at the cell as determined by a Spectra-Physics Model 404 power meter. It was found that approximately 30% of the laser power at the head was delivered to the cell compartment.

Each spectra was labeled with the pulses per second full scale (PPS FS) and only for 1000 (1K) PPS FS does the y-axis indicate the absolute photon counts acquired. The y-axis reflects the percentage of full scale counts acquired at settings other than 1K PPS FS. Thus the spectra in Figure 18 was acquired at -250 mV vs. SSCE and 2K PPS FS. The large peak at 1550cm^{-1} is approximately 500 on the y-axis, or 50% of full scale, and represents 1000 counts.

6.2 RESULTS

The Raman spectra of the "as-grown" films of PP, PNMP, and PNPP are shown in Figures 13 through 15 respectively. The spectra of PP and PNMP compare favorably with those published by Kanazawa *et al*[54] for oxidized, free-standing films. The comparison indicates that the films are produced in the partially oxidized state. The one notable difference is the

absence of the band at ≈1200cm^{-1} in Kanazawa's spectrum of PNMP.

The outstanding feature of all three spectra is the band at ≈1600cm^{-1}. The 1200-1500cm^{-1} region is cluttered with poorly resolved peaks and a solvent band at ≈1375cm^{-1}. It is in the 900-1200cm^{-1} region that the spectra for the three films are noticeably different. The spectrum of PP has a set of three weak peaks centered about 1000cm^{-1}. The spectrum of PNMP has a peak of moderate strength at 1175cm^{-1}. The spectrum of PNPP has peaks similar to both PP and PNMP with a peak at ≈1200cm^{-1} and a set of poorly resolved peaks at 1000cm^{-1}. The bands at 1000cm^{-1} may be associated with the phenyl substituent and not the pyrrole moiety. This is the first known reported Raman spectrum of the "as-grown" film of PNPP.

The spectra for a PP film subjected to different oxidation and reduction potentials are shown in Figures 16 through 22. They are presented in order, from the most oxidized to the most reduced, for discussion purposes only and were acquired in the opposite manner. The 514.5 nm laser line was used at an incident power of 30 mW. A cyclic voltammogram of PP is provided in Figure 23.

For the following discussion, it is helpful to arrange the spectra into three categories: oxidized, partially oxidized

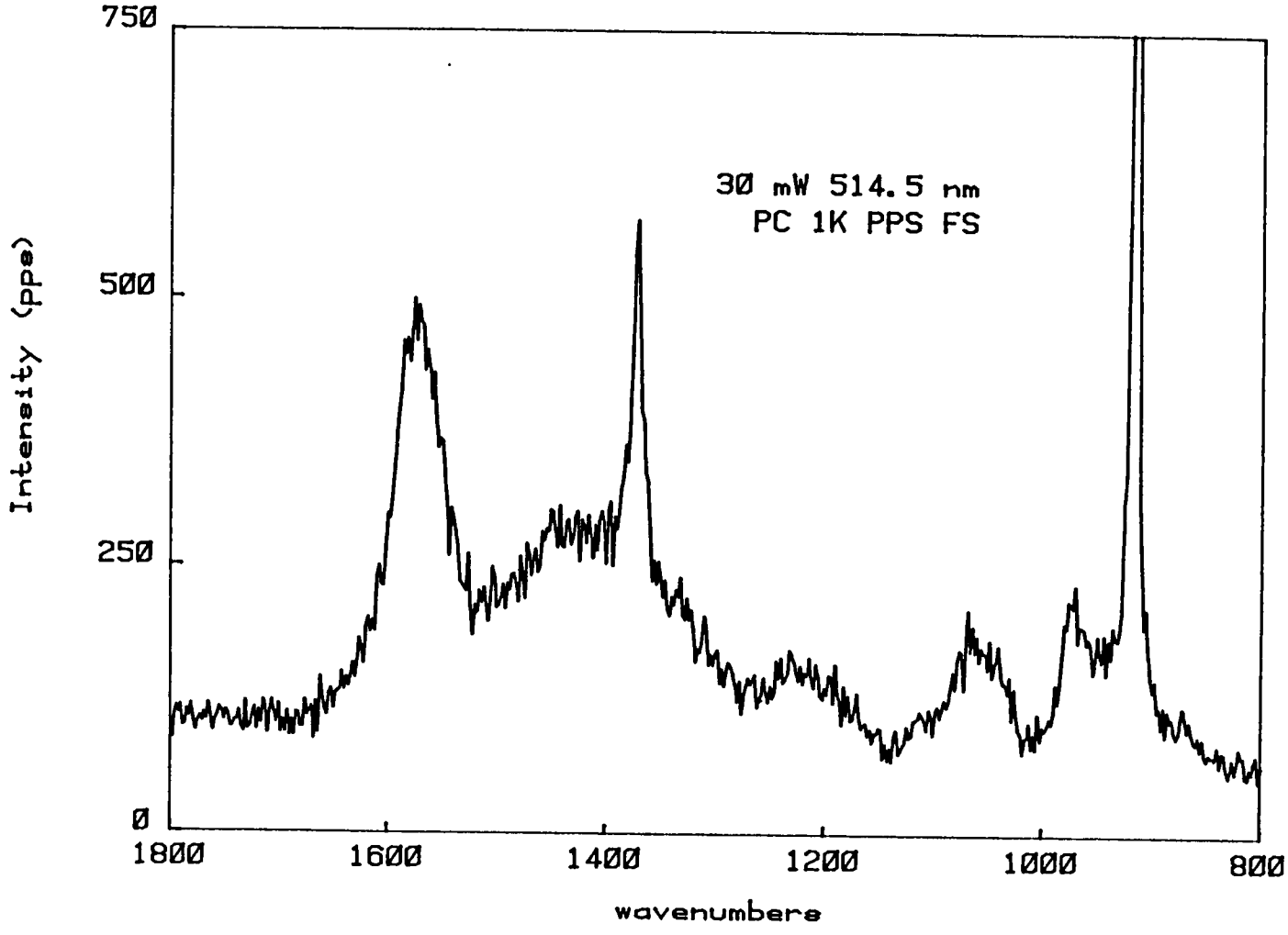

Figure 13. Raman spectrum of as-grown Polypyrrole.

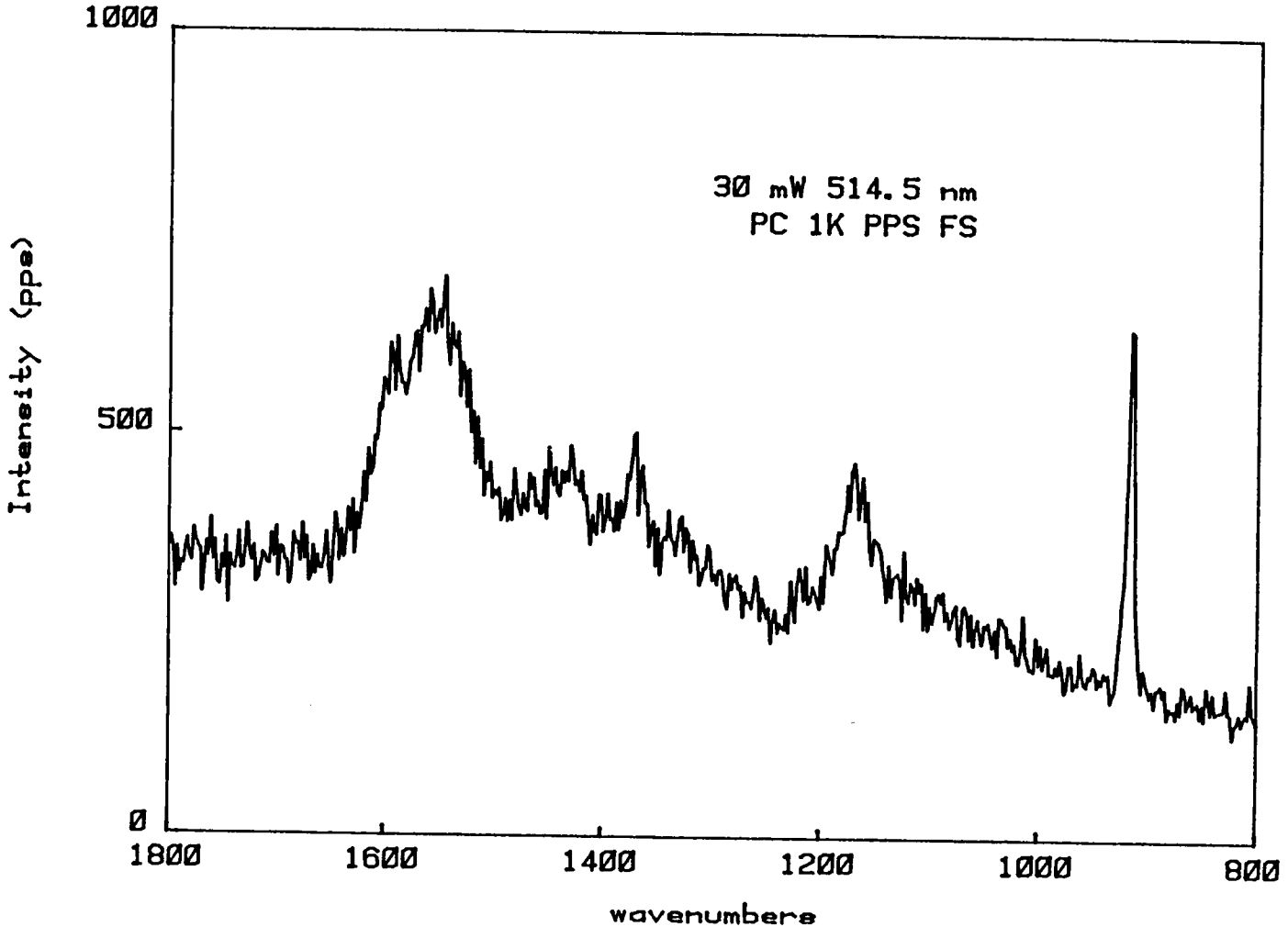

Figure 14. Raman spectrum of as-grown PNMP.

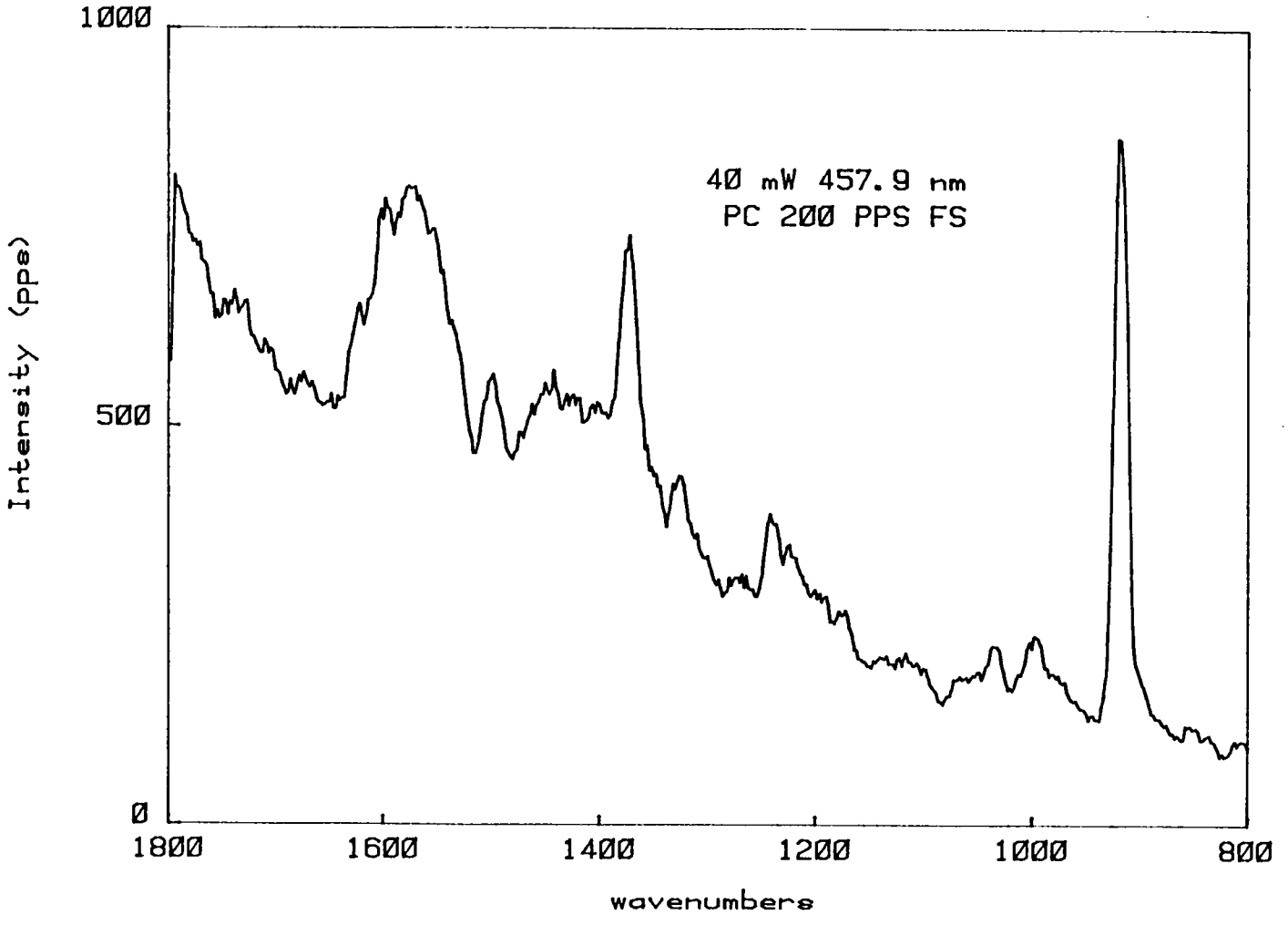

Figure 15. Raman spectrum of as-grown PNPP.

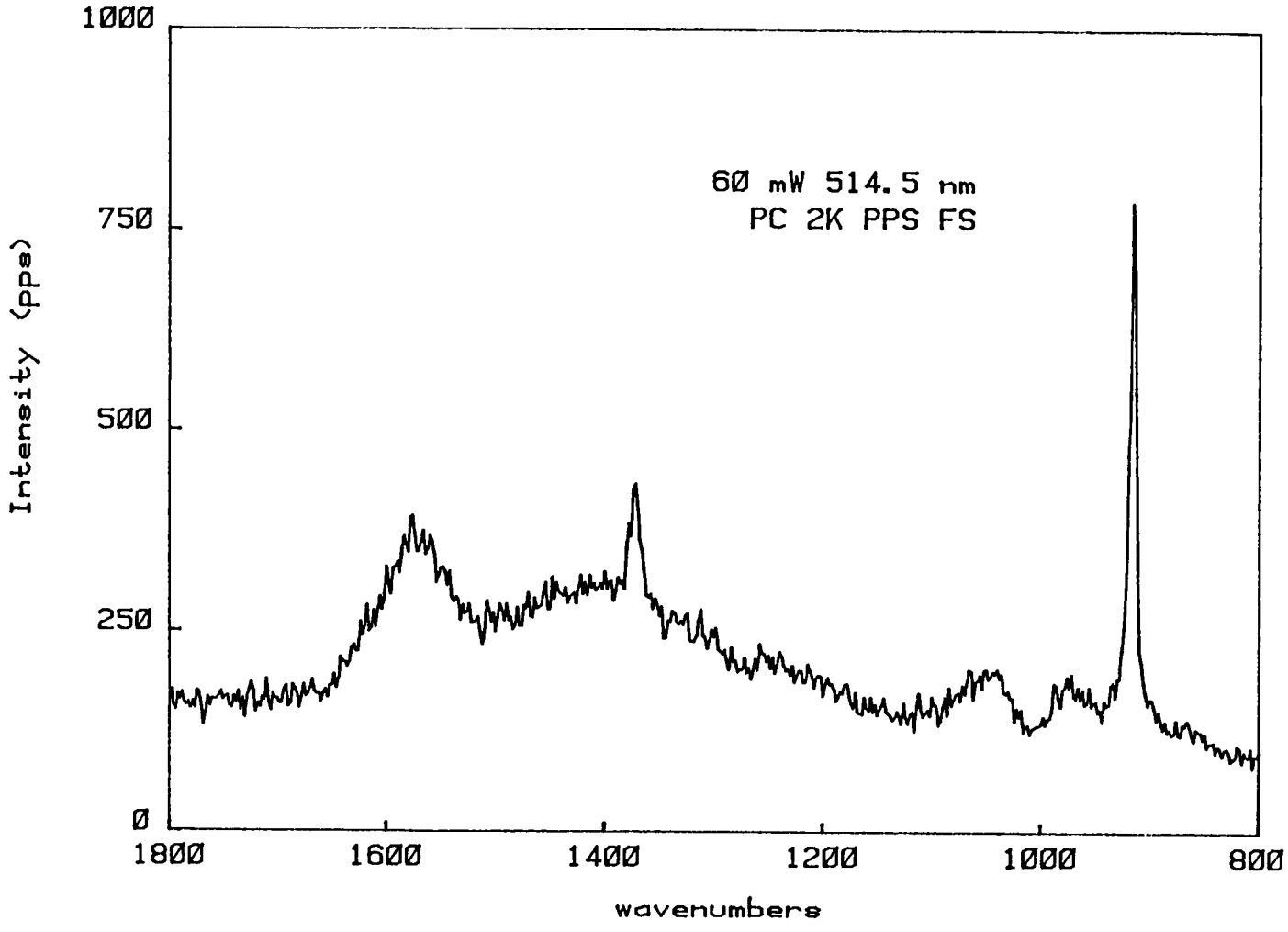

Figure 16. Raman spectrum of oxidized PP: E(applied)= +250 mV vs. SSCE.

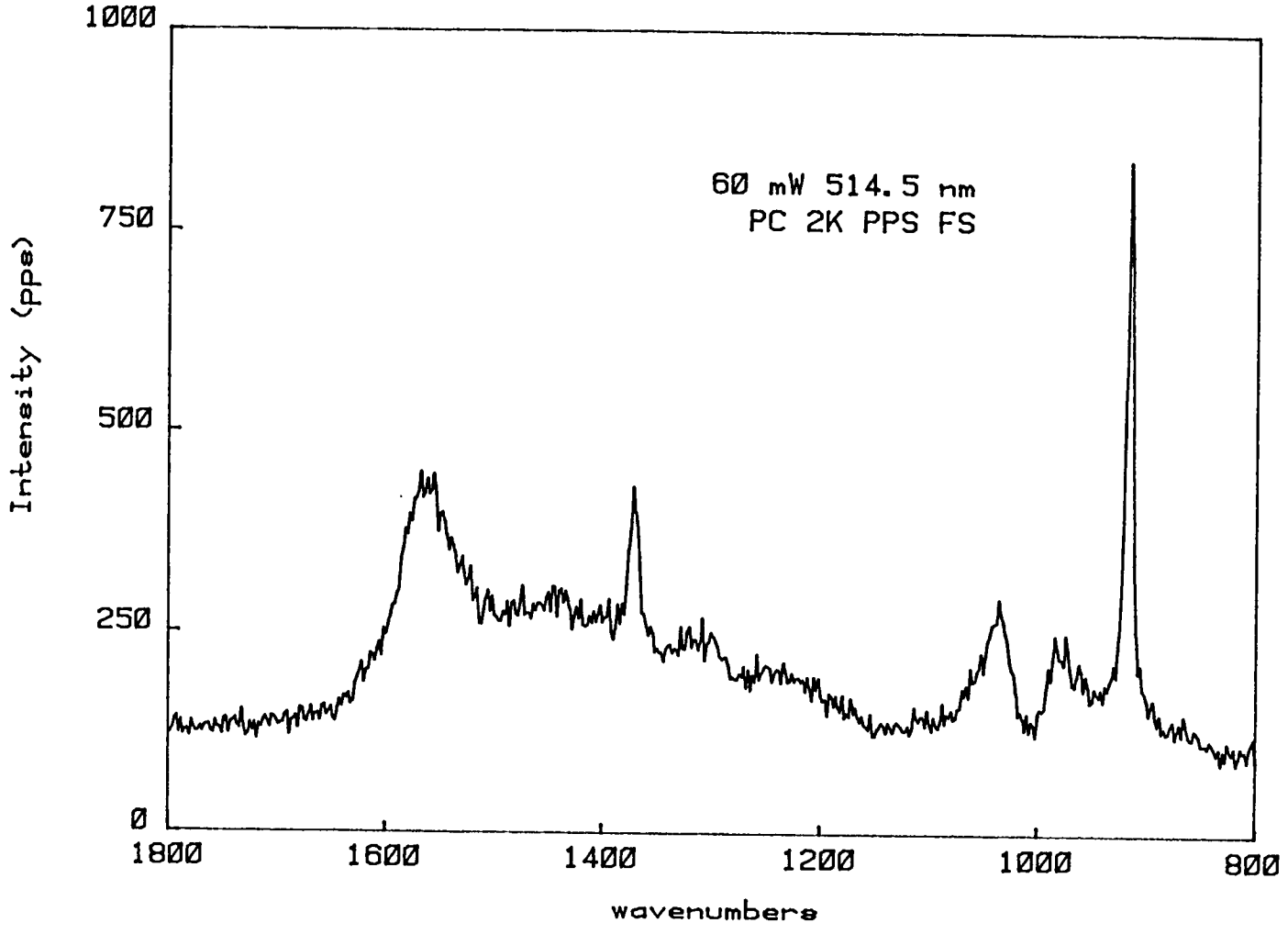

Figure 17. Raman spectrum of oxidized PP: E(applied)= -125 mV vs. SSCE.

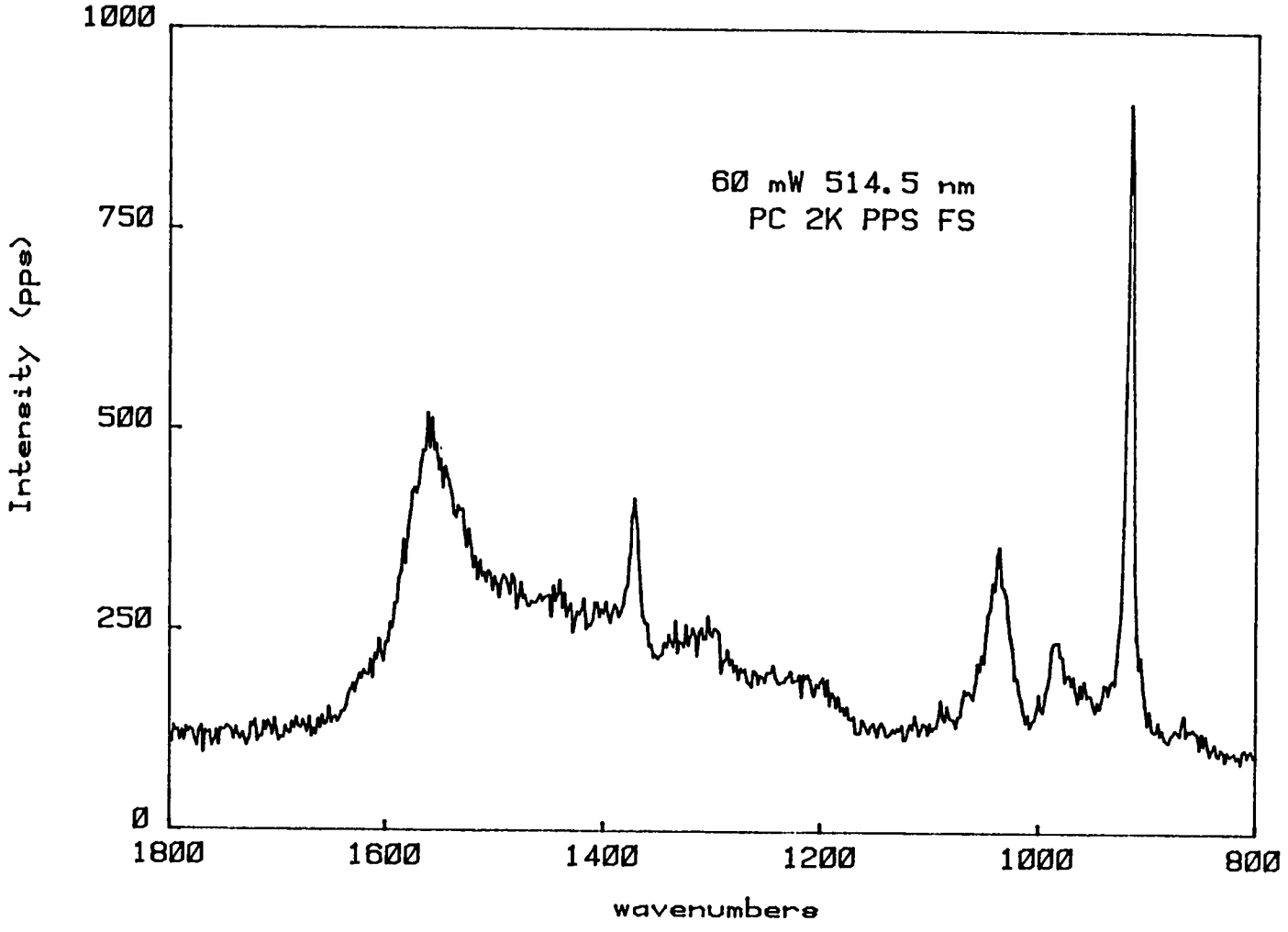

Figure 18. Raman spectrum of oxidized PP: E(applied)= -250 mV vs. SSCE.

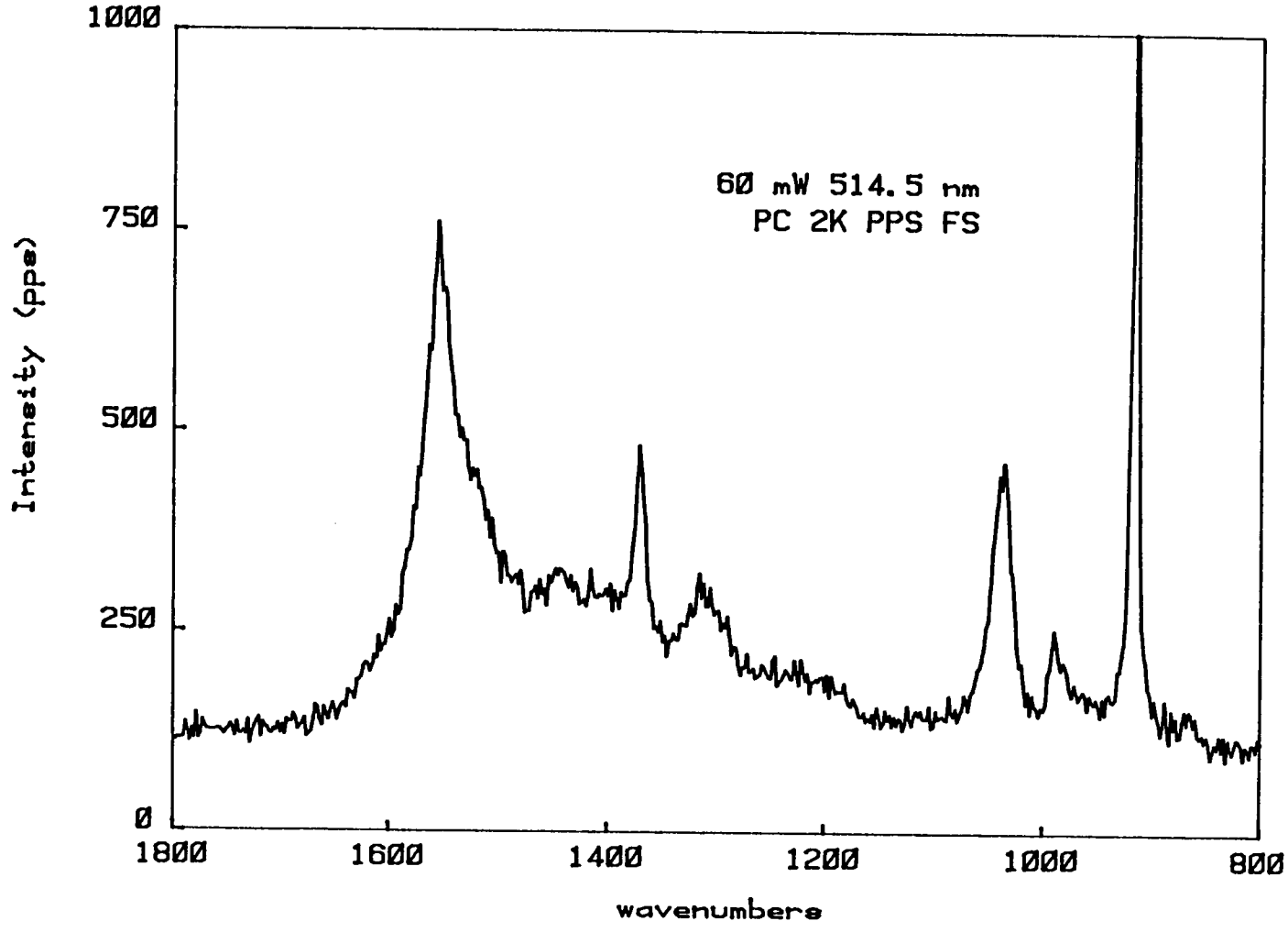

Figure 19. Raman spectrum of reduced PP: E(applied)= -375 mV vs. SSCE.

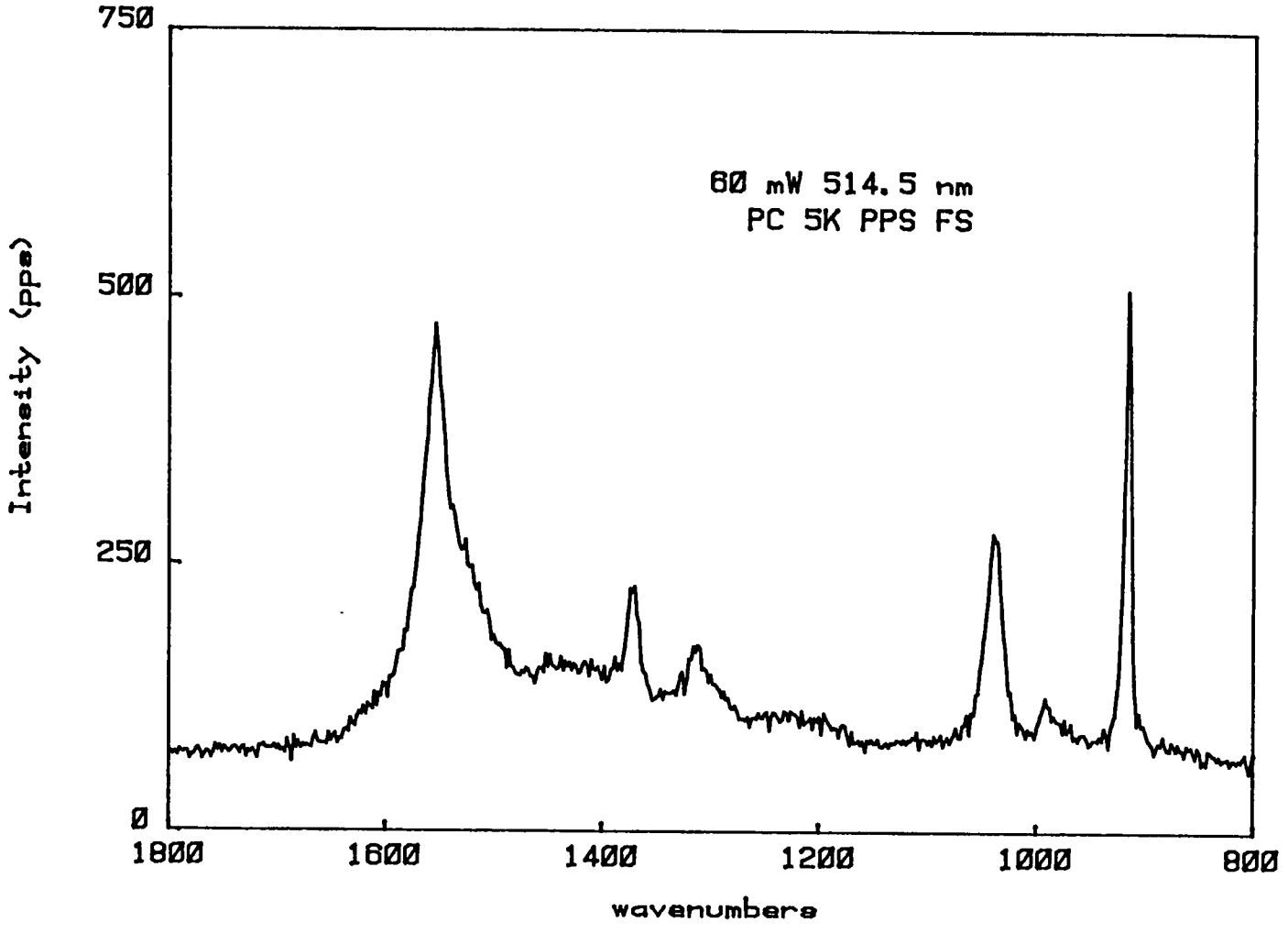

Figure 20. Raman spectrum of reduced PP: E(applied)= -500 mV vs. SSCE.

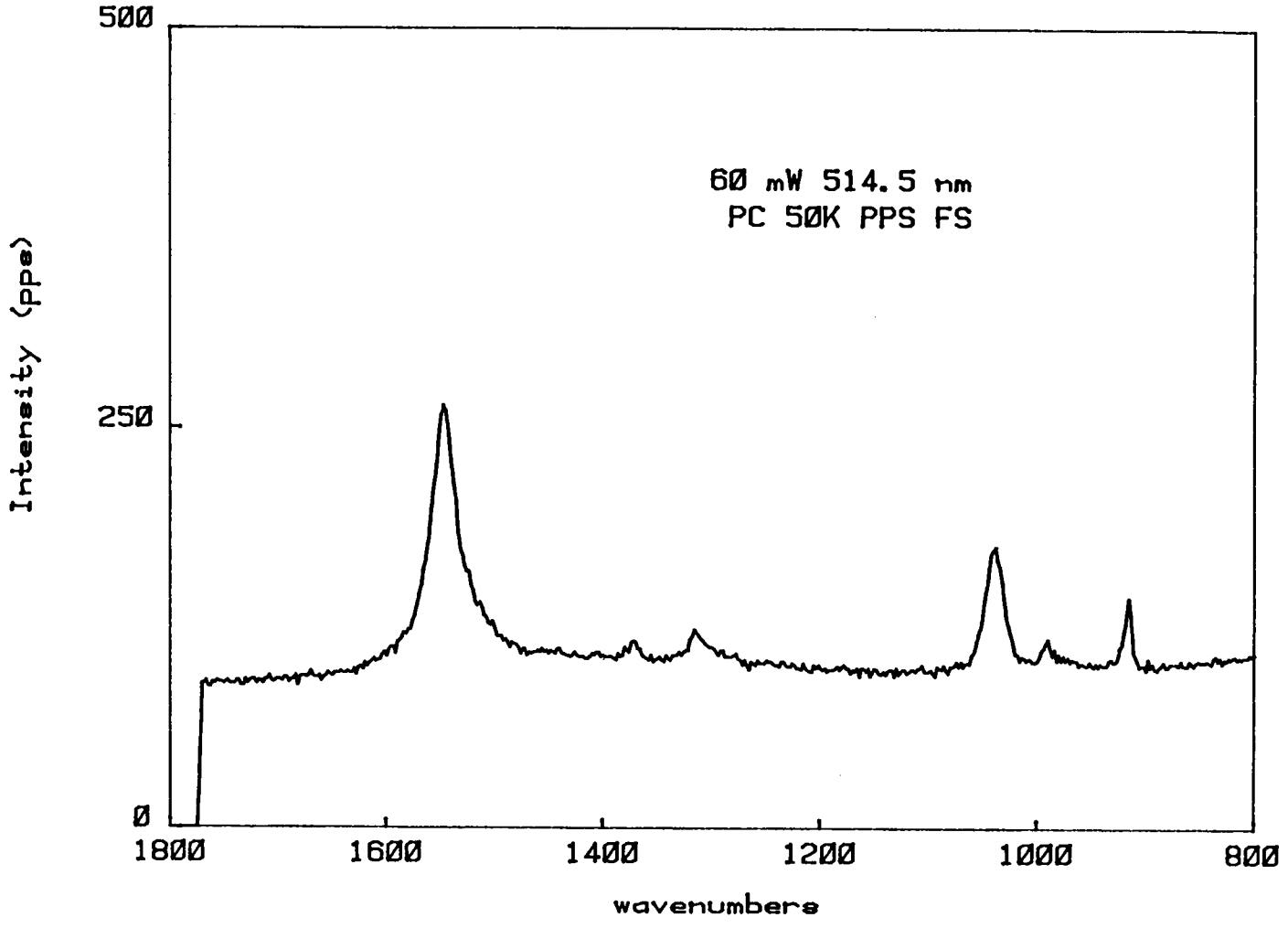

Figure 21. Raman spectrum of reduced PP: E(applied)= -1000 mV vs. SSCE.

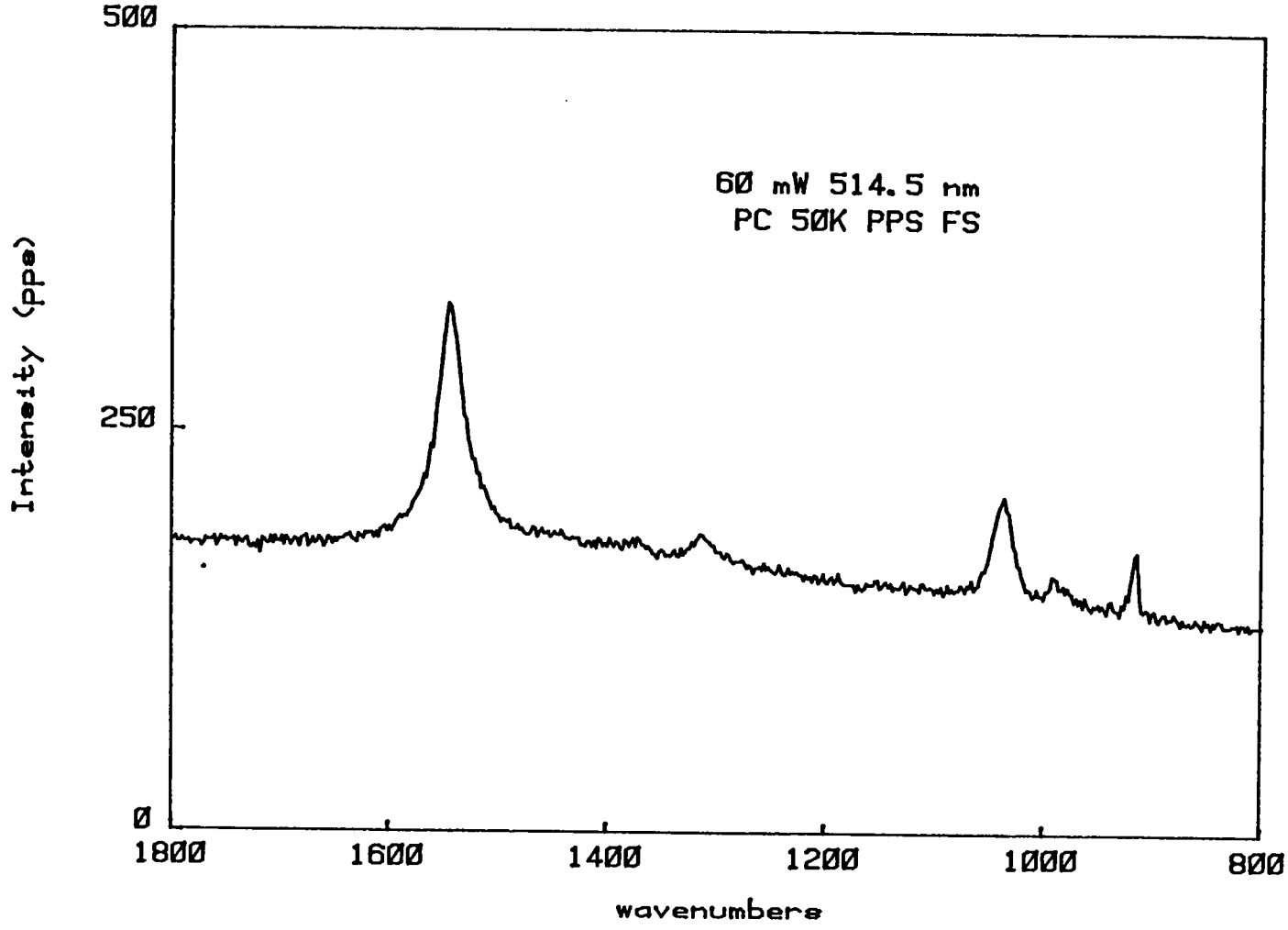

Figure 22. Raman spectrum of reduced PP: E(applied)= -1500 mV vs. SSCE.

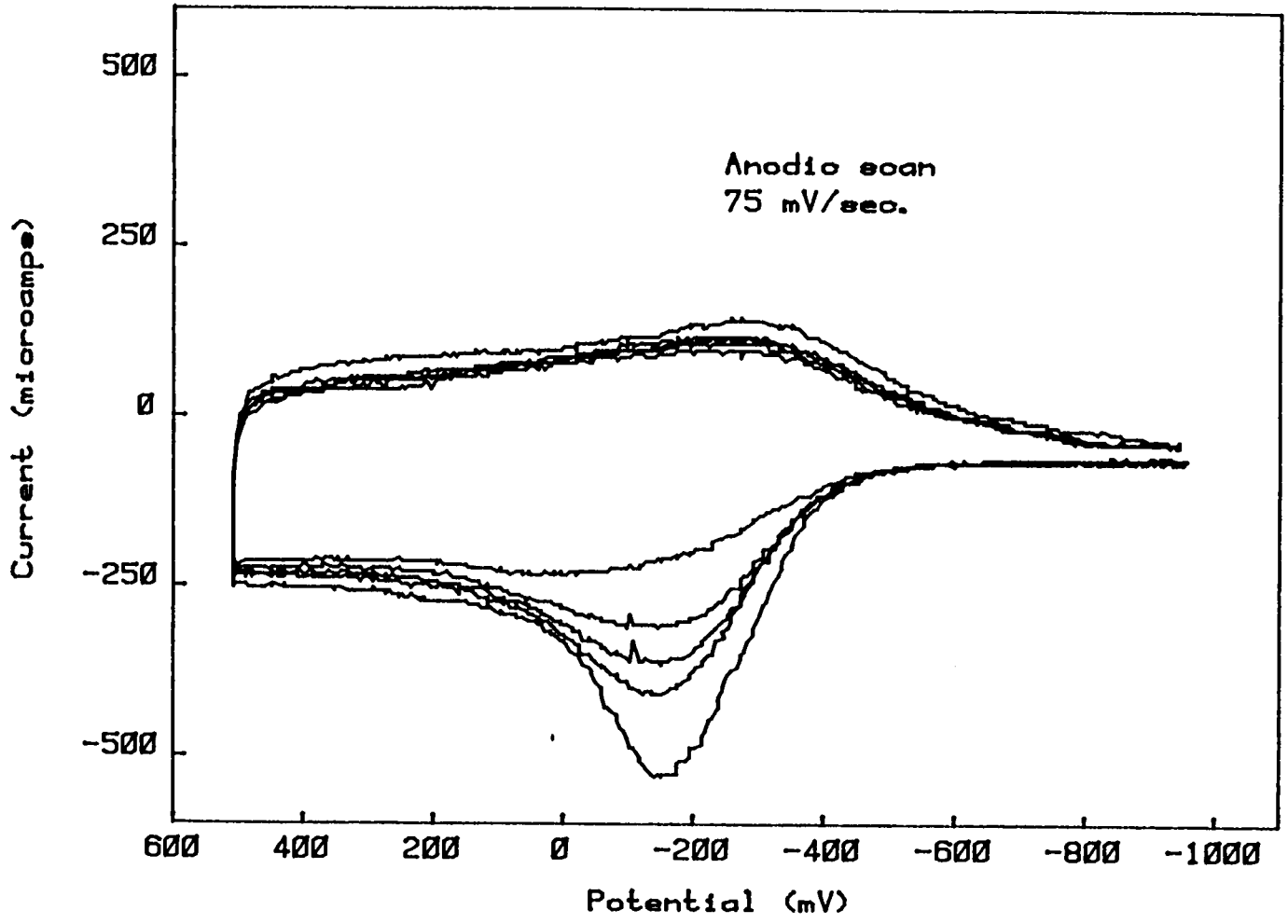

Figure 23. Anodic scans of Polypyrrole on Pt.

(reduced), and reduced. Spectra of oxidized PP were acquired at potentials greater than 0 mV. Those acquired in the potential region from 0 mV to -500 mV were considered characteristic of partially oxidized or reduced film. Spectra of reduced polypyrrole were obtained at potentials less than -500 mV. These divisions were made using the cyclic voltammogram of PP (Figure 23) as a guide.

A distinctive trend is noticeable in the spectra as the film was reduced. The spectra of the oxidized films (Figs.16 and 17) show diminished peak intensities at 1550cm^{-1} and 1040cm^{-1} when compared to the spectrum of the "as-grown" film. As the film is partially reduced at -250 mV (Fig.18), -375 mv (Fig.19), and -500 mV (Fig.20) the intensity and sharpness of these bands increase and the spectra resemble those of the "as-grown" film. Also, as the extent of reduction was increased from -250 mv (Fig.18) to -500 mV (Fig.20) the Raman peaks at ≈1550cm^{-1} and 1050cm^{-1} increased compared to the other bands. The two peaks centered at 1000cm^{-1} have intensity ratios of approximately 1:1 in the oxidized film (Fig.13) and were more near 2:1 in the spectra at -375 mV (Fig.19). Similarly, the weak band at 1550cm^{-1} in the oxidized film (Fig.16) increases dramatically as the film is reduced, and acquires an intensity about twice that of the peak at 1050cm^{-1} in Figure 19.

At the stronger reduction potentials of -1000 mV and -1500 mV the spectra (Figs.21 and 22) acquired another characteristic. The intensity of the baseline in these spectra was greater than in previous scans. The background counts at 1800cm^{-1} in Figure 22 is 10 times that displayed in Figure 20, and 100 times greater than that in Figure 16.

The spectra obtained from a thin switchable film of PNMP acquired at various potentials are presented in Figures 24 through 28. All spectra were acquired using the 488.0 nm laser line. A cyclic voltammogram of PNMP is provided in Figure 29. As with PP, the spectra can be divided into three categories, yet the divisions are shifted some 500 mV anodically due to the difference in the redox chemistry between the films. The oxidized film region is positive of +500 mV, the intermediate region is from 0 mv to +500 mV, and the reductive region is cathodic of 0 mV.

The spectra of PNMP at a strong oxidative potential (Fig. 24) has very weak Raman bands at 1600cm^{-1} and 1175cm^{-1} as compared to the "as-grown" film (Fig. 14). The spectra was acquired at 500 PPS FS and the baseline scatter is quite weak, ≈20% of full scale. Figure 25 shows the spectrum acquired at +500 mV (near the E_0 for the film) which resembles closely the spectrum of the "as-grown" film. The slight reduction has resulted in the increase in the Raman

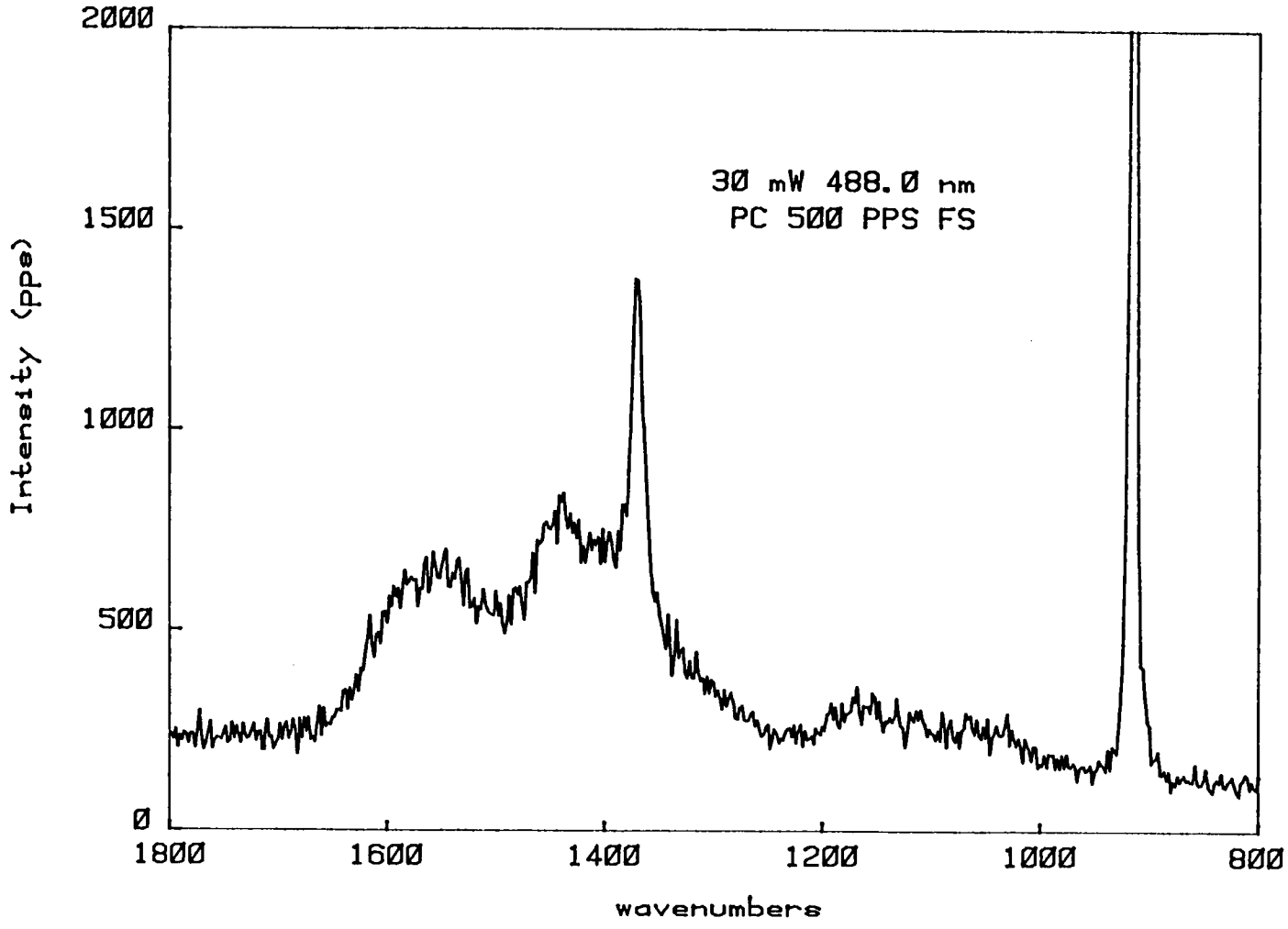

Figure 24. Raman spectrum of oxidized PNMP: E(applied)= +1000 mV vs. SSCE.

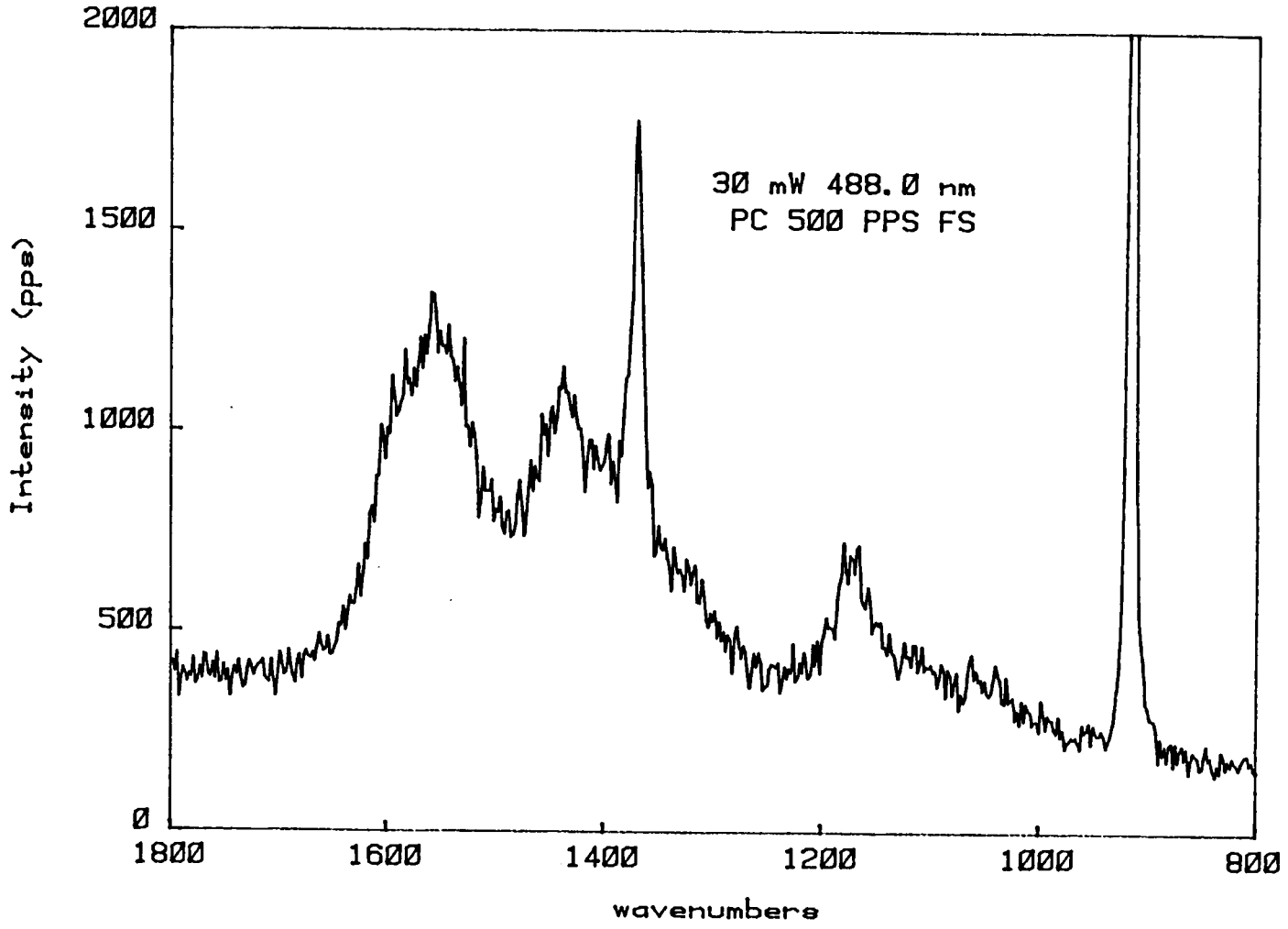

Figure 25. Raman spectrum of oxidized PNMP: E(applied)= +500 mV vs. SSCE.

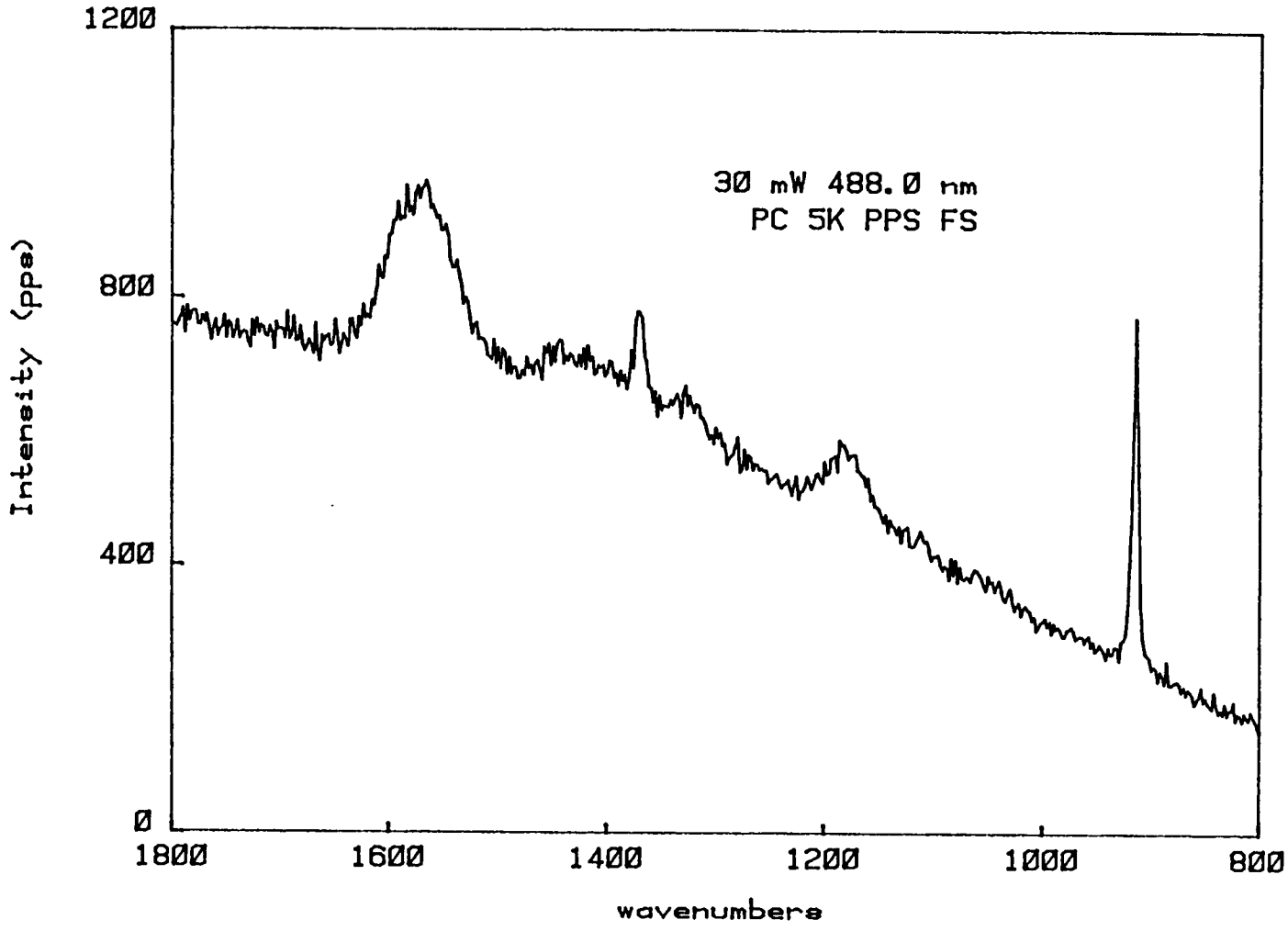

Figure 26. Raman spectrum of reduced PNMP: E(applied)= 0.0 mV vs. SSCE.

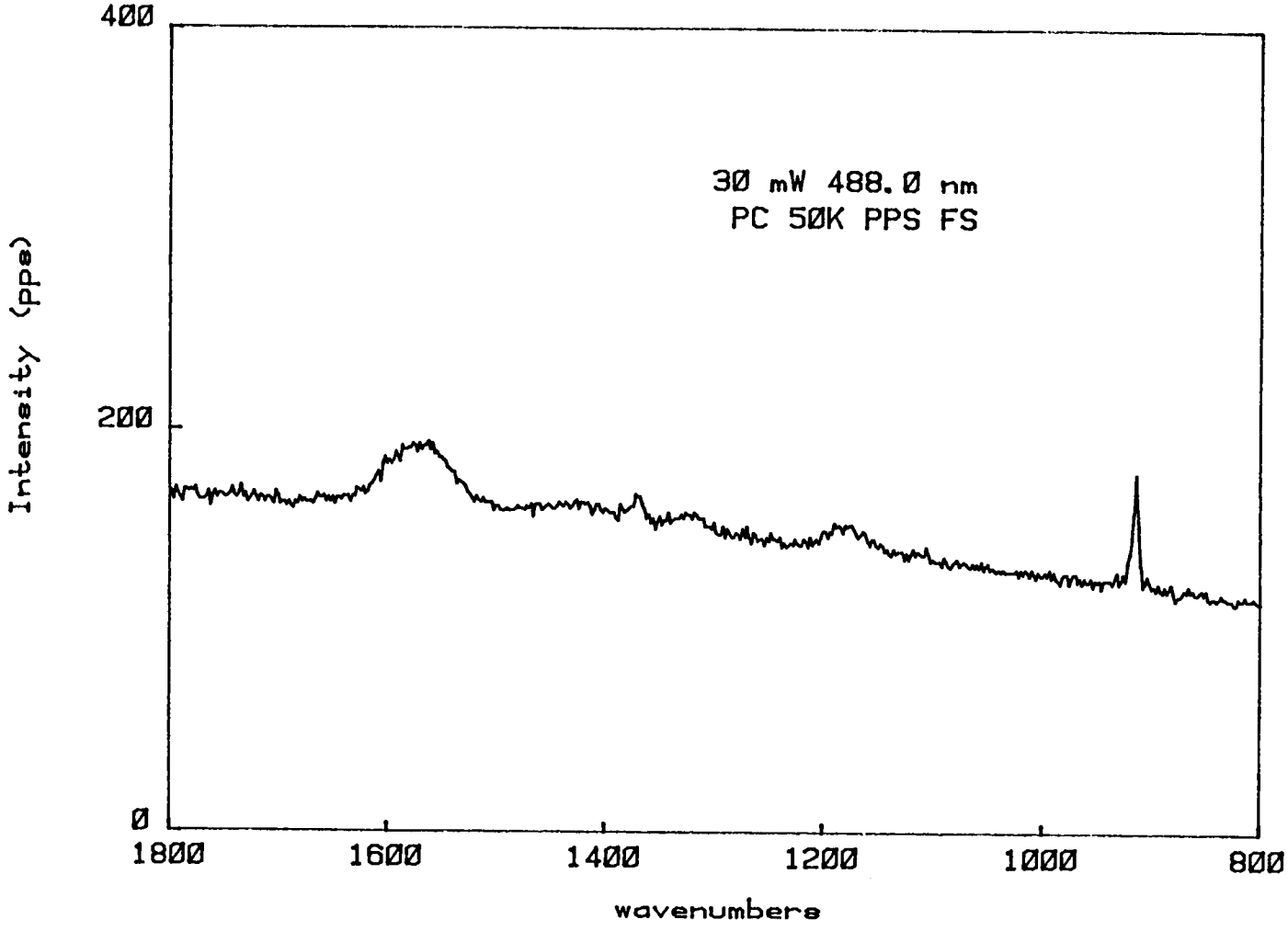

Figure 27. Raman spectrum of reduced PNMP: E(applied)= -500 mV vs. SSCE.

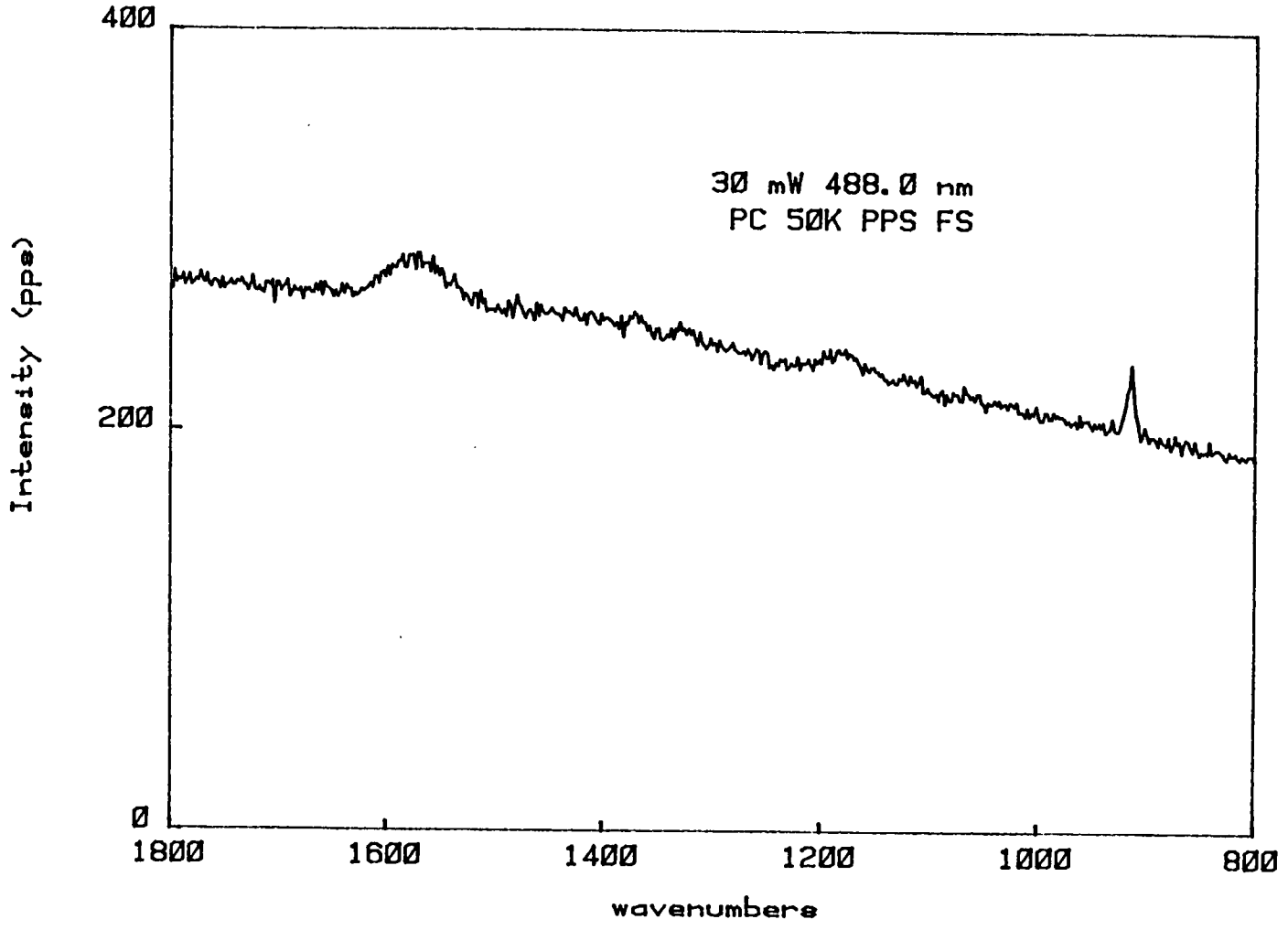

Figure 28. Raman spectrum of reduced PNMP: E(applied)= -1000 mV vs. SSCE.

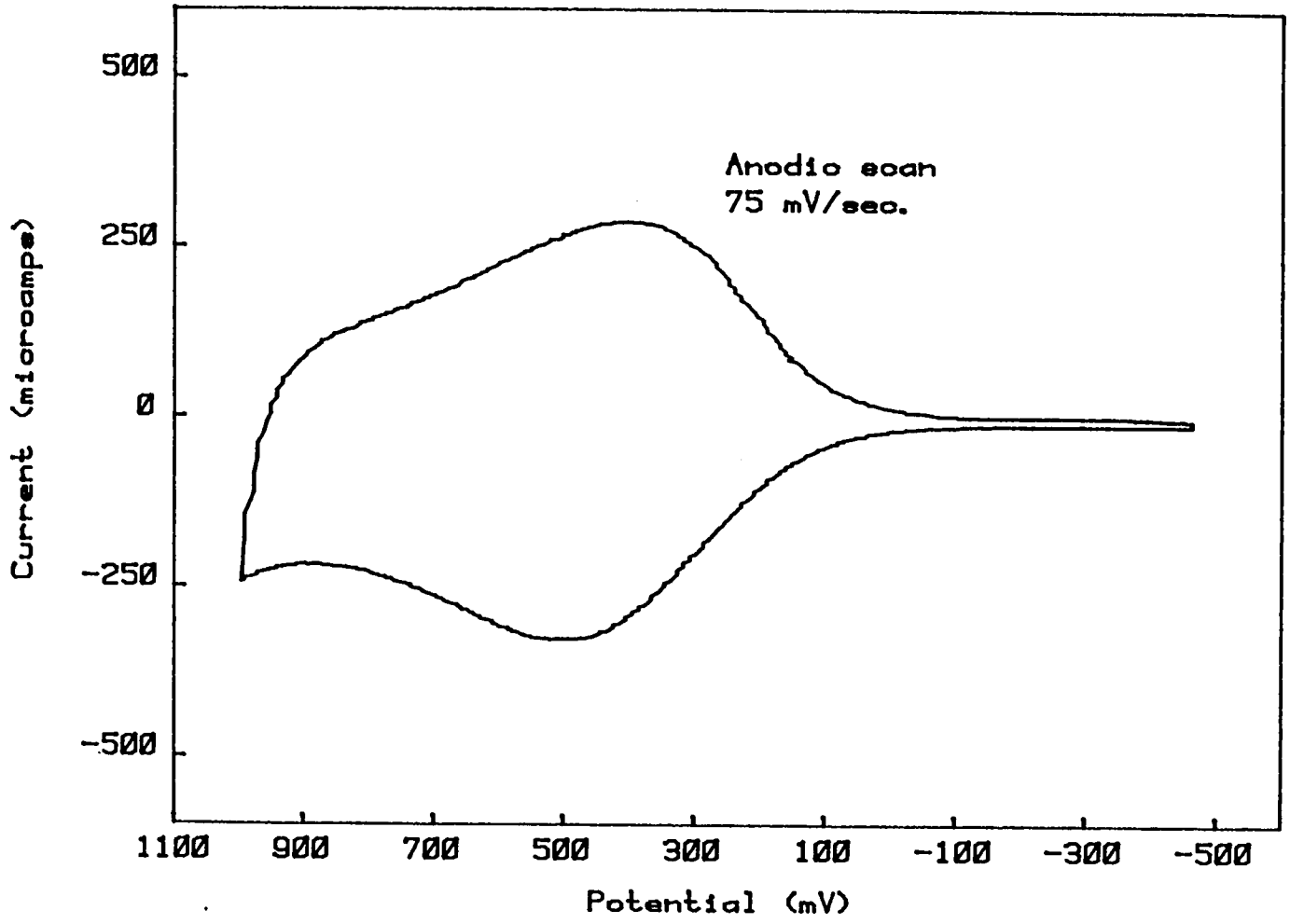

Figure 29. Anodic scan of PNMP on Pt.

intensities of the carbon-carbon stretching frequencies. Upon reduction at 0mV (Fig. 26) the baseline counts increase dramatically (note the sloping baseline and the 10-fold increase in the full scale counts). Baseline scatter at $\approx 1800 cm^{-1}$ is 80% of full scale or 4K counts. Unlike PP° (reduced PP), the Raman bands in the C-C stretching region for PNMP° (reduced PNMP) at intermediate reduction potentials remain weak and broad. At the strong reduction potentials of -500 mV and -1000 mV (Figs. 27 and 28 respectively) the spectra show very little change in the Raman peak intensities when compared to the baseline. However, the baseline scatter has increased markedly. Comparing the spectra at 0 mV, -500 mV, and -1000 mV in the $1800 cm^{-1}$ region, the counts increased from 4000 to 8000 to ≈13,500 respectively.

6.3 DISCUSSION

Several questions arise upon examination of the Raman spectra for the two families of oxidized and reduced films. First, what information does the Raman data yield about the transformation of the film from the oxidized to reduced states. Second, what explanation can be given for the strong Raman signals from PP°? Third, why do the Raman spectra for PNMP° differ so dramatically from PP°? Fourth, what is responsible for the large increase in the background intensity present in spectra of PP° and PNMP°? The answer

to the first two questions requires an understanding of the changes in optical properties that the film undergoes upon oxidation or reduction. Linking these changes to the Raman process provides a suitable explanation.

Examination of the absorption spectrum published for oxidized and reduced PP shows two features[25]. First, the reduced form has a strong absorption in the 400-500 nm region, verified visually from films reduced in this work. The films have a yellow-green color indicative of strong absorption of blue light. Such uv-vis absorption by conjugated π-electron systems involves a $\pi \rightarrow \pi^*$ transition between the Highest Occupied Molecular Orbital (HOMO) and the Lowest Unoccupied Molecular Orbital (LUMO). Second, the oxidized form has reduced absorption in the 400-500 nm area and increased absorption of red light. This was confirmed visually. This change can be attributed to the creation of low energy transitions resulting from the loss of one π-electron from the HOMO.

How does this effect the Raman process? Excitation is accomplished with blue-green laser light within the absorption band of the reduced form of the film. The stretching frequencies most affected and most enhanced by the resonance Raman process are those that are related to the absoption process. Since the absorption involves the

π-electrons of the carbon-carbon backbone, it follows that the C-C stretching frequency intensities, both single and double bond, will be enhanced when there is significant absorption by the film. The Raman bands at 1550cm^{-1} and 1040cm^{-1} in the reduced film of PP are resonance enhanced by the process just described. This has been shown to be true for polyacetylene (PA), another system of conjugated double bonds[51]. PA yields remarkably similar Raman spectra, as noted in Chapter 3. Oxidation reduces absorption at the blue-green wavelengths. Thus all Raman spectra of oxidized films suffer from weak intensities of the carbon-carbon stretches due to a lack of resonance enhancement.

It follows from the previous discussion that the absence of Resonance enhanced bands, like those present in the spectra of PNMP° could be attributable to reduced absorption at the chosen excitation wavelengths. Currently, absorption spectra of the reduced and oxidized forms of PNMP do not exist. However, visual inspection of the transformation is one from a copper-brown oxidized form to one of a pale yellow, reduced film. The fact is that PNMP° yields poor Raman spectra at the same wavelengths of excitation that yield excellent spectra in PP°. This suggests a difference in conjugation between the two films because aborption is directly related to conjugation. Diaz et al[28] have speculated that PNMP is

less conjugated than PP due to the steric effects of the methyl substituent.

Finally, both PP° and PNMP° exhibit strong, featureless background signals not present in their oxidized counterparts. This is due to the creation of a luminescing species, probably a reduced, conjugated segment within the chain, as a result of the reduction of the film. The fluorescence of reduced films will be covered in the following chapter. It is not unusual for conjugated π-electron systems to fluoresce, and similar results have been reported for polyparaphenylene[55] and polyacetylene[56].

6.4 CONCLUSION

Raman spectra of the "as-grown" films of PP, PNMP, and PNPP confirm the formation of the film in the oxidized state. Reduced films of PP gave excellent resonance Raman spectra on top of a photoluminescent background, while oxidized films yielded spectra with weak Raman bands. The oxidation process in heteroaromatic chain polymers involves homogeneous charge extraction from the π-electron system. The two strongest bands in the spectra for PP° are assigned to the carbon-carbon stretches, double and single bond, respectively. These bands are quite similar to those reported for polyacetylene and can be used in a similar

fashion for the determination of the exact conjugation lengths present in PP[51].

The spectra for PNMP° exhibit little resonance enhancement and are accompanied by a strong photoluminescence background. The fluorescence background is sensitive to the applied reduction potential and is nonexistent in the spectra of the oxidized film. The poor quality of the Raman spectra for PNMP° suggests that the extent of conjugation is different from that present in PP° It is difficult to state whether the potential dependence associated with the photoluminescence is due to an increase in polymer absorption or attributable to a conformational change within the chain that effectively increases the quantum efficiency of the luminescing moiety.

7.0 CONJUGATION AND LUMINESCENCE STUDIES OF PP AND PNMP

7.1 OVERVIEW

The strong resonance Raman spectra of PP° and the luminescence of reduced films of PP and PNMP were studied further, and the results are presented in the following two parts. In Part A, the dependence of the C=C stretching frequency ($\bar{\nu}_2$) on the wavelength of excitation and the reduction potential are examined. These data will be useful in determining the extent of conjugation and the distribution of conjugation lengths in PP and PNMP. Part B will characterize the photoluminescence of PP° and PNMP° as a function of excitation wavelength and reduction potential.

7.2 EXPERIMENTAL - PARTS A AND B

Films of PP and PNMP were synthesized as stated in Chapter 5, Film Preparation Methodology. All films were reduced for 10 to 15 minutes prior to the acquisition of the Raman spectra. PP films were characterized at three reduction potentials -500 mV, -1000 mV, and -1500 mv vs. SSCE. The films were uniformly light yellow-green at these potentials. An attempt was made, when possible, to use equivalent output powers for all excitation lines.

For Part A, Raman spectra of the C=C stretching frequency at ≈1550cm^{-1} for PP and ≈1575cm^{-1} for PNMP were acquired in the region of 1475cm^{-1} to 1625cm^{-1} at 1.0cm^{-1} resolution. Scan rates were 30 $cm^{-1}min.^{-1}$ to 60 $cm^{-1}min.^{-1}$ as noted in the results section for each spectra.

Acquisition of the spectra for Part B involving the region from 500cm^{-1} to 4000cm^{-1}(or 6000cm^{-1} in the case of PNPP), were accomplished with 5cm^{-1} resolution at scan rates of 300 $cm^{-1}min.^{-1}$. These wide scans were effective for characterization of the broad luminescence associated with the reduced films. Spectra were obtained for PP, PNMP, and PNPP.

7.3 RESULTS- PART A

Figure 30 contains the results of the characterization of the C=C strtetching frequency as a function of excitation wavelength and reduction potential. A total of nine scans were obtained at 3 different reduction potentials and 3 excitation wavelenghts. The spectra in Figure 30 are arranged in frames according to the applied reduction potential. Values of the C=C stretching frequency are presented in Table 3.

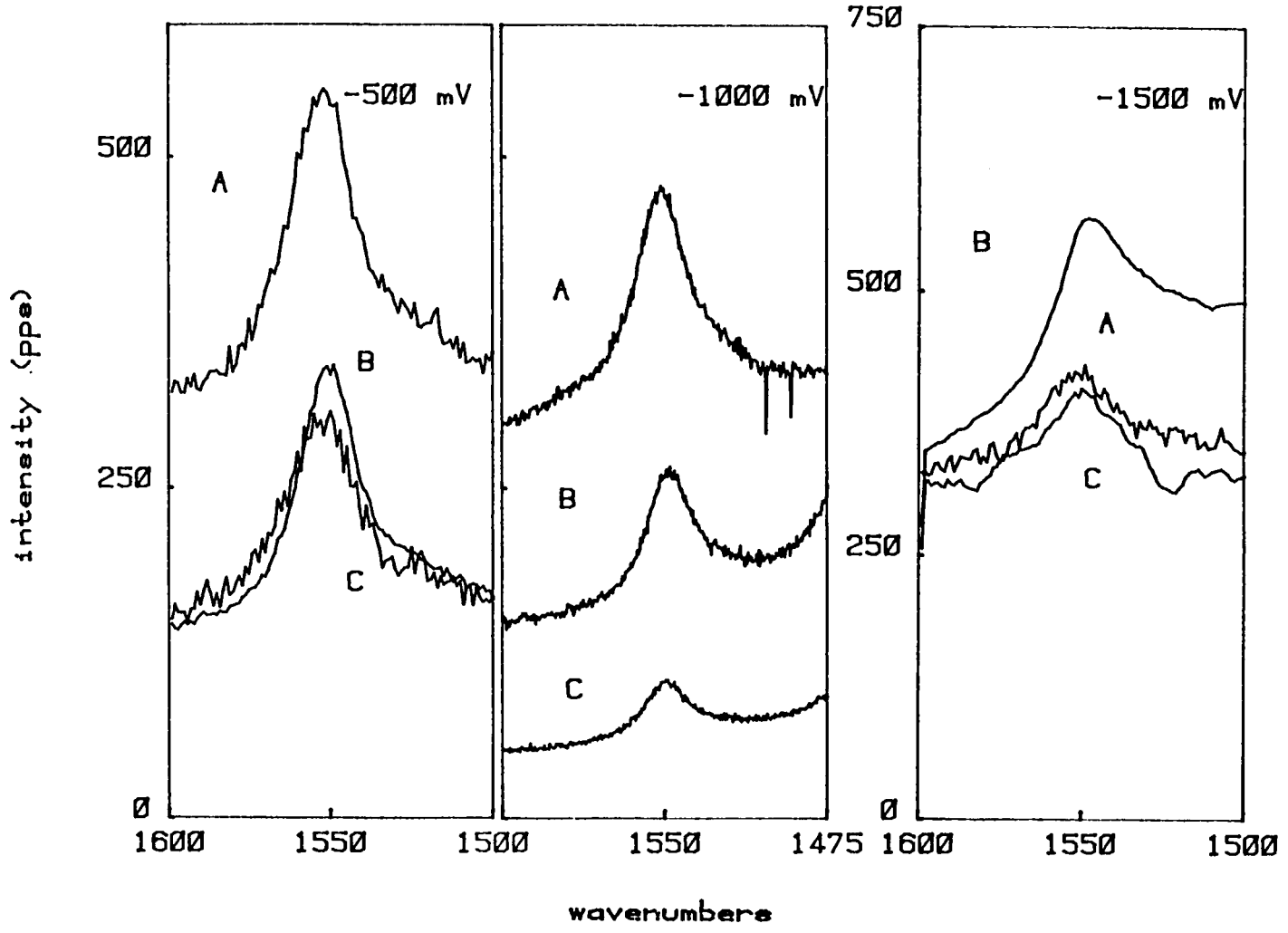

Figure 30. Raman spectrum of reduced PP:
A: 454.5 nm B: 488.0 nm C: 514.5 nm.

Table 3. Experimentally observed $\bar{\nu}_2$ values for PP.

	$\bar{\nu}_2$ (cm^{-1})		
λ(ex)	E(applied) (mV)		
(nm)	-500	-1000	-1500
454.5	1553	1553	1553
488.0	1551	1548	1548
514.5	1553	1550	1548

The left frame contains three scans acquired at the weakest reduction potential (-500 mV). There is no noticeable shift in the peak position as the excitation wavelength is changed from blue to green. The peak labeled A is of greater intensity due to the increased luminescence with the violet (454.5 nm) excitation wavelength. The lack of change is indicative of a narrow distribution of conjugation lengths within the polymer chain.

The middle frame contains spectra acquired at a scan rate of 30 $cm^{-1}min.^{-1}$ and give a good indication of the symmetry of the C=C stretch. Asymmetric Raman band profiles would be indicative of a complex resonance Raman process resulting from a wide distribution of conjugation lengths and has been reported in resonance Raman spectra of PA[4,8]. More specifically, the tailing of the C=C band towards low energy (reduced wavenumbers) is a result of Raman scatter from conjugation lengths slightly off resonance at this excitation wavelength. There is a barely perceptible tail in the peaks obtained at -1000 mV, using the 454.5 nm laser line which is suggestive of a narrow distribution of conjugation lengths in PP.

At the strongest reduction potential, -1500 mV, only a slight decrease is seen in the C=C stretching frequency as the excitation wavelength is red-shifted. This can be seen in

column 3 of Table 3. Yakushi et al[37] states that the stronger reduction potentials reduce cations of longer conjugated segments. These segments contain conjugated double bonds whose stretching vibration is resonantly enhanced at longer excitation wavelengths. The frequency of the C=C stretch is also decreased indicative of a weaker bond for a more conjugated system.

The spectra are rearranged in Figure 31 according to excitation wavelength. The right frame contains the data obtained with the 514.5 nm line and shows a slight trend to decreased C=C stretching frequency as the reduction potential is increased. The values for the C=C stretches are in row 3 of table 1 and support the production of longer conjugated reduced segments at the stronger reduction potentials. The C=C stretching frequency decreases as the reduction potential increases.

Figure 32 has data obtained from another PP film, and the right frame shows the C=C stretch in PP° before and after oxidation at +250 mV for 10 minutes. The spectra were acquired with the 488.0 nm line and at an applied potential of -1000 mV. Oxidation of the film for prolonged periods did not effect the position of the C=C stretch significantly. Therefore the extent of conjugation is not subject to

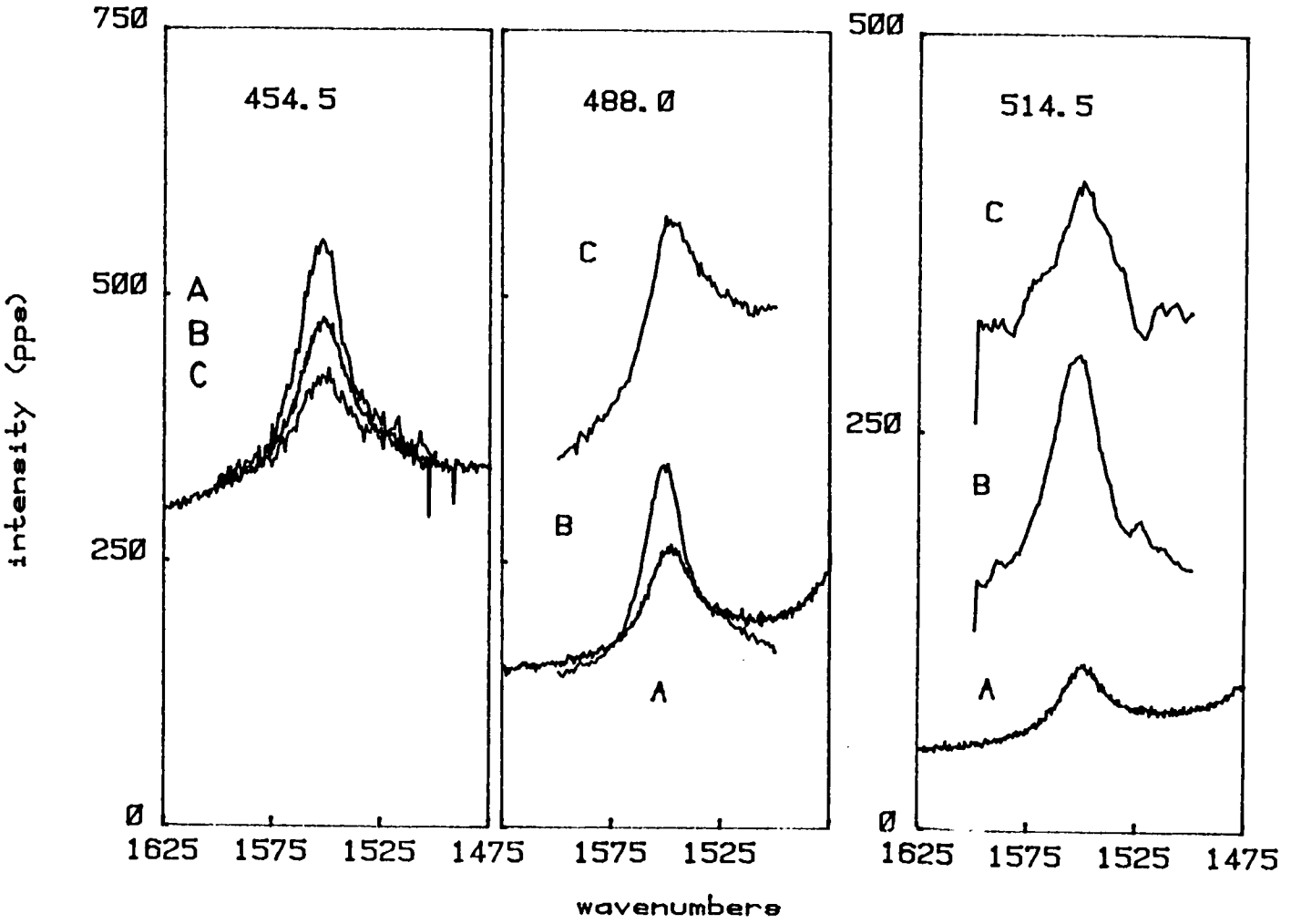

Figure 31. Raman spectrum of reduced PP:
A: -500 mV B: -1000 mV C: -1500 mV.

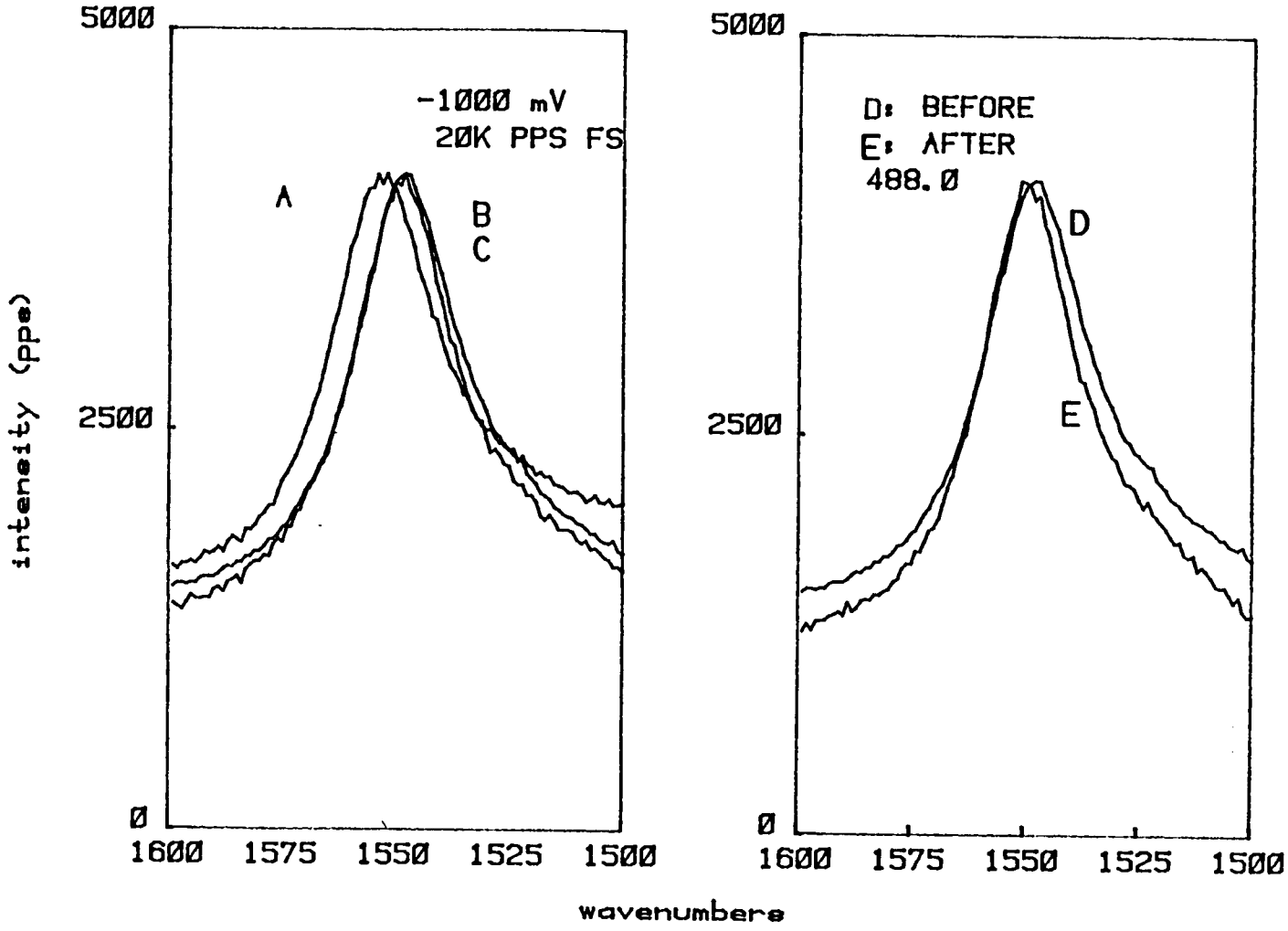

Figure 32. Raman spectrum of reduced PP: before and after oxidation.

modification by electrochemical oxidation for prolonged periods of time. The oxidized form of PP is stable.

The results of conjugation studies for PNMP° are presented in Figure 33 and Table 4. PNMP° is more difficult to characterize by this method due to the poor quality of the resonance Raman spectra and the large luminescence background. For that reason only the lower reduction potentials yield a sufficiently resolveable peak to warrant analysis here. As can be seen in Figure 33 the C=C stretching frequency was greater than that of PP by $\approx 20cm^{-1}$. This decreases slightly when the excitation wavelength is red shifted. The shift is slightly larger than that of PP ($10cm^{-1}$ as compared to $5cm^{-1}$).

7.4 CONCLUSION - PART A

The value of n, the conjugation sequence length, can be calculated from the measured C=C stretching frequencies using the equation developed by Baruya, Gerrard, and Maddams[50]. Figure 34 is a plot of $\bar{\nu}_2$ as a function of N (the conjugation sequence length) using the equations listed in Table 2 from Chapter 3. It is provided as a reference for the following analysis. The results of these calculations are presented in Table 5 for PP and Table 6 for PNMP.

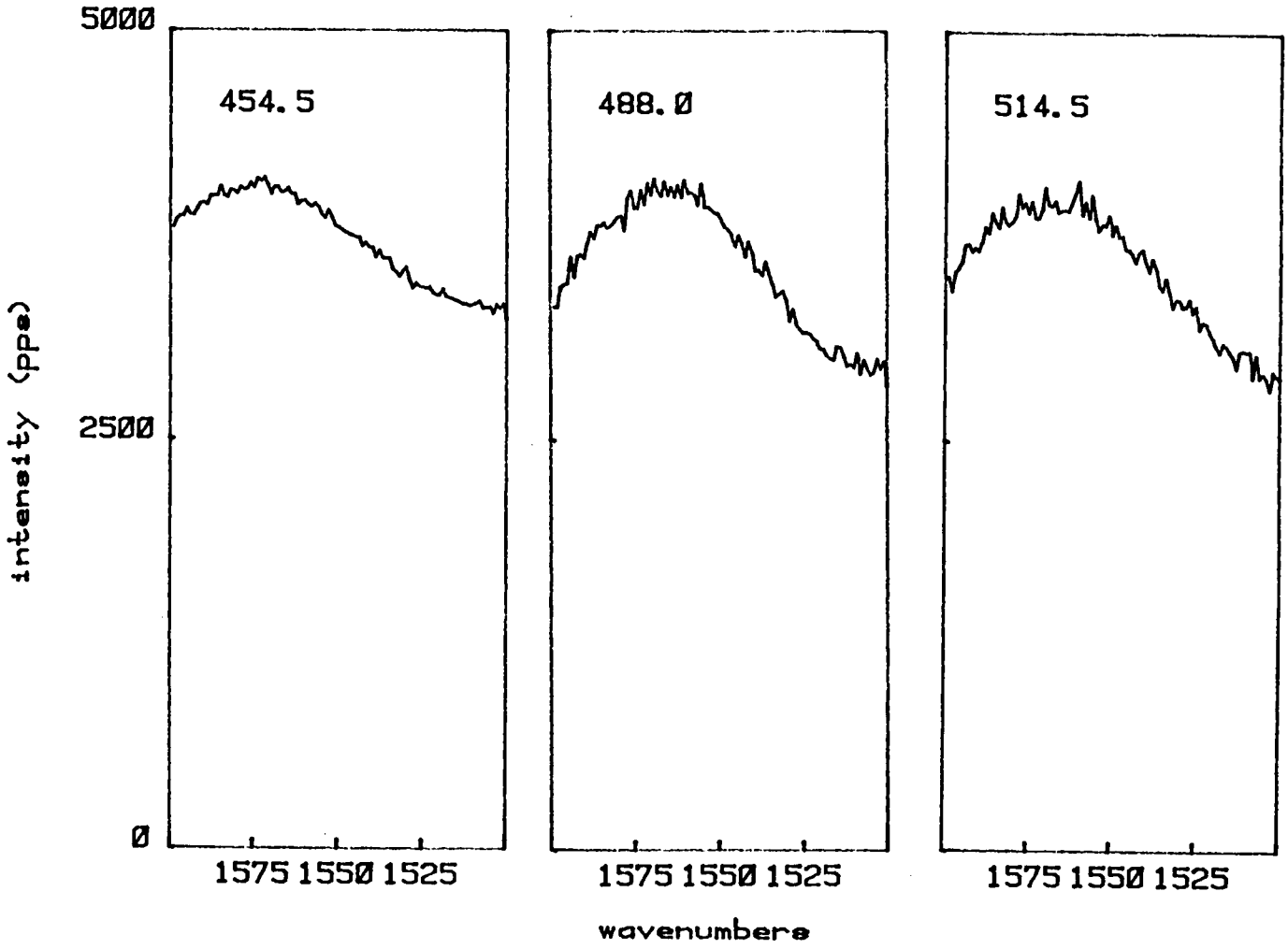

Figure 33. Raman spectrum of reduced PNMP: E(applied)= -500 mV vs. SSCE.

Table 4. Experimentally observed $\bar{\nu}_2$ values for PNMP.

PNMP	
$\lambda_{(ex)}$	E(applied) = -500 mV
(nm)	$\bar{\nu}_2$ (cm^{-1})
454.5	1574
488.0	1565
514.5	1565

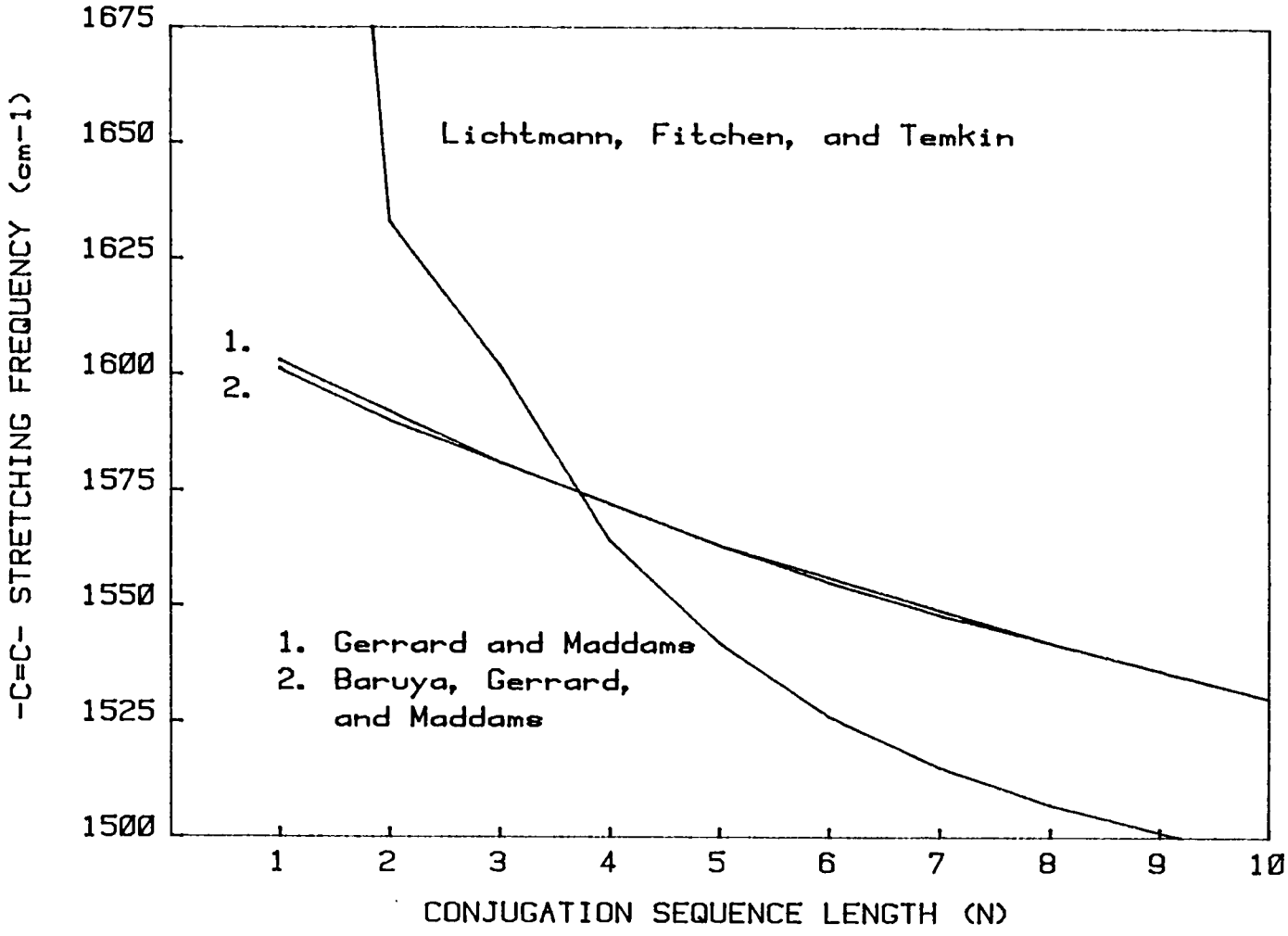

Figure 34. Plot of ν_2 versus N.

Table 5. Analysis of n from ν_2 for PP.

	E(applied)					
	-500 mV		-1000 mV		-1500 mV	
(ex) (nm)	$\bar{\nu}_2$ (cm^{-1})	n	$\bar{\nu}_2$ (cm^{-1})	n	$\bar{\nu}_2$ (cm^{-1})	n
454.5	1553	6.4	1553	6.4	1553	6.4
488.0	1551	6.6	1548	7.1	1548	7.1
514.5	1553	6.4	1550	6.8	1548	7.1

Table 6. Analysis of n from $\bar{\nu}_2$ for PNMP.

E(applied) = -500 mV		
(ex) (nm)	$\bar{\nu}_2$ (cm^{-1})	n
454.5	1574	3.6
488.0	1565	4.8
514.5	1565	4.8

The longest conjugation length observed, 7.1, resulted at the strongest reduction potential and the reddest excitation wavelength. This compares with the shortest conjugation length observed, 6.4. The conjugation length increased by approximately one double bond due to the increase in the applied reduction potential. PP is composed of conjugated segments of 3-4 pyrrole rings (two double bonds per pyrrole ring). PP thus involves a narrow distribution of conjugation lengths and is dominated by a single conjugation length. This result is consistent with the data from the cyclic voltammogram which showed a single peak in the redox wave. This suggests that the disorders are regular and may reflect the reactivity of the oligomeric cation species to hydrogenation during the polymerization reaction. If, during the polymerization reaction, an oligomeric cation of 3-4 rings is highly reactive to hydrogenation then this may explain the observed narrow distribution of conjugation lengths.

The small shifts in the C=C stretch, as both the applied reduction potential and excitation wavelength are changed, are consistent with a narrow distribution of conjugation lengths that does not change appreciably, even at strong reduction potentials.

The calculated n for PNMP varies from 3.6 to 4.8. The larger n values are obtained with the data from the long wavelength excitation (514.5 nm). PNMP chains contain conjugated segments of 2 to 3 pyrrole rings. PNMP chains are less conjugated than Polypyrrole. However, both systems consist of primarily of one conjugation length. This is the first direct spectroscopic evidence to establish the extent of conjugation in PP and PNMP.

7.5 RESULTS - PART B

Results of the photoluminescence studies of PP are presented in Figures 35 and 36. Figure 35 contains two spectra obtained from oxidized (+250 mV) and reduced (-1000 mV) PP in the region from 500cm^{-1} to 4000cm^{-1}. In the spectra of oxidized PP (left frame of fig. 35), the weak film bands are present at ≈1600cm^{-1} and 1100cm^{-1} and the sharp solvent peaks are at ≈2250cm^{-1} and 3000cm^{-1}. The baseline scatter signal is small (≈100 counts) and no photoluminescence is present. Upon reduction at -1000 mV (right frame of fig.35) the broad luminescence appears with a peak intensity between 2000cm^{-1} and 2500cm^{-1}. However, the strong Raman bands from the film are still present, on top of the luminescence signal.

Figure 36 contains spectra obtained from PP reduced at 4 different reduction potentials with a 454.5 nm excitation

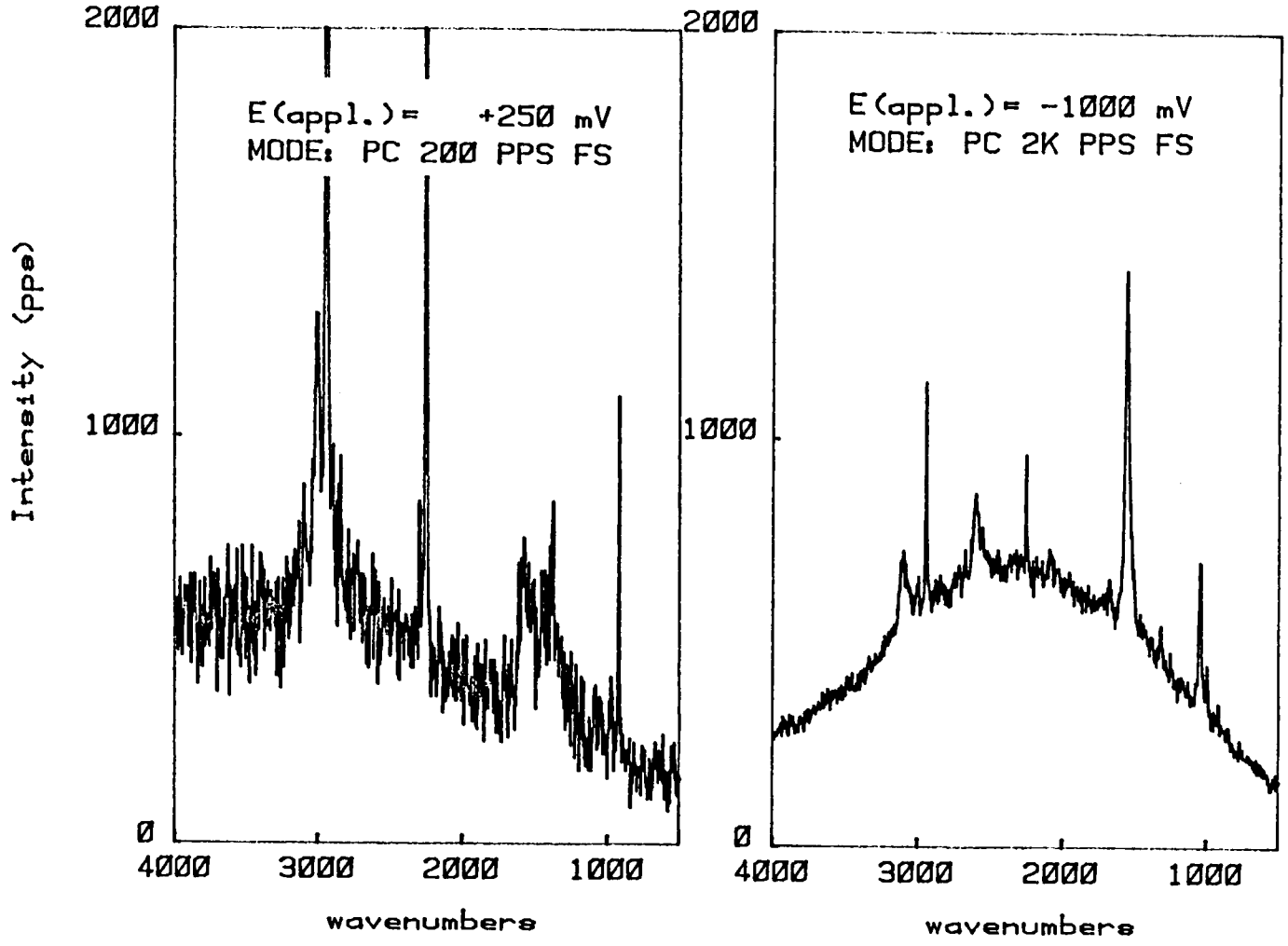

Figure 35. Raman spectrum of oxidized and reduced PP.

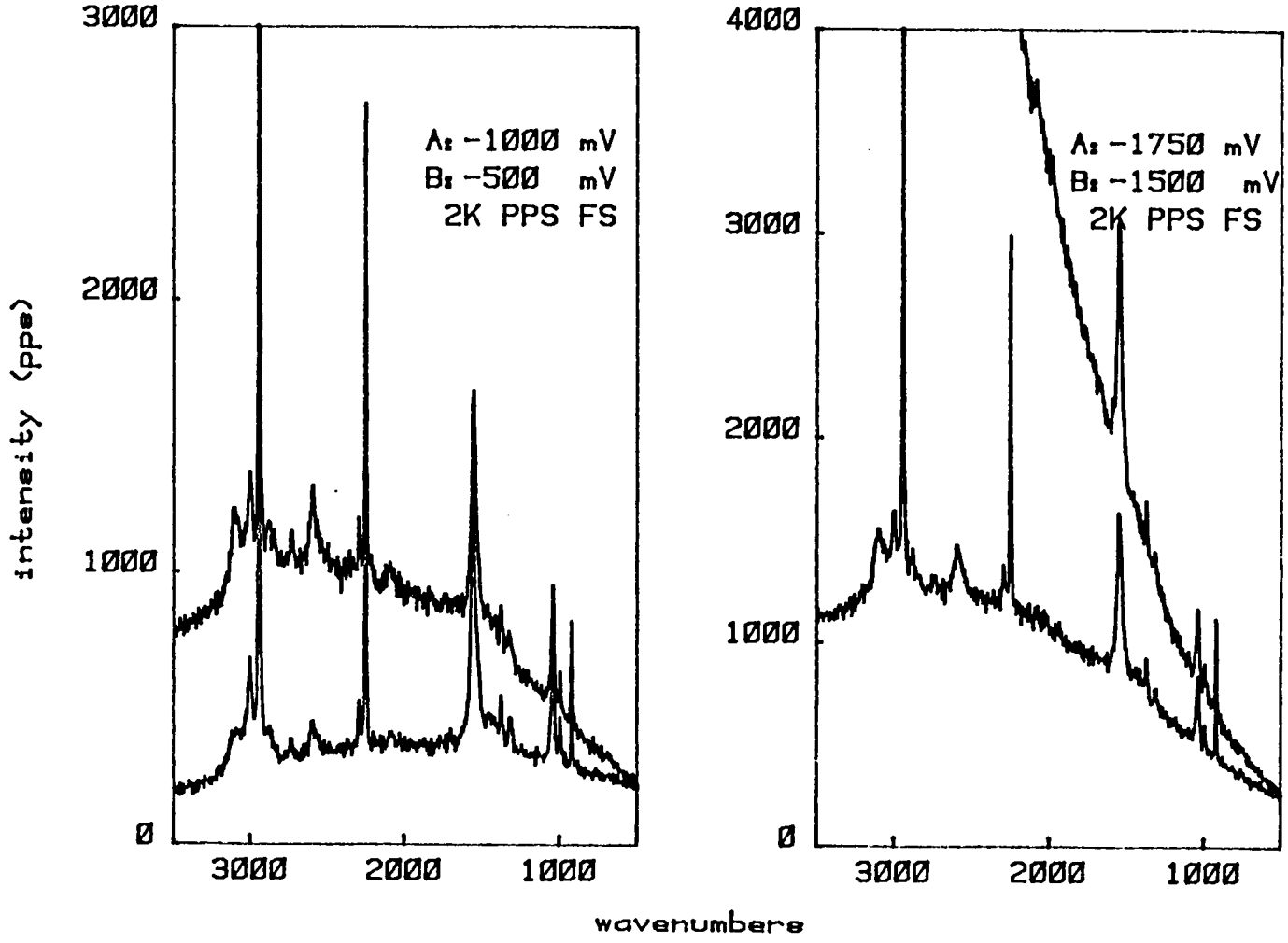

Figure 36. Raman spectrum of reduced PP: Acquired at four different reduction potentials.

line. At very strong reduction potentials (-1750 mV), an immense luminescence signal is present. Less luminescence is seen at the other reduction potentials. This is a curious phenomenom when one considers that very little cathodic current flows into the film when the potential is switched from -1500 mV to -1750mV. The luminescence intensity is strongly influenced by the reduction potential and increases as the potential is increased.

The results for PNMP are presented in Figures 37, 38, 39, and 40. The four spectra in Figures 37 and 38 show the progression from oxidized to reduced film, with a concomitant generation of significant luminescence at 0 mV and -250 mV. The luminescence is similar to PP, peaking in the 2000cm^{-1} to 2500cm^{-1} region. In Figure 39, a comparison of the luminescence obtained from PNMP° using 454.5 nm and 514.5 nm excitation lines are shown. Clearly the blue line excites more luminescence in the film. As expected the two spectra show that the strongest signals are created from the most reduced films.

The reproducibility of the luminescence after prolonged oxidation of the film was studied. Figure 40 contains luminescence data on PNMP° before and after oxidation at +750 mV for 10 minutes. Little change in either the intensity or shape of the luminescence is seen. Clearly the luminescence

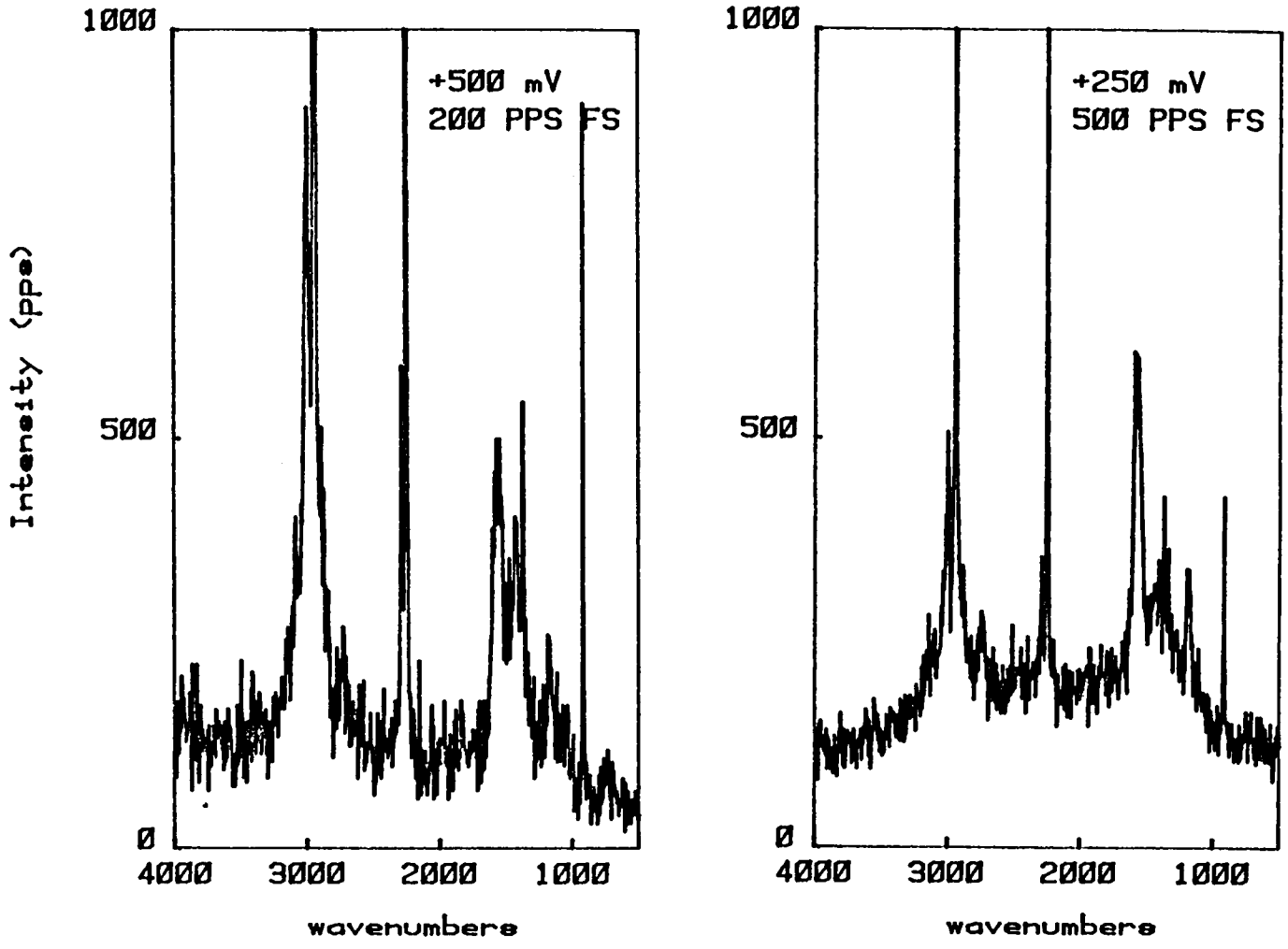

Figure 37. Raman spectrum of oxidized PNMP: wide scans to include luminescence.

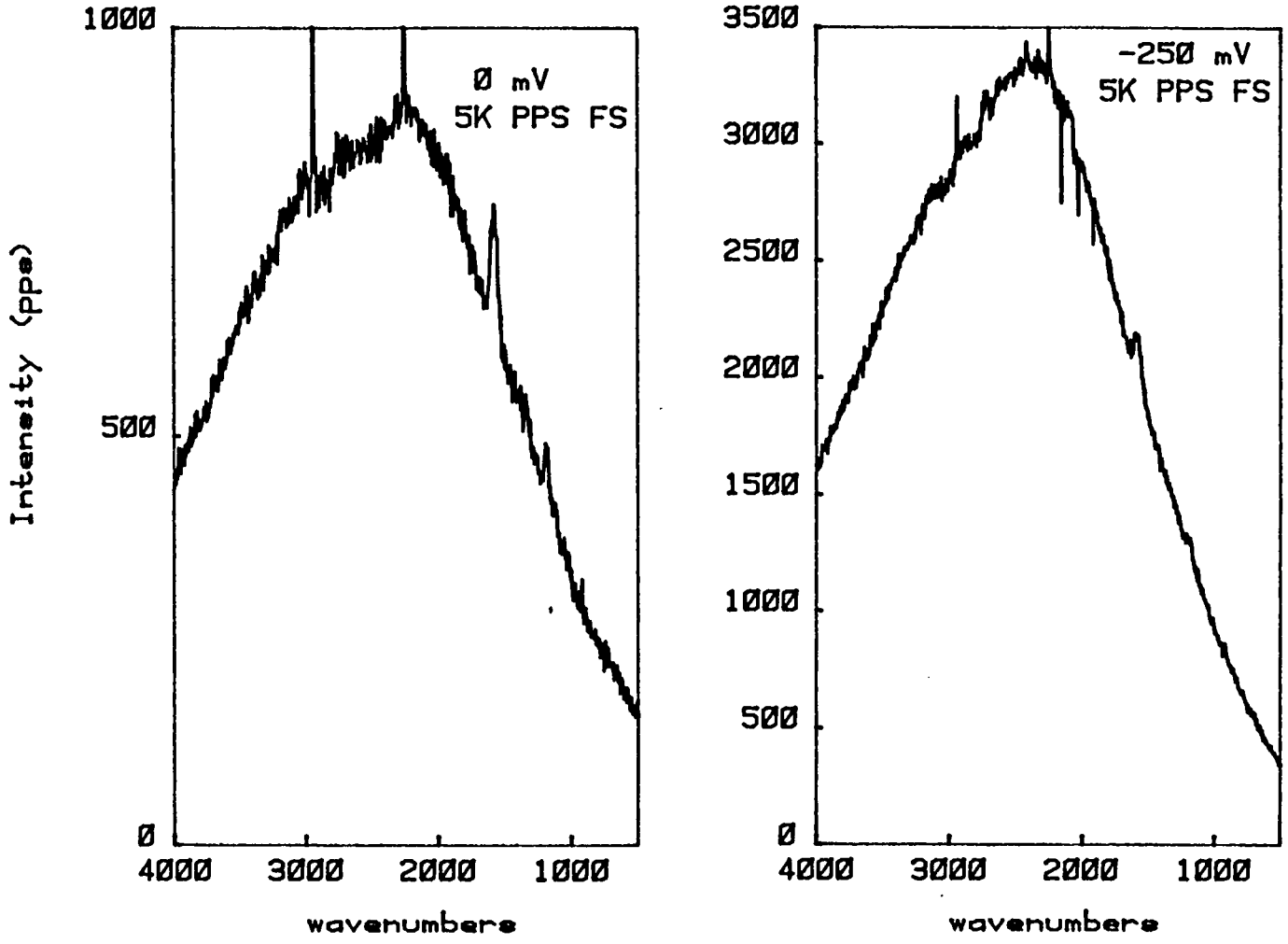

Figure 38. Raman spectrum of reduced PNMP.

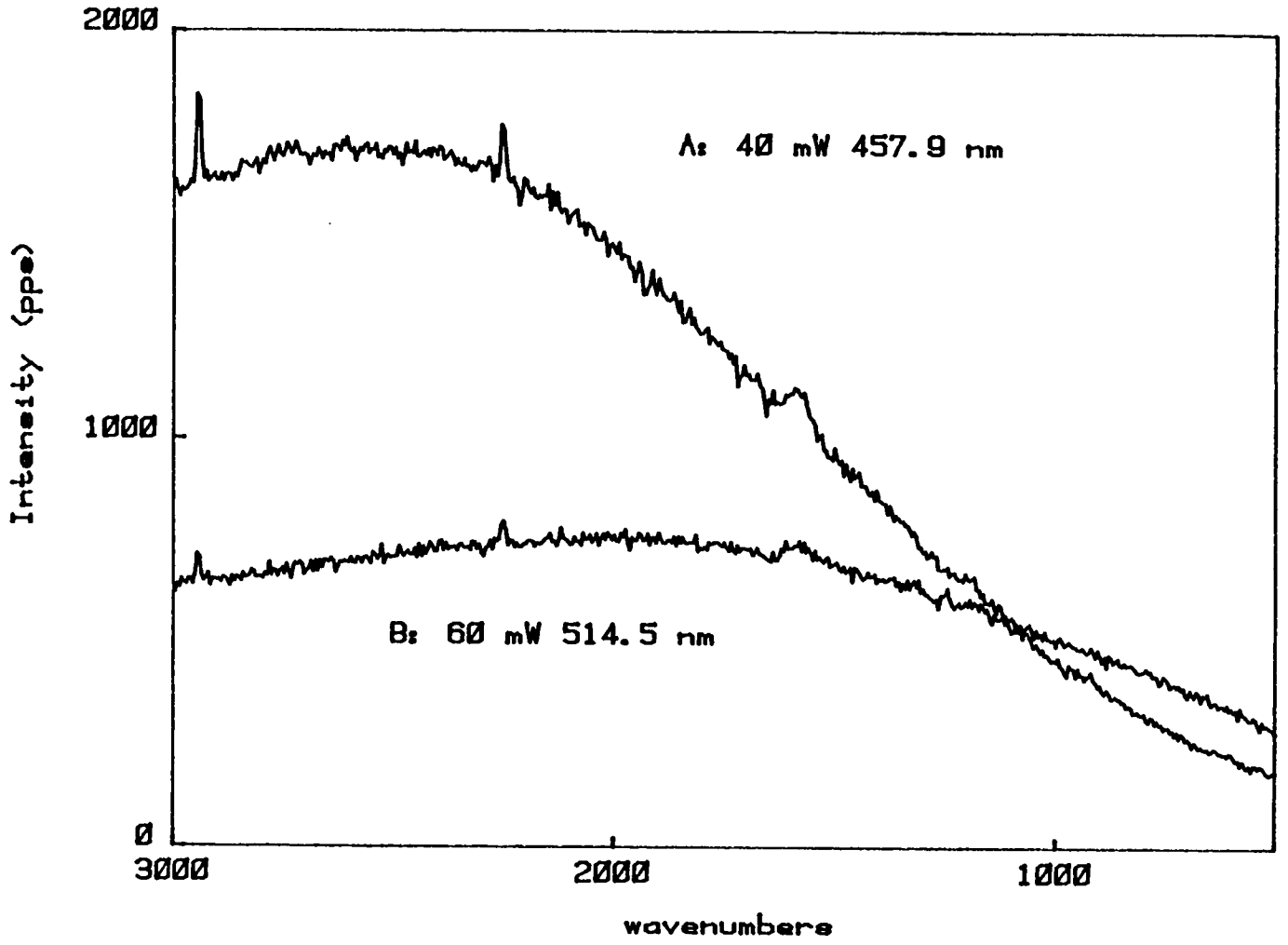

Figure 39. Luminescence of reduced PNMP film: A: 457.9 nm excitation, B: 514.5 nm excitation.

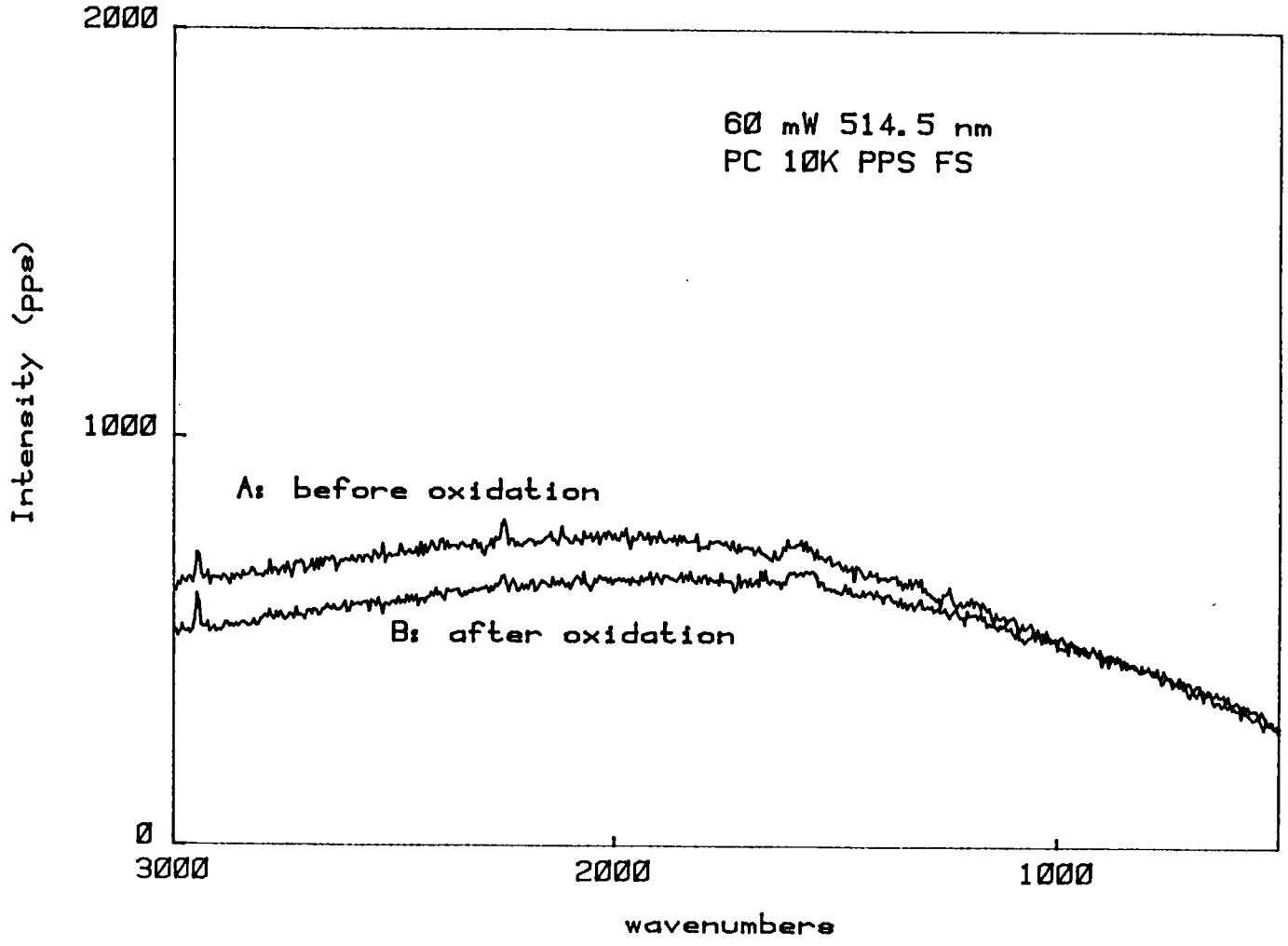

Figure 40. Luminescence of reduced PNMP: Acquired before and after oxidation.

is associated with the π-electron system of the polymer backbone.

Further evidence in support of this assertion was obtained from PNPP. If the phenyl substituent is in conjugation with the pyrrole rings, then a red shift in the luminescence would be expected. Luminescence spectra of PNPP° are presented in Figure 41. The peak intensity of the luminescence is in the region of 3500-4000cm^{-1}. This represents a red-shift in the lumnescence of PNPP° of 1000-1500cm^{-1}. Reduced films of PNPP behave similar to those of PP and PNMP because they luminesce more strongly at the stronger reduction potentials.

7.6 DISCUSSION - PART B

The fact that PP and its N-substituted derivatives fluoresce or phosphoresce is no surprise, nor is the fact that oxidation effectively quenches the luminescence. Extraction of the π-electron density from the pyrrole ring reduces the absorption and therefore the luminescence. What is surprising is the increase in the luminescence as the reduction potential is increased in a region where very little cathodic current flows into the film. In other words, a small amount of film reduction produces a large increase in luminescence intensity. Why?

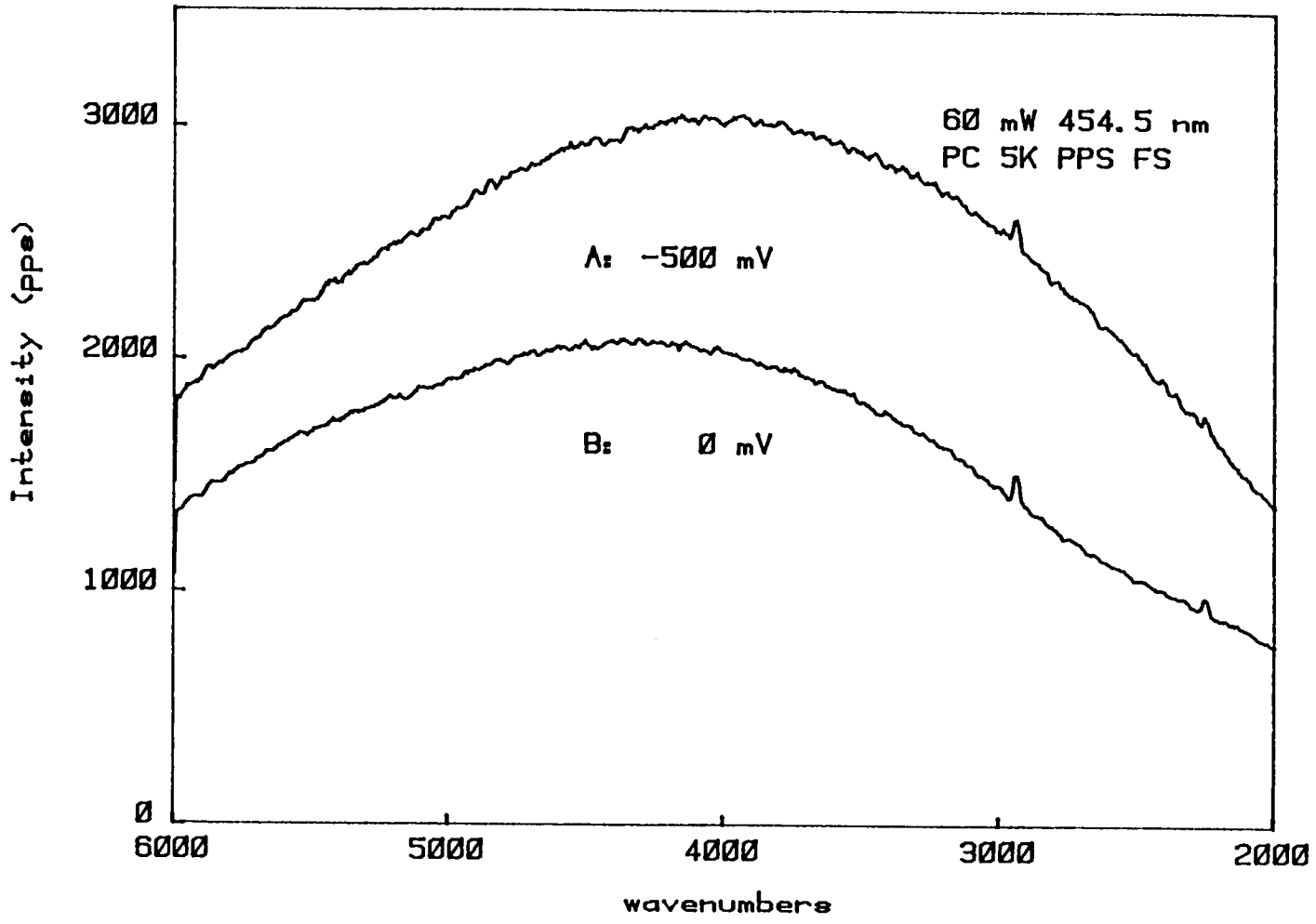

Figure 41. Luminescence of reduced PNPP.

There are two possible explanations for the luminescent behavior of the reduced films. First, the small amount of reduction at the stronger reduction potentials creates a more efficient luminescent species. The Raman studies of the conjugation in reduced PP and PNMP did show a slight increase in the conjugation length as the reduction potential is increased. The longer conjugated segments may absorb and emit more light. Second, absorption remains constant but the relative quantum efficiency of luminescence increases for the emitting species. The absorption of light is constant but the efficiency of the emission is dependent upon the reduction potential.

The first explanation is supported by the results from Chapter 6. The conjugation of reduced PP increases by ≈1 double bond at the stronger reduction potentials. The longer segment may possess a higher absorption coefficient and a larger quantum efficiency of emission. Furthermore, the cation centers present at the weaker absorption potentials have long wavelength absorption bands which may absorb the luminescence from the film.

The second argument involving quantum efficiency is less straight forward. The environment of the luminescent moiety (a 3 to 4 ring conjugated portion of PP) may inhibit or promote emission. The quenching of the luminescence by

vibrational deactivation may be reduced at the stronger reduction potentials. These processes would involve the solvent or counter-ion coupled to the luminescer to effectively deactivate the the excited state by internal conversion. A potential induced rearrangement of the double layer may reduce the quencher-luminescer interaction resulting in an increase in the luminescence intensity. Solvent and ionic effects on the fluorescence quantum yields of solution species have been studied with varied results. Schulman[57] has concluded that the processes are not well understood at this time and further rersearch is necessary.

7.7 CONCLUSION - PART B

Reduced films of PP, PNMP, and PNPP exhibit strong luminescence. The intensity is dependent upon the reduction potential and increases as the applied reduction potential is increased. The exact explanation for this behavior is unknown at this time and may involve an increase in the concentration of the luminescer and a decrease in the quenching of the luminescence by the solvent or counter-ion.. The two are not mutually exclusive.

The emission maximum does not change with an increase in reduction potential. This is consistent with the previous

finding that the reduced films are made up of primarily one conjugation length.

8.0 SUMMARY

Raman spectroelectrochemistry is a suitable method for the analysis of the carbon-carbon backbone structure of polypyrrole and its N-substituted derivatives. The Ar-ion laser is an excellent choice for obtaining resonance enhanced Raman spectra from the reduced films. The combination of electrochemistry and Raman spectroscopy allows characterization of both oxidized (conductive) and reduced (insulative) forms of the polymer in a single experiment. This is a unique opportunity to view the changes the polymer undergoes during the transformation.

One of the most puzzling questions about PP is the extent of conjugation within a polymer chain. It is very difficult to obtain this information. Radiochemical techniques have been used to determine the chain length in PP but provide little useful information on the conjugation length. However, Raman spectroscopy has been successful in analyzing the conjugation segment length in polyacetylene and polyvinylchloride.

The extent of conjugation in PP and PNMP have been examined by Raman spectroscopy. The frequency of the C=C stretching vibration was used to calculate the conjugation length. Results indicate that the conjugation lenght is limited to

3-4 rings in PP and 2-3 rings in PNMP. No evidence was found of the presence of long conjugation lengths (>10 rings). The conjugation length increases no more than one double bond as the applied reduction potential is increased to 1200 mV cathodic of the E_0 of the film (-200 mV for PP and +450 mV for PNMP). PP and PNMP are therefore made up of mostly one conjugation length.

Electrochemical data suggests that PP may have conjugation lengths as long as 10 rings. This assertion is not supported by the Raman data. However, the data does support the previous assertion that a single conjugation length predominates based on the presence of only one redox wave in the cyclic voltammogram.

Thin reduced films of PP and PNMP exhibits strong luminescence. This luminescence has been characterized at a number of applied reduction potentials. The broad featureless bands disappear upon oxidation and must be associated with the injection of π-electron density into the polymer backbone.

The curious characteristic of the luminescence is the strength of the signal in a region of little faradaic activity. Applying a slightly more cathodic potential to the film in a region cathodic of the reduction wave, where minute

quantities of reductive current flowed into the film, resulted in a marked increase in the luminescence intensity. The explanation for this behavior is still not clear.

Is the increase due to the lengthening of the conjugated segment by approximately one double bond as discovered in the Raman data? Creation of a segment that has a larger absorption coefficient at the excitation wavelength and a larger quantum efficiency of light emission would be a possible explanation for this behavior. It is not known why the required concomitant increase in the Stokes shift is not detected.

Another possible explanation for the luminescence behavior of the reduced films is that the conjugation and absorption remain constant but the quantum efficiency of emission is increased dramatically. This may be linked to a chain rearrangement sensitive to the applied reduction potential. It is an accepted fact that ion-migration occurs as the film is reduced, resulting in chain movement within the film. This movement might result in a chain conformation that promotes luminescence by reducing the amount of radiationless deactivation of the excited state. This effectively increases the quantum efficiency.

Future research may require the use of a traditional fluorescence spectrometer to adequately characterize the luminescence of the reduced films. Absorption data would be helpful in the determining the effect of reduction potential on the molar absorptivity of the film. Excitation and emission spectra would verify the the creation of a longer conjugation length by noting the Stokes shift.

APPENDIX A. FORTH SOFTWARE LISTINGS

The following 11 pages contain all of the FORTH software for electrode pretreatment, film preparation, cyclic voltammetry, and data storage (both electrochemical and Raman). The software ran on an LSI-11 microcomputer with 16K words of dynamic RAM.

399 LIST

Non-ASCII

400 LIST

```
 0 ( Electrochemistry  constants and LOAD block     dec 83 wsc  )
 1 ( pfpc clock constants for start and freq. select )
 2 OCTAL  106  CONSTANT  ONE.HERTZ         105  CONSTANT  TEN.HERTZ
 3          0  CONSTANT  KILL              104  CONSTANT  100.HERTZ
 4 ( ADAC & pfpc register addresses )      103  CONSTANT  1K.HERTZ
 5 176770  CONSTANT  CSRADC         176760  CONSTANT  ODAC
 6 176772  CONSTANT  BUFADC         170000  CONSTANT  ACLOCK
 7
 8 DECIMAL     : THRU 1+ SWAP DO I LOAD LOOP ;
 9 ( current gain multiplier for absolute current  )
10 CREATE  MULTIPLIER  1000     , 100       , 10        ,
11                     1        ,
12                   (  263 281 THRU       EXIT   )
13 263 LOAD 264 LOAD 265 LOAD
14 282 LOAD     283 LOAD             267 281 THRU
15
```

401 LIST

```
 0 ( Electrochemistry  polyFORTH wsc 8-83 )   DECIMAL
 1 VARIABLE -LIMIT    0 -LIMIT    !  VARIABLE  +LIMIT  0 +LIMIT  !
 2 VARIABLE SCAN_RATE 0 SCAN_RATE !  VARIABLE  #INT'S  0 #INT'S  !
 3 VARIABLE STEP_RATE 0 STEP_RATE !  VARIABLE  #PNTS   0 #PNTS   !
 4 VARIABLE INIT.POT  0 INIT.POT  !  VARIABLE  CLOCK   0 CLOCK   !
 5 VARIABLE 1CTR      0 1CTR      !  VARIABLE  2CTR    0 2CTR    !
 6 VARIABLE P.TIME    0 P.TIME    !  VARIABLE  CHECK#  2 CHECK#  !
 7 VARIABLE #DATA     0 #DATA     !  VARIABLE  ?AVG    0 ?AVG    !
 8 VARIABLE CURRENT.BLK 0 CURRENT.BLK ! VARIABLE BUFFER.CNT
 9 0 BUFFER.CNT !     VARIABLE BLK.ADDR  0 BLK.ADDR  !
10 VARIABLE   ADC#>I  1000  ADC#>I  !
11 ( I vs. V data array in XY pairs : 4400 bytes/2200 pairs       )
12 CREATE IVDATA      2200 2 * ALLOT      IVDATA 2200 2 * ERASE
13 VARIABLE IVPTR     IVDATA  IVPTR !
14 ( /2.5: divide by 2.5 or the DAC resolution                    )
15 : /2.5  10 25 */  ;        : RESET  IVDATA  IVPTR !   ;
```

402 LIST

```
 0 ( cyclic voltammetry initialize routines polyFORTH  wsc  1983 )
 1 ( user initialization of cv range, scan rate, & starting v    )
 2  : PARAMETERS  CR  ." Enter cathodic limit in mV " ASK -LIMIT !
 3  ( -- )        CR  ." Enter anodic limit in mV " ASK +LIMIT !
 4                CR  ." Enter scan rate in mV " ASK SCAN_RATE !
 5                CR  ." Enter initial potential " ASK INIT.POT ! ;
 6    ( conversion from mV's to dac numbers/steps          )
 7 : ABSOLUTE ( -- )  -LIMIT     @ /2.5      -LIMIT     !
 8                    INIT.POT   @ /2.5      INIT.POT   !
 9                    +LIMIT     @ /2.5      +LIMIT     !
10                    SCAN_RATE  @ /2.5      STEP_RATE  !
11                    100  STEP_RATE @  /     #INT'S     !      ;
12 ( loop counters for pos. & neg potential scans : 3 total      )
13 : PTRS&CTRS  +LIMIT @ -LIMIT @     -      /2.5   #PNTS !
14              +LIMIT @ INIT.POT @   -      /2.5    1CTR !
15              INIT.POT @   -LIMIT @     -  /2.5    2CTR !    ;
```

403 LIST

```
 0 ( Cyclic voltammetry polyFORTH wsc  10/83 )   OCTAL
 1 ( call to all initialize routines                              )
 2 : SET-UP ( -- )   PARAMETERS  PTRS$CTRS   ABSOLUTE    ;
 3
 4 ( isr for pfpc clock A  -- awakens task no more                )
 5 ASSEMBLER BEGIN    CLOCK I)  WAKE #  MOV
 6                    200  200   INTERRUPT
 7 ( increment WE potential by 2.5 mVolts                         )
 8  CODE   1+ODAC     -LIMIT  INC    ODAC  -LIMIT  MOV   NEXT
 9 ( decrement WE potential by 2.5 mVolts                         )
10  CODE   1-ODAC     +LIMIT  DEC    ODAC  +LIMIT  MOV   NEXT
11 ( delay interval between DAC inc/dec & data aquisition
12   actual time spent in this loop is a function of the 100 Hz
13   clock rate and the scan rate e.g.25,50,75,100 mV/s-1        )
14 : INTERVAL   #INT'S  @  0  DO  STOP  LOOP  ;  DECIMAL
15
```

404 LIST

```
 0 ( Cyclic voltammetry polyFORTH wsc 8-83  )            OCTAL
 1 ( data aquisition for both current and voltage
 2   software trigger    flag check
 3   adc0 = current      adc1 = potential                         )
 4
 5 CODE TAKE.DATA    0   IVPTR  MOV                  ( set pointer )
 6                   CSRADC 400 #   MOV     ( Trig. ADC channel 1 )
 7                   BEGIN CSRADC   TST B 0< END   ( Wait on done )
 8                   0 )   BUFADC   MOV          ( Store potential )
 9                   0 )+  NEG                   ( negate voltage  )
10                   CSRADC    0 #  MOV     ( Trig. ADC channel 0 )
11                   BEGIN  CSRADC  TST B 0< END         ( Done ? )
12                   0 )   BUFADC   MOV          ( Store currrent  )
13                   0 )+  NEG                   (  negate current )
14                   IVPTR  0  MOV  NEXT         ( replace pointer )
15 DECIMAL
```

405 LIST

```
 0 ( Cyclic voltammetry polyFORTH wsc 10/83        )
 1 ( allows for current equilibrium at initial potential before
 2   starting cv scan          total time = 10 seconds              )
 3 : EQUILIBRATE    ( -- )  CLOCK  GET
 4                  ONE_HERTZ    ACLOCK   !   INIT.POT @ ODAC !
 5                  10 0  DO  STOP    LOOP ( wait 10 seconds   )
 6                  KILL     ACLOCK    !
 7                  CLOCK    RELEASE     ;
 8
 9 ( positive potential scan from initial V to the anodic limit   )
10 : FIRST.+SCAN  INIT.POT @ -LIMIT !     1CTR @ 2 / 0 DO  INTERVAL
11                TAKE.DATA     1+ODAC  INTERVAL  1+ODAC  LOOP     ;
12
13 ( negative potential scan from anodic limit to cathodic limit )
14 : -SCAN      #PNTS @ 2 /    0 DO    INTERVAL  TAKE.DATA    1-ODAC
15              INTERVAL    1-ODAC     LOOP                          ;
```

406 LIST

```
 0 ( Cyclic voltammetry polyFORTH wsc 8-83 ) DECIMAL
 1 ( positive potential scan from cathodic limit to initial V     )
 2 : SECOND.+SCAN  +LIMIT @ -LIMIT   !     2CTR @   2 /    0  DO
 3                 INTERVAL    TAKE.DATA      1+ODAC
 4                 INTERVAL    1+ODAC         LOOP                  ;
 5
 6 ( performs one complete anodic scan: i.p to +L to -L to i.p    )
 7 : ANODIC.SCAN   ( -- ) CLOCK GET  100.HERTZ  ACLOCK  ! ( start )
 8                 FIRST.+SCAN   ( anodic scan: ip to +l )
 9                 -SCAN    SECOND.+SCAN   ( +l to -l to ip )
10                 KILL ACLOCK !    CLOCK RELEASE      ( stop clock )
11                 RESET         ;       ( reset ivptr to ivdata )
12
13 : +LIMIT.RESET  #PNTS @  +LIMIT @  +  +LIMIT  !                ;
14 : +CYCLE ( #.scans -- ) SET-UP  INIT.POT @ ODAC !  EQUILIBRATE
15              0  DO  ANODIC.SCAN  +LIMIT.RESET  I 1 + .  LOOP    ;
```

407 LIST

```
 0 ( Cyclic voltammetry 100 mV s-1 scan routines oct 84 wsc        )
 1 ( 100 mV/s anodic scan uses different clock                     )
 2 : +FAST.SCAN ( -- )       CLOCK  GET 1K.HERTZ ACLOCK !
 3                       FIRST.+SCAN     -SCAN  SECOND.+SCAN
 4                       KILL ACLOCK !  CLOCK  RELEASE  RESET       ;
 5
 6 ( FORTH call word for 100 mV/s anodic scan                      )
 7 : +FAST ( #.scans -- ) SET-UP  25 #INT'S !  INIT.POT @ ODAC !
 8         EQUILIBRATE   0  DO  +FAST.SCAN  +LIMIT.RESET
 9         I 1 + .  LOOP                                           ;
10
11 ( prints message after successful disk transfer                )
12 : D.M  ( -- )     CR ." Block #" CURRENT.BLK ?
13                ." has been written to disk. " CR                ;
14
15
```

```
408 LIST

 0 ( Electrochemistry data storage routines nov 83 wsc ) DECIMAL
 1
 2 ( transfers data from stack to buffer then to disk            )
 3 : TXFR.BUFFR   ( n -- )   BLK.ADDR  @  !
 4         2  BLK.ADDR +!       ( store data in disk buffer )
 5         1  BUFFER.CNT  +!    ( inc ctr/buffr full ?)
 6         BUFFER.CNT @ 512 = IF UPDATE  (  Yes, write to disk )
 7         FLUSH  D.M  1 CURRENT.BLK  +!   (   next block )
 8         CURRENT.BLK  @  BLOCK  BLK.ADDR ! ( reset blk.addr )
 9         0  BUFFER.CNT !  THEN   ;        ( reset counter )
10
11 ( flushes remaining data to disk if buffer less than full    )
12 : TST.BUFFER  BUFFER.CNT @  0= NOT IF UPDATE FLUSH  D.M THEN ;
13
14
15


409 LIST

 0 ( EMPTY )  EXIT
 1
 2
 3
 4
 5
 6
 7
 8
 9
10
11
12
13
14
15


410 LIST

 0 ( cyclic voltammmetry post run average routines Jan 84 wsc )
 1
 2 VARIABLE X.PTR  0  X.PTR  !          VARIABLE Y.PTR  0 Y.PTR  !
 3
 4 ( reinitialize array pointers after each scan                 )
 5 : RESET/XY  IVDATA  DUP X.PTR ! 2 + Y.PTR ! ;  RESET/XY
 6
 7 ( multiplies the top of the stack by 4.88/ADC resolution      )
 8 : ADC.RES  ( n - n*4.88 ) 488 100 */                          ;
 9
10 ( X:potential * 4.88 transferred to disk                      )
11 : X.STORE  X.PTR @ @  ADC.RES  TXFR.BUFFR 4 X.PTR +!          ;
12
13 ( Y:current * 4.88 * gain transferred to disk                )
14 : Y.STORE  Y.PTR @ @  ADC.RES        ADC#>I @ 1000  */
15            TXFR.BUFFR   4 Y.PTR +!                           ;
```

411 LIST

```
 0 ( cyclic voltammetry post run average routines Jan 84 wsc )
 1 DECIMAL
 2 ( loop for data transfers to disk                          )
 3 : STORE.IV ( -- ) #PNTS @          0 DO
 4                   X.STORE
 5                   Y.STORE          LOOP
 6                   TST.BUFFER   RESET/XY                    ;
 7
 8
 9 ( fetches first data block from disk 0 fills and inits pointers)
10  : GET.BUFFER  ( blk # -- ) CR ." Enter block # for data "
11                ASK        DUP  CURRENT.BLK !       BLOCK
12                DUP        1024  ERASE               BLK.ADDR !
13                0  BUFFER.CNT !         CR                    ;
14
15
```

412 LIST

```
 0 ( polymerization programs  polyFORTH  Jan 84       ) DECIMAL
 1 ( initialize parameters for polymerization                    )
 2 : POLY.SET-UP  CR ." Enter polymerization potential in mV "
 3                ASK  /2.5  +LIMIT   !
 4                CR ." Enter initial potential in mV "
 5                ASK  /2.5  -LIMIT   !
 6                CR ." Enter polymerization time in seconds "
 7                ASK        P.TIME  !
 8                5   #INT'S     !   ( sets scan rate to 50 mV/s)
 9                +LIMIT @  ABS  -LIMIT @  -   #PNTS  !        ;
10
11 ( determine the # of dac steps from init.pot to poly.pot     )
12 : DAC.STEPS  ( -- ) +LIMIT   @  -LIMIT   @ -  /2.5  1CTR !   ;
13
14
15
```

413 LIST

```
 0 ( polymerization programs  polyFORTH  Jan 84       ) OCTAL
 1
 2 CODE TAKE.CURRENT   ( aquire polymerization current )
 3                     CSRADC    0 #  MOV  ( Trig. ADC channel 0 )
 4                     BEGIN  CSRADC  TST B 0< END ( Done ? )
 5                     IVPTR  BUFADC   MOV   ( Store currrent  )
 6                     IVPTR           NEG   (  negate current )
 7
 8                     NEXT                     DECIMAL
 9
10 ( data collection rate for p.scan is 10 Hz )
11 : P.SCAN   #PNTS @ 2 /   0 DO  INTERVAL  ( wait 5 ints)
12            1+0DAC ( inc dac 0 )INTERVAL  ( wait 5 ints)
13            TAKE.CURRENT ( read poly.i )  1+0DAC  ( inc dac 0)
14            LOOP                                          ;
15
```

414 LIST

```
 0 ( polymerization routines polyFORTH  Jan 84 - wsc -    ) DECIMAL
 1
 2 ( time.out: times the polymerization; reads i at 10 HZ )
 3 : TIME.OUT          CLOCK GET     TEN.HERTZ       ACLOCK !
 4   ( -- )            P.TIME @ 10 *  0    DO ( poly time x 10 Hz )
 5                     STOP TAKE.CURRENT  LOOP ( read poly.i & wait)
 6                     KILL  ACLOCK CLOCK RELEASE  ( stop clk )  ;
 7
 8 ( init.scan:  scans from init.pot to poly.pot at 50 mV s-1
 9   see p.scan for data collection -- poly current            )
10 : INIT.SCAN         CLOCK GET     100.HERTZ     ACLOCK    !
11   ( -- )            P.SCAN         KILL ACLOCK  CLOCK RELEASE    ;
12
13
14
15
```

415 LIST

```
 0 ( Electrochemical polymerization  polyFORTH  wsc )
 1 ( initialize value for the conversion of binary to current    )
 2 : GAIN  CR ." Enter switch position 1,2,3, or 4. "
 3         MULTIPLIER  ASK  1 - 2 *  +  @
 4         ADC#>I    !    CR
 5     ." Enter divisor 1, 2, or 5 . " ADC#>I @ ASK / ADC#>I ! ;
 6 ( transfer current to buffer then disk                        )
 7 : STORE.CURRENT  #DATA @    0  DO  IVDATA I 2 * + @
 8                  ( S>D FLOAT)  ADC#>I ( F@) @  ( F*) *
 9                  TXFR.BUFFR  LOOP  TST.BUFFER                 ;
10 ( electrooxidation of monomer at Pt electrode                  )
11 : POLY.SCAN    0 ODAC !    POLY.SET-UP       TAKE.CURRENT
12                INIT.SCAN  TIME.OUT          0 ODAC !
13                IVPTR @  IVDATA -  2  /       #DATA !
14              ( GET.BUFFER STORE.CURRENT )  RESET              ;
15 : POLYMERIZE  POLY.SCAN   ; ( call for polymerization         )
```

416 LIST

```
 0 ( Cyclic voltammetry cathodic scan routines polyFORTH 1/84 wsc)
 1 ( first leg of cathodic scan from init.pot to cathodic limit  )
 2 : 1'RST.-SCAN ( -- ) INIT.POT @ +LIMIT !  2CTR @ 2 / 0  DO
 3                      INTERVAL   TAKE.DATA       1-ODAC
 4                      INTERVAL   1-ODAC          LOOP         ;
 5
 6 ( final leg from anodic limit to init.pot                      )
 7 : 2'ND.-SCAN  ( -- ) -LIMIT @  +LIMIT  !  1CTR @ 2 /   0  DO
 8                      INTERVAL   TAKE.DATA       1-ODAC
 9                      INTERVAL   1-ODAC                LOOP   ;
10
11 ( second leg from cathodic limit to anodic limit              )
12 : +SCAN        ( -- ) #PNTS  @ 2 /    0  DO   INTERVAL
13                       TAKE.DATA    1+ODAC
14                       INTERVAL    1+ODAC       LOOP   ;
15
```

```
417 LIST

     0 ( Cyclic voltammetry cathodic scan routines Jan 84 --wsc--      )
     1
     2 ( cathodic cv scan )
     3 : CATHODIC.SCAN ( cathodic scan ) ( -- )
     4                 CLOCK GET   100.HERTZ  ACLOCK  !
     5                 1'RST.-SCAN  +SCAN  2'ND.-SCAN
     6                 KILL  ACLOCK  !      CLOCK   RELEASE
     7                 RESET                                          ;
     8
     9 ( reset cathodic limit after first scan for multiple  scans    )
    10 : -LIMIT.RESET  1CTR @ 2CTR @ +  MINUS  -LIMIT  +!              ;
    11
    12 ( user call for cathodic cv scans                               )
    13 : -CYCLE ( #.scans -- ) SET-UP  INIT.POT @ ODAC ! EQUILIBRATE
    14          0 DO  CATHODIC.SCAN  -LIMIT.RESET   I 1 + . LOOP      ;
    15


418 LIST

     0 ( Cyclicvoltammetry 100 mV s-1 scan routines oct 84 wsc )
     1
     2 ( 100 mV/s cathodic scan routine                                 )
     3 : -FAST.SCAN ( -- )   CLOCK  GET  1K.HERTZ  ACLOCK !
     4                       1'RST.-SCAN  +SCAN  2'ND.-SCAN
     5                       KILL ACLOCK !  CLOCK RELEASE  RESET      ;
     6
     7
     8 ( user call for 100 mV/s cathodic scans                          )
     9 : -FAST  ( #.scans -- ) SET-UP  25 #INT'S  ! INIT.POT @ ODAC !
    10                         EQUILIBRATE   0  DO  -FAST.SCAN
    11                         -LIMIT.RESET   I 1 + .   LOOP          ;
    12
    13
    14
    15


419 LIST

     0 ( Electrochemical electrode pretreatment routines polyFORTH wsc)
     1   VARIABLE T.TIME 0 T.TIME !
     2 : 1HZ.START  CLOCK GET    ONE.HERTZ ACLOCK !                     ;
     3 : ACLK.STOP  0 ACLOCK !   CLOCK RELEASE                          ;
     4 ( anodic, cathodic and neutral potentials for pretreatment       )
     5 : POSITIVE   1800 /2.5  ODAC ! ; : NEGATIVE -400 /2.5 ODAC !    ;
     6 : NEUTRAL     200 /2.5  ODAC ! ;
     7 ( timing loop for pretreatment at each of the 3 potentials       )
     8 : TREAT  1HZ.START T.TIME @ 0 DO STOP  LOOP ACLK.STOP            ;
     9 ( calls for potentistating of electrode                          )
    10 : +.TREATMENT POSITIVE TREAT ; : -.TREATMENT NEGATIVE TREAT      ;
    11 : 0.TREATMENT NEUTRAL TREAT  ;
    12 ( user call for electrode pretreatment                          )
    13 : PRETREATMENT ( -- ) CR ( 3 cycles:+,-,0 )
    14          ." Enter cleaning time in seconds "  ASK T.TIME ! CR
    15          +.TREATMENT  -.TREATMENT  0.TREATMENT                  ;
```

420 LIST

```
 0 ( Cyclic voltammetry BOXcar routines polyFORTH wsc 7/84 )
 1 OCTAL
 2 VARIABLE WIDTH  10   WIDTH !
 3 VARIABLE HTEMP   0   HTEMP !    VARIABLE LTEMP  0 LTEMP !
 4
 5 ( trigger adc and wait on done then store data in array      )
 6 CODE V.STORE     0    IVPTR     MOV      ( set pointer )
 7                  CSRADC  400 #   MOV  ( Trig. ADC channel 1 )
 8                  BEGIN CSRADC   TST B 0< END ( Wait on done )
 9                  0 )   BUFADC   MOV  ( Store potential )
10                  0 )+  NEG    ( negate due to poor design )
11                  IVPTR  0  MOV  NEXT  ( replace pointer )
12
13
14
15 DECIMAL
```

421 LIST

```
 0 ( cyclicvoltammetry BOXcar routines polyFORTH  7/84 wsc) OCTAL
 1 CODE BOXCAR          R  -)  W   MOV
 2 ( boxcar avg of i)   2   7 #  MOV   HTEMP  CLR   LTEMP  CLR
 3                  CSRADC   0 # MOV BEGIN CSRADC TST B 0< END
 4                      LTEMP  BUFADC   MOV       HTEMP   SXT
 5                  BEGIN  CSRADC    0 # MOV BEGIN CSRADC  TST B
 6                      0< END   1  BUFADC  MOV
 7                      0      SXT      CLC   LTEMP   1    ADD
 8                      0      ADC      HTEMP   0   ADD
 9                      2   DEC   0=   END
10                      1   LTEMP  MOV     0   HTEMP   MOV
11                      10 #   0   DIV     0   NEG
12                      1  IVPTR   MOV     1 )+ 0  MOV
13                      IVPTR  1   MOV  W  R )+    MOV     NEXT
14 ( acquire both potential and boxcar of current                 )
15 : TAKE.DATA   V.STORE     BOXCAR        ;      DECIMAL
```

422 LIST

Non-ASCII

```
423 LIST

    Non-ASCII
```

```
424 LIST

    Non-ASCII
```

```
425 LIST

 0 ( SCAMP serial interface  ikc -- feb 1984 -- )
 1 ASSEMBLER
 2 CREATE <DUMB.EXPECT>   U ' H @ # SUB
 3      PTR U) ) DEVICE 2+ U) ) MOV B    PTR U) INC   CTR U) INC
 4        0= IF   U ) WAKE # MOV   THEN   U R )+ MOV   RTI
 5
 6 : ECHO.OFF  ( -- )  'EXPECT 8 + @  BESAVE !
 7         <DUMB.EXPECT> 'EXPECT 8 + ! ;
 8
 9 : ECHO.ON   ( -- )  BESAVE @  'EXPECT 8 + ! ;
10
11
12 : THRU 1+ SWAP DO I LOAD LOOP ;
13
14 285  289 THRU
15
```

```
426 LIST

 0 ( SCAMP serial interface  ikc  -- feb 1984 -- )
 1
 2 : ACK  CONSTANT  DOES>  @  DUP  1000 0 DO LOOP  EMIT
 3         1000 0 DO LOOP  EMIT ;
 4
 5 OCTAL   322 ACK 1ACK   244 ACK 2ACK  110 ACK 3ACK  DECIMAL
 6
 7 : SEND_FUT   ( -- )  ( send file usage table )
 8       129 0 DO  0 EMIT  LOOP ;
 9
10 : CONT.SEQ     ( -- )  ( set a control sequence )
11        PAD 7 EXPECT ;
12
13 : DATA.SEQ   ( -- )  ( receive a data sequence )
14        PAD 131 EXPECT ;
15


427 LIST

 0 ( SCAMP serial interface  ikc  -- feb 1984 -- )
 1
 2 OCTAL
 3
 4 CODE REPACK  ( n -- n )   S ) SWB   S ) ASR   S ) ASR   S ) ASR
 5        S ) ASR   S ) 170000 # BIC   NEXT
 6
 7 CODE REFORMAT  ( f -- f )   2 S) SWB   S ) SWB   S -) S ) MOV
 8        S ) TST B   0< IF   SEC   ELSE   CLC   THEN
 9        S ) ROR   S ) 177 # BIC   2 S) 177600 # BIC
10        S ) S )+ BIS   NEXT
11 DECIMAL
12
13
14
15


428 LIST

 0 ( SCAMP serial interface  ikc  -- feb 1984 -- )
 1
 2 : SECTOR   ( -- )  ( receive a sector of data )
 3      CONT.SEQ  1ACK  DATA.SEQ  2ACK ;
 4
 5 : FUT   ( -- )  ( send/receive  the file usage table )
 6       CONT.SEQ  1ACK  2ACK  SEND.FUT  SECTOR  3ACK  ;
 7
 8 : STORE.SECTOR   ( -- )   PAD 1+ PAD 128 CMOVE
 9      PAD 128 + PAD DO   I @  REPACK  BLK.ADDR @ !
10        2 BLK.ADDR +!  2 +LOOP  ;
11
12
13
14
15
```

```
429 LIST

 0 ( SCAMP serial interface   ikc   -- feb 1984 --  )
 1 2048. E 0  2CONSTANT  11BITS
 2 2VARIABLE QFACTOR     2VARIABLE QOFFSET
 3 2VARIABLE QTIME       2VARIABLE QFLAG
 4
 5 : 1ST.SECTOR  ( -- )  ( recv 1st sector of quadrant )
 6     SECTOR     PAD DUP 1+  SWAP  16 CMOVE  PAD 2@   REFORMAT
 7     11BITS F/    QFACTOR 2! PAD 4 + 2@   REFORMAT  QOFFSET 2!
 8     PAD 8 + 2@   REFORMAT   QTIME 2!
 9     PAD 12 + 2@   REFORMAT     QFLAG 2!    3ACK ;
10
11 : 1/2.QUADRANT  ( blk# -- ) ( recv/store one FORTH blk of data)
12        BLK.ADDR !   8 0 DO  SECTOR  STORE.SECTOR  3ACK  LOOP ;
13
14
15


430 LIST

 0 ( SCAMP/LSI-11 SERIAL INTERFACE  -ikc- feb 1984 )
 1
 2 : QUADRANT  ( blk# -- )  ( receive a data quadrant )  ECHO.OFF
 3    DUP 1+ BLOCK UPDATE SWAP BLOCK UPDATE ." >"  FUT  1ST.SECTOR
 4      1/2.QUADRANT  1/2.QUADRANT  ECHO.ON  FLUSH  CR ." DONE" ;
 5
 6
 7 : >CPS  ( i -- f )  ( convert SCAMP integer fraction to actual)
 8                     ( counts per second                        )
 9         0 FLOAT  11BITS F-  QFACTOR 2@ F*   QOFFSET 2@  F+ ;
10
11
12
13
14
15


431 LIST

 0 ( EMPTY )
 1
 2
 3
 4
 5
 6
 7
 8
 9
10
11
12
13
14
15
```

APPENDIX B. EQUPMENT LIST FOR SPEX INC. LASER RAMAN.

- 1403 Ramalog double spectrometer, 0.85m double monochromator, f/7.8, with wavenumber Compudrive, 4 slits.

- 18H 1800 groove mm^{-1} (425-850 nm) gratings (2).

- 1729F Thermoelectric Cryostat, silica optics, side window for Hammamatsu R955 PMT; requires water and drain.

- R955 Hammamatsu Photomultiplier Tube, multialkali, 200-700 nm cooled.

- DPC-2 Digital Photometer, PMT power supply, preamp, and PC/DC amplifier.

- 1467 Periscope Viewer, for viewing sample area through entrance slit.

- 1461 Polarization Scrambler, in mount.

- 1459 UVISIR Illuminator and sample chamber, 50 mm focusing lens, f/1.4 elliptical mirror, sample image projection screen, and safety shutter. 1460 Lasermate,

laser monochromator for isolating laser wavelengths from 200-2000 nm, 1200g/mm 500 nm grating.

- SC32 SCAMP, spectrometer controller, data acquisition, and data processing system.

APPENDIX C. RAMAN SPECTRA OF POLY-N-PHENYLPYRROLE

Appendix C contains the Raman spectra of electrochemically oxidized and reduced poly-N-phenylpyrrole in Figures 42 through 45. The spectra were acquired at three different applied potentials. The spectra suffer from poor resolution resulting from the absence of resonance enhancement and competition from a strong luminescent background in the reduced form. These two factors complicated the analysis of the conjugation lengths present in PNPP.

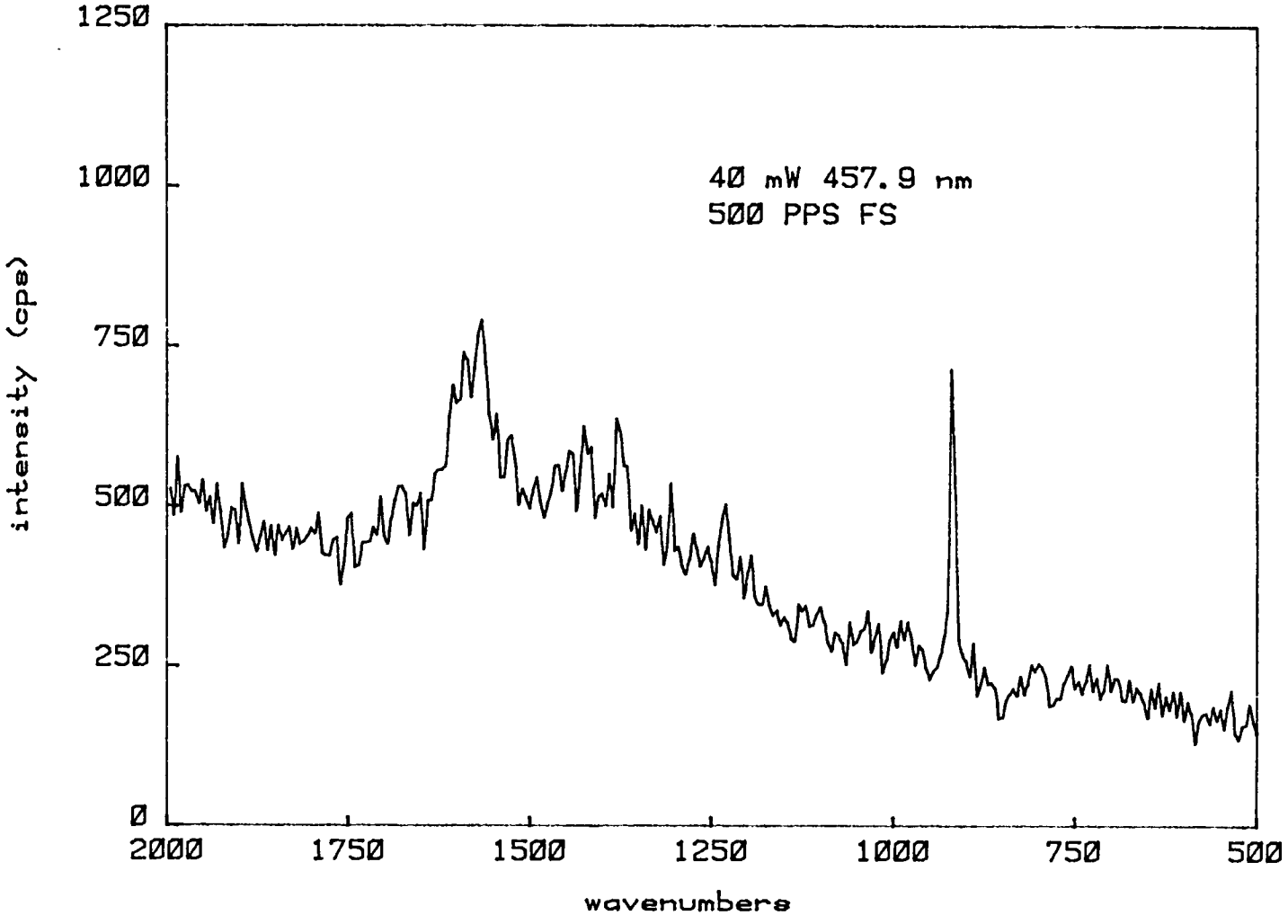

Figure 42. Raman spectrum of oxidized PNPP: E(applied)= +500 mV vs. SSCE.

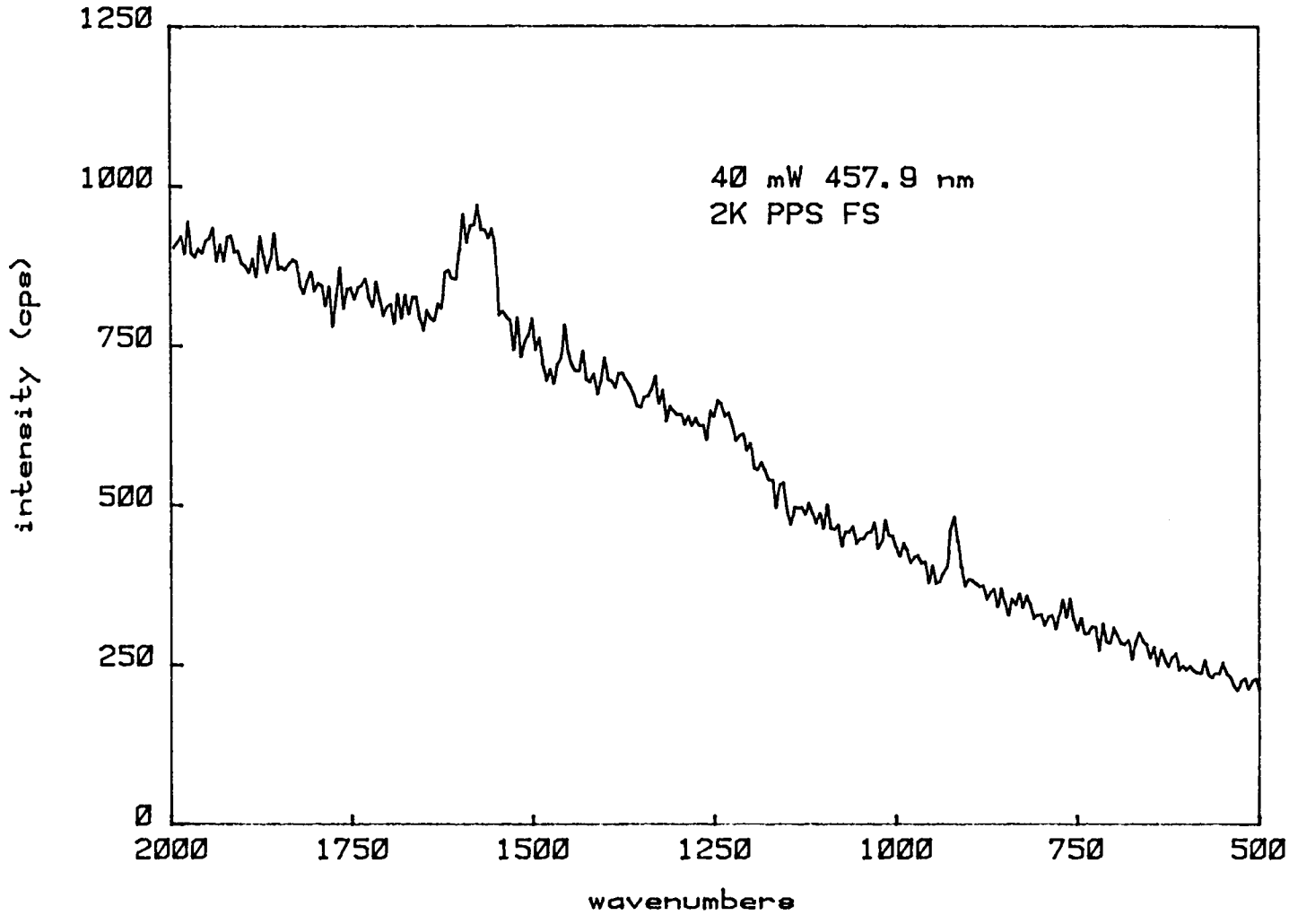

Figure 43. Raman spectrum of reduced PNPP: E(applied)= 0 mV vs. SSCE.

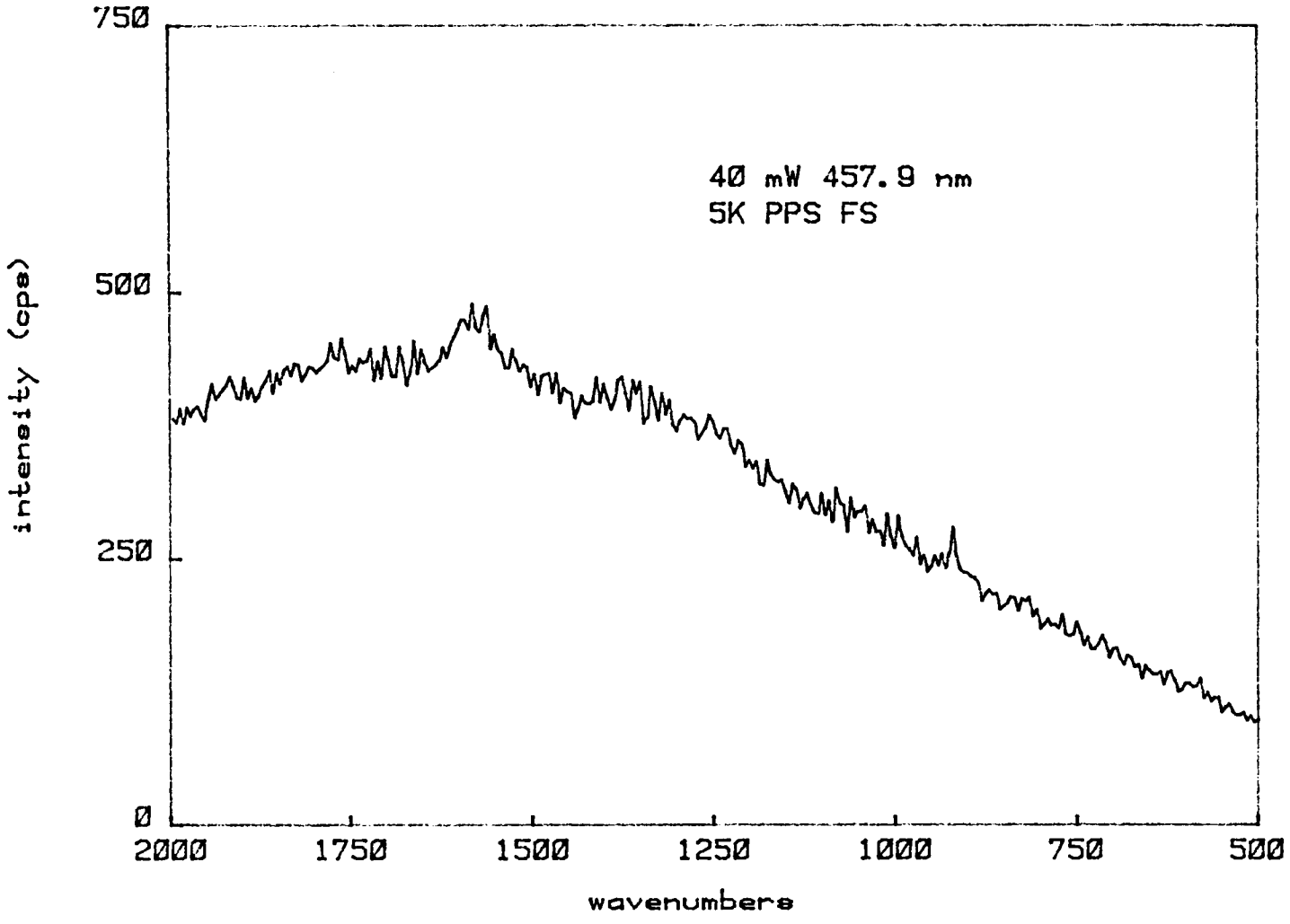

Figure 44. Raman spectrum of reduced PNPP: E(applied)= -500 mV vs. SSCE.

APPENDIX D. PLOT OF E(APPLIED) VS. LOG(X) FOR PP.

Appendix D contains a Nernst plot of applied potential against log(X) for a polypyrrole film. The value for log(X) is equal to [Red]/[Ox] and is obtained from Figures 17, 19, and 20. The quantity [Red] was obtained from the maximum intensity of the C=C stretching frequency at $\approx 1550 cm^{-1}$. The quantity [Ox] was calculated by subtracting the [Red] value from the maximun intensity of the C=C stretching frequency for the totally reduced film (Figure 22). All of these values are corrected for the baseline scattering internsity. The values of Log(X) are -1.06 for -125 mV, -0.71 for -375 mV, and -0.46 for -500 mV. The slope of the Nernst plot is 630 mV indicative of a highly irreversible system.

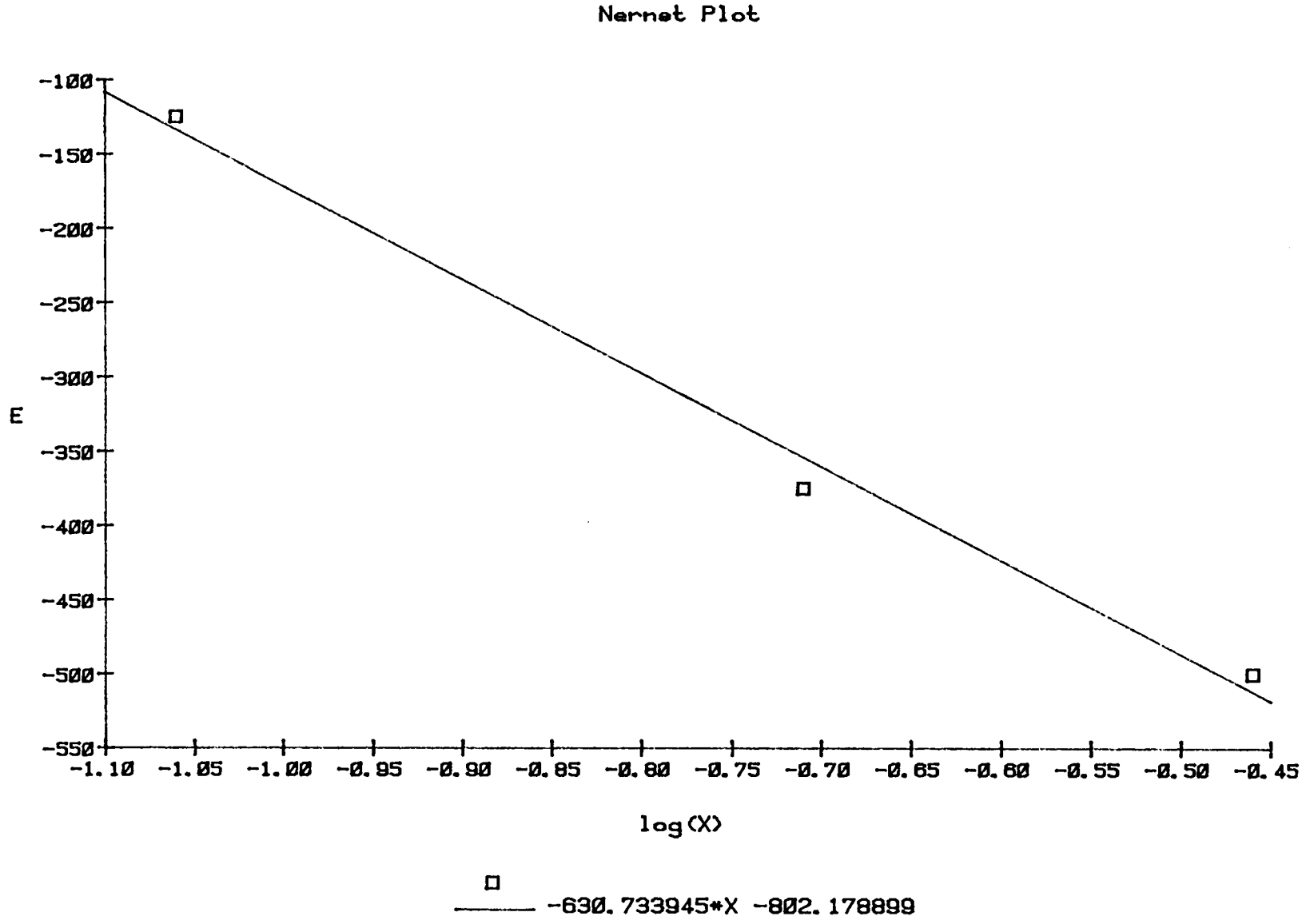
Nernst Plot
-100
-150
-200
-250
-300
-350
-400
-450
-500
-550
E
-1.10
-1.05
-1.00
-0.95
-0.90
-0.85
-0.80
-0.75
-0.70
-0.65
-0.60
-0.55
-0.50
-0.45
log(X)
-630.733945*X -802.178899

BIBLIOGRAPHY

1. A. F. Diaz and K. K. Kanazawa, Chemica Scripta 17, 145 (1981).

2. E. M. Genies, G. Bidan, and A. F. Diaz, J. Electroanal. Chem., 149, 101 (1983).

3. R. A. Bull, F.R. Fran and A. J. Bard, J. Electrochem. Soc. 130, 1636 (1983).

4. P. Burgmayer and R. W. Murray, J .Am. Chem. Soc., 104, 6139 (1982).

5. R. A. Bull, F. R. Fan and A. J. Bard, J. Electrochem. Soc., 130, 1636 (1983).

6. T. Skotheim, O. Inganas, J. Prejza and I. Lundstrom, Mol. Cryst. Liq. Cryst. 83, 329 (1982).

7. K. K. Kanazawa, A. F. Diaz, W. D. Gill, P. B. Grant, G. B. Street, G. P. Gardini and J. F. Kwak, Syn. Met., 1, 329 (1980).

8. P. Pfluger, U. M. Gubler and G. B. Street, Solid St. Commun., 49, 911 (1984).

9. T. Skotheim, M. I. Florit, A. Melo and W. O. O'Grady, Phys. Rev. B, 30, 4846 (1984).

10. G. B. Street, T. C. Clarke, M. Krounbi, K. Kanazawa, V. Lee, P. Pfluger, J. C. Scott and G. Weiser, Mol. Cryst. Liq. Cryst., 83, 253 (1982).

11. J. C. Scott, P. Pfluger, T. C. Clarke and G. B. Street, Polym. Preprints, 23, 119 (1982).

12. J. L. Koenig in "Applied Spectroscopy Reviews," ed. by E. G. Brame, Marcel Dekker, New York, (1971) chapter 5.

13. J. Robinson in "Specialist Periodical Report: Electrochemistry," Volume 9, ed. by D. Pletcher, The Royal Society of Chemistry, London, (1984) chapter 3.

14. A. Angeli and L. Alessandri, Gazetta 46, 283 (1916).

15. A. Dall'Olio, Y. Dascola, V. Varucco and V. Bocchi, C. R. Acad. Sci. Ser. C 267, 433 (1968).

16. A. F. Diaz, K. K. Kanazawa and G. P. Gardini, J. C. S. Chem. Commun., 635 (1979).

17. A. F. Diaz and J. I. Castillo, J. C. S. Chem. Commun., 397 (1980).

18. A. F. Diaz, J. I. Castillo, J. A. Logan, W-Y Lee, J. Electroanal. Chem., 129, 115 (1981).

19. G. B Street, T. C. Clarke, M. Krounbi, K. K. Kanazawa, V. Lee, P. Pfluger, J. C. Scott and G. Weiser, Mol. Cryst. Liq. Cryst., 83, 253 (1982).

20. E. M. Genies, G. Bidan and A. F. Diaz, J. Electroanal. Chem., 149, 101 (1983).

21. A. F. Diaz, A. Martinez, K. K. Kanazawa and M. Salmon, J. Electroanal. Chem., 130, 181 (1981).

22. K. K. Kanazawa, A. F. Diaz, R. H. Geiss, W. D. Gill, J. F. Kwak J. A. Logan, J. F. Rabolt and G. B. Street, J. C. S. Chem. Commun., 854 (1979).

23. J. Hornstra and L. J. van der Pauw, J. Electronics Control, 7, 169 (1959).

24. K. K. Kanazawa, A. F. Diaz, W. D. Gill, P. B. Grant, G. B. Street, G. P. Gardini and J. F. Kwak, Syn. Metals, 1, 329 (1980).

25. A. F. Diaz and K. K. Kanazawa, "Extended Linear Chain Compounds,"Vol. 3, Ed. by J. S. Miller, Plenum Press, New York, (1983) p. 417.

26. F. B. Kaufmann, A. H. Schroeder, E. M. Engler and J. Q. Chambers, J. Am. Chem. Soc., 102, 483 (1980).

27. A. F. Diaz, J. I. Castillo, J. A. Logan and W. Y. Lee, J. Electroanal. Chem. 129, 115 (1981).

28. A. F. Diaz, J. I. Castillo, K. K. Kanazawa, J. A. Logan, M. Salmon and O. Fajardo, J. Electroanal. Chem., 133, 233 (1982).

29. M. Salmon, A. F. Diaz, J. A. Logan, M. Krounbi and J. Bargon, Mol. Cryst. Liq. Cryst., 83, 265 (1982).

30. A. F. Diaz, Chem. Scr., 17, 145 (1981).

31. A. F. Diaz, J. Crowley, J. Bargon, G. P. Gardini and J. B. Torrance, J. Electroanal. Chem., 121, 355 (1981).

32. G. B. Street, T. C. Clarke, R. H. Geiss, V. Y. Lee, A. Nazzal, P. Pfluger and J. C. Scott, J. de Physique Coll., C3, 599 (1983).

33. G. B. Street, S. E. Lindsey, A. I. Nazzal and K. I. Wynne, to appear in Mol. Cryst. Liq. Cryst.

34. P. Pfluger and G. B. Street, J. Chem. Phys., 80, 544 (1984).

35. W. K. Ford, C. B. Duke and W. R. Salaneck, J. Chem. Phys., 80, 544 (1984)

36. A. Nazzal and G. B. Street, J. C. S. Chem. Commun., 83 (1983).

37. K. Yakushi, L. J. Lauchlan, T. C. Clarke and G. B Street, J. Chem. Phys., 79, 4774 (1983).

38. J. L. Bredas, K. Yakushi, J. C. Scott, and G. B. Street, Phys. Rev. B, 30, 1023 (1984).

39. Smekals ref. about prediction of Raman

40. C. V. Raman and K. S. Krishnan, Nature, 121, 501 (1928).

41. N. B. Colthup, L. H. Daly, S. E. Wiberly, "Introduction to Infrared and Raman Spectroscopy," Academic Press, N. Y., 1975, p. 57.

42. D. P. Strommen and K. Nakamoto, J. Chem. Ed., 54, 474 (1977).

43. A. Albrect, J. Chem. Phys., 34, 1476 (1961).

44. D. L. Gerrard, Chem. Britain, Aug. 1984 p. 715.

45. F. Sondheimer, D. A. Ben-Efraim and R. Wolovsky, J. Am. Chem. Soc., 83, 1675 (1961).

46. C. Tric, J. Chem. Phys., 51, 4778 (1968).

47. T. M. Ivanova, L. A. Yanovskaya and P. P. Shorygin, Opt. Spectroscopy, 18, 75 (1965).

48. L. S. Lichtmann, D. B. Fitchen and H. Temkin, Syn. Met., 1, 139 (1979).

49. D. L. Gerrard and W. F. Maddams, Macromol., 14, 1356 (1981).

50. A. Baruya, D. L. Gerrard and W. F. Maddams, Macromol., 16, 578 (1983).

51. H. Shirakawa, T. Ito and S. Ikeda, Polymer J. 4, 460 (1973).

52. A. Campion, J. K. Brown and V. M. Grizzle, Surf. Sci. Lett., 115, L153 (1982).

53. J. J. VanBenschoten, J. Y. Lewis, W. R. Heineman, D. A. Roston and P. T. Kissinger,J. Chem. Ed., 60, 772 (1983).

54. K. K. Kanazawa, A. F. Diaz, M. T. Krounbi and G. B. Street, Syn. Metals 4, 119 (1981).

55. I. Harada, Y. Furukawa, M Tasumi, H. Shirakawa and S. Ikeda, J. Chem. Phys. 73, 4746 (1980).

56. S. Krichene, S. Lefrant, G. Froyer, F. Maurice and F. Pelous, J. Phys. Colloq. C3, 733 (1983).

The vita has been removed from the scanned document